九州大学学術情報リポジトリ
Kyushu University Institutional Repository

Enhanced Oil Recovery from Heterogeneous Reservoir by Blocking Performance with In/situ Formed Sodium Carbonate Gel

サムニアン, チア

https://doi.org/10.15017/4060153

出版情報：Kyushu University, 2019, 博士（工学）, 課程博士
バージョン：
権利関係：

Enhanced Oil Recovery from Heterogeneous Reservoir by Blocking Performance with *In-situ* Formed Sodium Carbonate Gel

Samneang Chea

Enhanced Oil Recovery from Heterogeneous Reservoir by Blocking Performance with *In-situ* Formed Sodium Carbonate Gel

A DOCTORAL DISSERTATION

By

Samneang Chea

Department of Earth Resources Engineering,

Graduate School of Engineering,

Kyushu University, Japan

2020

Enhanced Oil Recovery from Heterogeneous Reservoir by Blocking Performance with *In-situ* Formed Sodium Carbonate Gel

Submitted to the Department of Earth Resources Engineering, Graduate School of Engineering, Kyushu University, Japan
In Partial Fulfilment of the Requirement for the Degree of Doctor of Philosophy

By
Samneang Chea

Supervised by
Professor Kyuro Sasaki

2020

Abstract

Injected fluids conformance is one of challenges in producing oil by water flooding and enhanced oil recovery operations from a heterogeneous reservoir with large permeability variation layers or fractures. When the displacement process of reservoir fluids, such as oil or gas, is applied in the heterogeneities reservoir, the injected fluids tend to flow through the highest permeability pathway between injecting and producing wells. This breakthrough of the injected fluids causes decreasing in the production with the excessive fluids production through the pathway. In such case, blocking fluids flow to shut-off the short-cut pathway in thief zone in the heterogeneous reservoir.

The scope of this research considered characterizing and evaluating the potential of *in-situ* sodium carbonate gel (SC-gel) as blocking performance in heterogeneous reservoirs for enhanced oil recovery by forming from alkaline water-solution of sodium metasilicate ($Na_2SiO_3 \cdot 9H_2O$; S-MS) reacted with dissolved CO_2 gas. To apply the SC-gel blocking to enhanced oil recovery after water flooding, the permeability and flooding tests were also carried out using sandstone cores.

This dissertation consists of five chapters.

Chapter 1 is the introductory chapter, which addresses the importance of the oil recovery process from heterogeneous reservoirs by blocking high permeable pathways, and its challenges. The overviews of oil recovery mechanism starting from primary to tertiary oil recovery and previous researches on water-shut off treatment methods. The approach of enhanced oil recovery method was highlighted comprehensively in this chapter for both megascopic and microscopic oil displacement efficiency.

Chapter 2 describes the experimental research process with an overview of qualitative and quantitative methods, data collection, recording and analysis. It also presents the materials, such as crude oil and chemicals, used in gel formation coreflooding experiments and interfacial tension measurement (IFT) between oil and the S-MS water solutions including the experimental setups measurement instrument. Furthermore, Raman spectroscopy and scanning electron microscopy/energy dispersive x-ray (SEM-EDS) spectroscopy that were used to analyse molecular compounds and chemical characterization of the gel formed in the experiments is explained. The sandstone core was used to measure the threshold pressure gradient (TPG) after *in-situ* forming SC-gel in it. The cylindrical heterogeneous core (43.4 mm in diameter and 72.0 mm in length) was constructed by combining two semi-cylindrical Berea sandstone cores with different

permeability (300 mD and 50 mD). It was used for coreflooding test after injecting saline water and the Japanese light crude oil (JLO-I) into the core to evaluate the blocking effect in the heterogeneous reservoir.

Chapter 3 explains the gel characterization and evaluation by using the sodium metasilicate (S-MS) solution and dissolved CO_2 gas. The characterization process based on the chemical and physical properties of the gel formed from different S-MS concentration, CO_2 gas pressure, temperature, time, salinity and divalent ion. The gel properties were measured based on both chemical and physical methods. The physical characterization was presented on the gelation time, gel strength, and gel stability through the controlling parameters such as sodium metasilicate concentrations (1-10 wt%), CO_2 Gas pressure (2-7.5 MPa), temperature (25-80 ºC), salinity (NaCl; 0.1-10 wt%), divalent ion (Ca^{2+}; 10-10000 ppm), and light crude oil interaction (JLO-I). Both Raman and SEM-EDS spectroscopies revealed that the gel was a sodium carbonate type (SC gel). Gelation time after CO_2 gas injection was around 1 to 24 h depending on temperature and pressure. Gel strength increased with higher S–MS concentration and CO_2 gas pressure. The baseline concentration of S-MS solution was selected for the detailed investigation of the effect of supercritical CO_2 injection, salinity (NaCl), divalent ion (Ca^{2+}), and crude oil interaction with the gel property, as well as the gel behaviour in the porous media.

Measurements of gas permeability and threshold pressure gradient (TPG) were carried out to evaluate the blocking effect by forming SC-gel in the sandstone core. It was confirmed that TPG and gas permeability of the sandstone core increased by 2.6 times and decreased about 1/10 to that of water saturation by filling *in-situ* SC-gel.

Chapter 4 evaluates the blocking performance of *in-situ* formed SC-gel on oil recovery from the heterogeneous sandstone core. Firstly, the alkaline flooding of S-MS solution can be applied after water flooding and before blocking operations to improve the oil recovery, because IFT between oil and S-MS solution and oil was reduced to around 0.1 mN/m from 27 mN/m of the case of water. It was confirmed that micro-emulsion consisting water droplets (0.5-50 μm) in oil and stable up to three weeks at temperature of 55°C was generated by mixing 0.5-2 wt% of S-MS solution including 0.1-10 wt% of NaCl.

The coreflooding test was applied to the heterogeneous sandstone core prepared from two different permeability sandstone cores. The water flooding using the saline water (2 wt% of NaCl concentration) was conducted until oil recovery became 57%. Then 1 wt% of S-MS solution of 0.5 pore-volume (PV) at 0.1 mL/min was injected as the alkaline

flooding. Then 0.3 PV of 5wt% of S-MS solution at the same flow rate and CO_2 gas was injected at 2.0 MPa. After the injections, the core was immediately shut-in to form in-situ gel for 2 days in which the pressure drop of 1.6 MPa was recorded due to CO_2 gas dissolution and forming the gel. Meanwhile the pH, pressure drop in the core, oil and water/solution volumes in produced micro-emulsion were also monitored during the core flooding to investigate fluids properties in the core. When 2 PV water injection at the same flow rate took place again after shut-in, the pressure drop increased to 1.5 times (permeability reduced to 67% reduced) with increasing 9 % in oil recovery ratio due to the *in-situ* formed gel in the core. It was concluded that the operation of blocking with *in-situ* formed SC-gel by injecting S-MS solution and CO_2 gas was effective for the heterogeneous oil reservoir after water and alkaline floodings.

Chapter 6 is a summary and conclusion of the major findings of present research, including the research interest in the future study.

Acknowledgement

I would like to express my gratitude to Professor Kyuro SASAKI for his invaluable guidance, time, encouragement and his excellent supervision during this research. No achievement without him.

I also would like to gratefully thank to Assoc. prof. Yuishi Sugai for his kind support, assistance and discussion during the laboratory experiment.

Acknowledgement and appreciation go to Asst. prof. Ronald Nguele for his helpfulness, discussion and suggestion during my research.

I am thankful to all members of Resources Production and Safety Engineering Laboratory and also all professors and department office staffs of Earth Resources Engineering Department for their helpfulness and kindness.

I would like to give my sincere gratitude to KIZUNA program (JICA) for the scholarship and financial supports for my research.

I gratefully acknowledge Dr. OM Romny, General Director of the Institute of Technology of Cambodia for giving this golden chance to pursue my study.

Last but not least, special thanks are extended to my beloved wife and family for their support, encouragement and loves during my study.

Table of contents

List of figures

List of tables

Chapter 1: Introduction

Oil is a fundamental energy source and also an important chemical raw material. 95% of worldwide oil production is used to provide energy purpose. However, the oil resources are being depleted rapidly. In addition, to increase the oil production replying the growing of global demands of fossil fuel, some oil recovery operation and technique have been developed from primary, secondary and tertiary process to enhance the oil recovery. Tertiary recovery is the most important method used to remove the residual oil trapping the pore space in the reservoir which cannot be produced by primary and secondary process.

The water breakthrough has been a main problem during the enhanced oil recovery (EOR) process in the heterogeneous reservoir consisting of fracture or a short-cut layer with much higher permeability than that of other layers resulting in low oil recovery ratio.

1.1 Oil Recovery Mechanisms

Oil recovery operation traditionally has been subdivided into three stages: primary, secondary and tertiary. Primary recovery is the oil recovery from the natural drive energy existing in the reservoir. Secondary recovery is usually implemented after the primary stage by water flooding, pressure maintenance and gas injection process. Tertiary is any technique applied after secondary recovery by using miscible gases, chemicals, or thermal energy to displace the residual oil trapped in the pore space after the secondary recovery process became uneconomic (Green and Willhite, 1998; Lake, 1996). The recovery factor by primary and secondary process is around 35 to 50 % of the original oil in place. But the residual oil in the part of the reservoir swept by water flooding largely remains about 20% to 35%, so the oil may still exist about 50-60 % (Green & Willhite, 1998). In this case, the tertiary recovery or EOR process is expected to remove the remaining oil. By the way, the EOR process somehow can be applied after the primary stage so the stage of oil recovery is not always in chronological order. The oil recovery process is comprehensively provided in **Figure 1.1**.

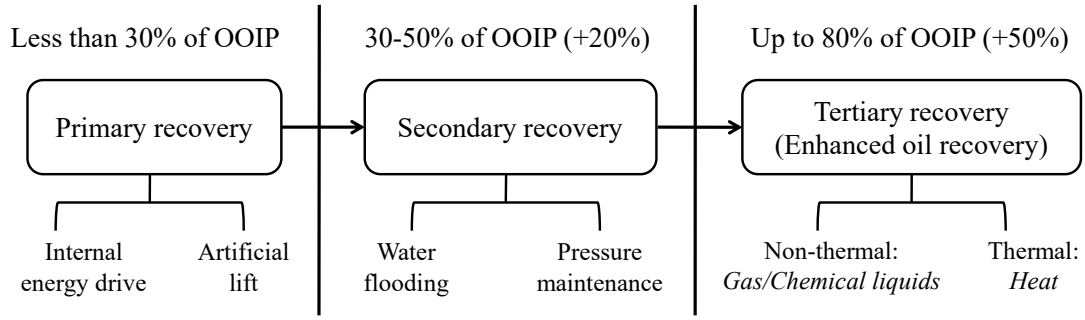

Figure 1.1 Oil recovery process

Enhanced oil recovery, principally results from the injection of gases, or liquid chemicals and/or the use of thermal energy which do not normally present in the natural reservoir. Enhanced oil recovery can be in term of tertiary oil recovery and it can be carried out after the secondary oil recovery. Somehow, EOR processes are also implemented as a primary production stage. The classification scheme of oil recovery clearly shown in **Figure 1.1**.

Gases used in EOR processes are hydrocarbon gases, CO_2, nitrogen, and flue gases. A number of liquid chemicals are commonly used, including the polymer, surfactants, and hydrocarbon solvents. Thermal processes typically consist of the use of steam, hot water, or rely on the *in-situ* generation of thermal energy through oil combustion in the reservoir rock. Table, et al., 1997 listed down a detailed EOR method applying in the oil industries (see **Table 1.1**).

The selection of any EOR technique is really depended on the oil type, reservoir rock, formation type, reservoir temperature, as well as the oil saturation, and the history of the past operation (Green and Willhite, 1998). Carman (1956) provided comprehensive screening criteria for enhanced oil recovery methods as shown in **Table 1.2**.

Table 1.1 Methods of enhanced oil recovery (Taber et al., 1997)

Thermal methods	Chemical methods	Gas (and hydrocarbon solvent) methods
In-situ combustion	Alcohol-miscible solvent flooding	" Inert" gas injection
Standard forward combution	Micellar/polymer (surfactant) flooding	Nitrogen injection
Wet combustion	Low IFT waterflooding	Flue gas injection
O_2 enriched combustion	Alkaline flooding	Hydrocarbon gas injection
Reverse combustin	ASP flooding	CO_2 flooding
Steam and hot-water injection	Polymer floodng	
Hot-water flooding	Gels for wate-shutoff	
Steam stimulatin	Microbial injection	
Stem flooding		
Surface mining and extraction		

EOR processes ideally consider on the overall displacement efficiency, including the microscopic and macroscopic displacement efficiencies. Microscopic displacement

relates to the displacement or mobilization of oil at the pore space and reflects the oil saturation. It is a measure of the effectiveness of the displacing fluid in moving the oil at where the displacing fluid contacts the oil. Macroscopic displacement efficiency concerns the sweep efficiency conformance of displacing fluids in contacting the reservoir volume. It is a measure of effectiveness of the displacing fluid sweeps out the volume of a reservoir, both horizontally and vertically, as well as how effectively the displacing fluid moves the displaced oil toward the production wells.

Table 1.2 Summary of screening criteria for EOR methods(Carman, 1956)

EOR methodA2:J32	Oil properties			Reservoir characteristics					
	Gravity ºAPI	Viscosity (cp)	Composition	Oil saturation (%PV)	Formation type	Net thickness (ft)	Average permeability (md)	Depth (ft)	Temperature (ºF)
Gas injection methods (misible)									
Nitrogen (& flue gas)	>35 ↗ 48↗	<0.4↘	High % of C_3-C_7	>40↗ 75↗	Sandstone or carbonate	Thin unless dipping	N.C.[2]	>6000	N.C.
Hydrocarbon	>23↗ 41↗	<3↘ 0.5↘	High % of C_2-C_7	>30↗ 80↗	Sandstone or carbonate	Thin unless dipping	N.C.	>4000	N.C.
Carbon dioxide	>22↗ 36 ↗	<10↘ 1.5↘	High % of C_6-C_{12}	>20↗ 55↗	Sandstone or carbonate	(Wide range)	N.C.	>2500	N.C.
Chemical									
Micellar/-polymer, Alkaline/-polymer (ASP), and alkaline flooding	>20↗ 35↗	<35↘ 13↘	Light, intermedia. Some organic acids for alkaline floods	>35↗ 53↗	Sandstone preferred	N.C.	>10↗450↗	<9000 ↘ 3250	<200 ↘80
Polymer flooding	<15 <40	<150, >10	N.C.	>70↗ 80↗	Sandstone preferred	N.C.	>103↗800↗	<9000	<200 ↘140
Thermal									
Combustion	>10ä 16→?	<5000 → 1200	Some asphaltic components	>50↗ 72↗	High porosity sand/ Sandstone	>10	>50[5]	<11500↘3500	>100 ↗ 135
Steam	>8-13.5→?	<200000 ↘ 4700	N.C.	>40↗ 66↗	High porosity sand/ sandstone	>20	>200[5]	<4500 ↘ 1500	N.C.

1. Underlined values represent the approximate mean or average for current filed projects, ↗ indicated higher value of parameter is better
2. N.C.=not critical
3. >S md from some carbonate reservoirs
4. Transmissibility >20 md ft/cp
5. Transmissibility >50 md ft/cp

Several physical/chemical interactions occur between the displacing fluids and oil that can improve the efficiency of microscopic displacement (low oil saturation). These phenomena are including the miscibility between the fluids, decreasing the interfacial tension (IFT) between fluids, oil volume expansion, and reducing oil viscosity. Macroscopic displacement is improved by maintaining of favourable mobility ratios between all displacing and displaced fluids throughout the process (Green and Willhite, 1998).

The large density difference between displacing and displaced fluids might be advantaged by flooding in an up dip or down dip direction.

1.1.1 Microscopic Displacement of Fluids in a Reservoir

An important aspect of any EOR process is the effectiveness of process fluids in removing oil from the rock pore at the microscopic scale. Microscopic efficiency is mainly controlled by capillary and viscous forces governing phase trapping and mobilization of fluids in porous media. So the understanding of these forces is required to understand the recovery mechanism involved in the EOR process (Green and Willhite, 1998).

The forces related to phase trapping and mobilization in multiphase fluid system in porous media including the interfacial tension (IFT), rock wettability, and capillary pressure.

Surface Tension and Interfacial Tension, IFT:

IFT is the surface energy related to the fluid interfaces influence the saturation, distributions, and displacement of the phases when immiscible phases coexisted in a porous medium. The surface tension term refers to the surface energy between a liquid and its vapour or air. If the surface energy is between two different liquids, or between a liquid and a solid, so the term is the interfacial tension, IFT (**Figure 1.3**). IFT value, commonly encountered in water, hydrocarbon, water/hydrocarbon systems, and some water/ hydrocarbon /surfactant systems. IFT can be measured by using either ring tension-meter, spinning-drop, or the pendant-drop methods.

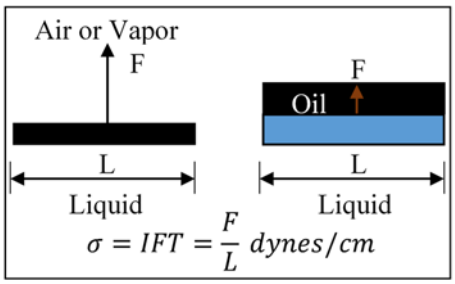

Figure 1.2 The concepts of surface and interfacial tension

A simplest way to measure the surface tension of a liquid is to use a capillary tube shown in **Figure 1.3**.

$$\sigma = \frac{rh(\rho_w - \rho_a)g}{2\cos\theta} = \frac{rP_c}{2\cos\theta} \quad (1.1)$$

where

r: capillary-tube radius, cm

h: height of water rise in the capillary, cm

ρ_w: water density, g/cm^3

ρ_a: air density, g/cm^3

g: gravity acceleration constant, 980 cm/s^2

θ: contact angle between water and capillary tube.

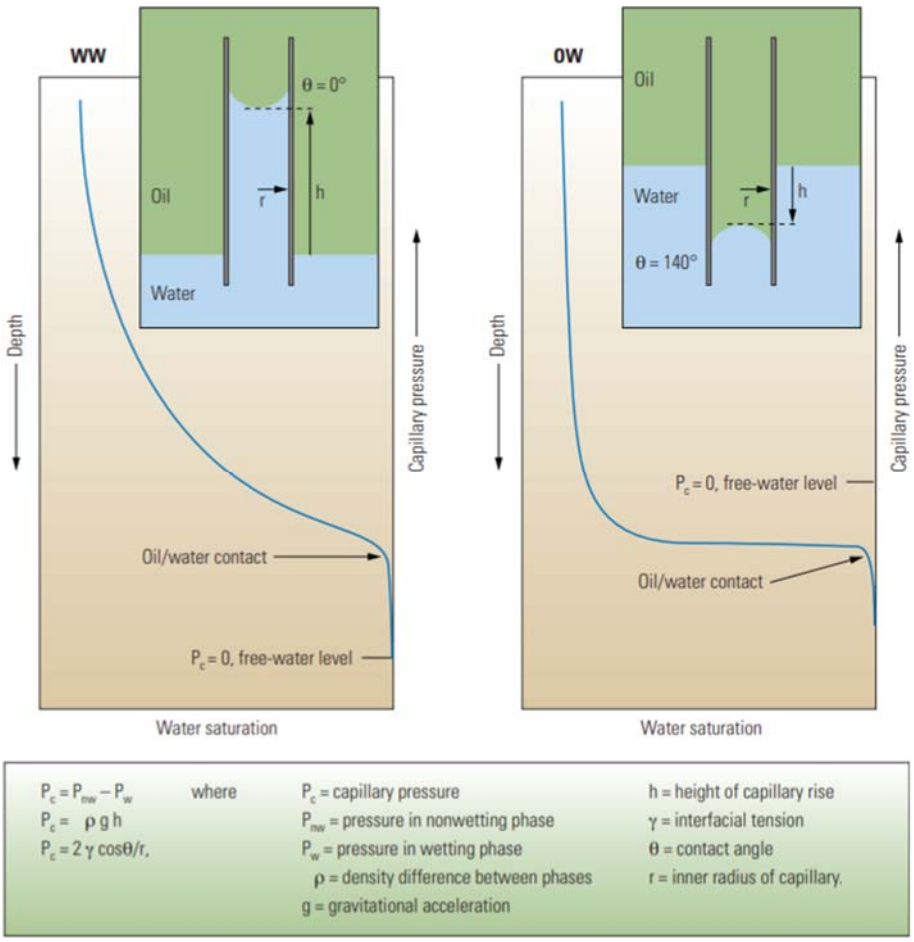

Figure 1.3 Capillary measurement method (Abdallah et al., 2007)

In the porous media, fluid distribution is not only affected by the forces at fluid/fluid interfaces, but also by the forces at fluid/solid interfaces. Wettability is the tendency of a fluid to spread on or adhere to a solid surface in the presence of a second fluid in the porous media. When two immiscible phases are placed in contact with a solid surface, one phase usually is attracted to the solid more strongly than the other phase (**Figure 1.4**). The more strongly attracted phase is called the wetting phase (Green and Willhite, 1998).

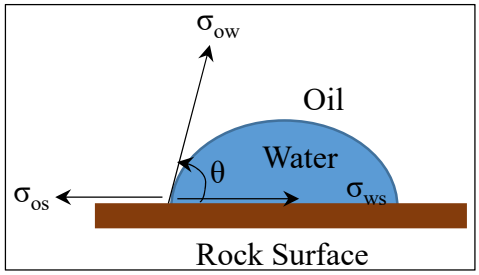

Figure 1.4 Wettability and interfacial tension (Green and Willhite, 1998)

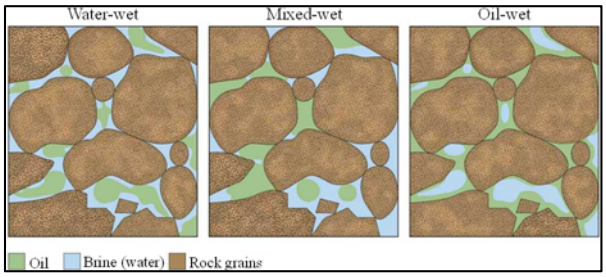

Figure 1.5 Effect of wettability on saturation (Abdallah, et al., 2007)

Rock wettability affects the nature of fluid saturation and the general relative permeability as mentioned in **Figure 1.5**.

The contact angle, θ, is used to measure the wettability. The solid is water-wet if θ<90° and oil-wet if θ>90°. A contact angle closes to 0° indicates a strong water-wet and an angle closes to 180° means a strongly oil-wet (Green and Willhite, 1998). The details, angles with different wettability are shown in **Table 1.3**. (Zolotukhin and Ursin, 2000).

Table 1.3 Contact angle in different wettability (Zolotukhin and Ursin, 2000)

Contact angle values	Wettability prerference
0-30	Strongly water wet
30-90	Preferentially water wet
90	Neutral wettability
90-150	Preferentially oil wet
150-180	Strongley oil wet

Capillary Pressure:

Capillary Pressure is a pressure difference existing across the interface (Abdallah et al., 2007; Green and Willhite, 1998). This pressure can be illustrated by the fluid rise in a capillary tube in **Figure 2.3** and calculated by **Eq. (1.2)**. The capillary pressure is related to the fluid/fluid IFT, the relative wettability of the fluids (through θ), and the size of capillary, *r*.

$$P_C = \frac{2\sigma_{ow}cos\theta}{r} \tag{1.2}$$

where

P_c: capillary pressure (mN/cm^2)

σ_{ow}: IFT between water and oil (mN/cm)

r: capillary tube radius (cm)

θ: contact angle (-)

Viscous Force:

Viscous forces in a porous medium are the magnitude of the pressure drop passing through the medium. It can be expressed by Darcy's law (Green and Willhite, 1998).

$$\Delta P = -\frac{\bar{v}\mu L\emptyset}{k} \tag{1.3}$$

where

ΔP: pressure drop across the porous medium P_2-P_1 (Pa)

$\bar{v}$: average velocity of fluid in the pores of the porous medium (m/s)

μ: fluid viscosity (Pa·s) (1 mPa·s=1 cP or 1000cP=1Pa·s)

L: length of the porous medium, (m).

ϕ: porosity of the porous medium (-)

k: permeability of reservoir (m^2) (1 mD = 0.987^{-15} m^2 or 1D = 0.987^{-12} m^2)

1.1.2 Macroscopic Displacement Efficiency

Oil recovery in any displacement process relies on the volume of reservoir contacted by the injected fluid. Macroscopic displacement efficiency is the volume sweep efficiency, which is controlled by the areal and vertical sweep efficiencies (Green and Willhite, 1998).

The four main parameters affecting areal displacement efficiency are:

- Injection/production well pattern
- Reservoir permeability heterogeneity
- Mobility ratio
- Relative importance of gravity and viscous forces.

The factors effecting vertical displacement efficiency are following:

- Gravity segregation caused by differences in density
- Mobility ratio
- Vertical to horizontal permeability variation
- Capillary forces

Mobility Ratio:

The mobility ratio, M, is an extremely important parameter in any displacement process. The oil displacement process is considered to have the mobility control if $M \leq 1$. The sweep efficiency increases if M decreases. M also effects on the stability of a displacement

process, with flow becoming unstable/viscous fingering (non-uniform displacement front) when M >1 (Green and Willhite, 1998).

The mobility ration can be calculated by **Eq. (1.4)**.

$$M = \frac{\lambda_D}{\lambda d} \tag{1.4}$$

where

λ_D: mobility of the injecting fluid phase such as surfactant solution (m^2/(Pa·s))

λ_d: mobility of the displaced fluid phase such as oil (m^2/(Pa·s))

The mobility of the fluid phase in porous media is given by **Eq. (1.5)**.

$$\lambda_i = \frac{k_i}{\mu_i} \tag{1.5}$$

where

λ_i: mobility of the fluid phase

k_i: effective permeability of phase i (m^2)

μ_i: fluid viscosity of phase i (Pa·s)

Mobility control concept is applicable to the development of EOR process, especially for the fluid flow in the porous media.

Green & Willhite (1998) suggested that the important factor of macroscopic efficiency is better considered in the heterogeneous reservoir geology.

The implementation of EOR technique is always affected by reservoir geology and reservoir geologic heterogeneities. This factor can cause the unexpected losses of injected fluids or bypassing of fluids because of channelling in high permeability zones or fractures. Similarity, fluid movement may be very non-uniform because of heterogeneity of reservoir rock.

1.2 Previous Research and Problem Definitions

1.2.1 Oil Recovery from Heterogeneous Reservoirs

A heterogeneous reservoir is defined as a reservoir consisting of shift zone, high permeability layer and/or fractures (Green and Willhite, 1998, pp. 1–4). These features are one of the major problems during water-flooding recovery processes as far as the oil recovery is concerned. This is due to the injected water is produced through the high permeability zone (short-cut zone) leaving unsweep low permeability zone. On the other hand, carbon dioxide (CO_2) leakage through the sealing potential of fractures and high

fault zone remains the main problem for carbon capture and storage (CCS) in the underground geological formation (Blackford et al., 2013; IPCC, 2005). Given the substantial volume of trapped oil within the low permeability zones or the need of a sealing agent, which prevents the CO_2 gas leakage from the underground reservoir, a conformance improvement treatment is crucial for either process.

Conformance improvement, also referred as water shut off treatments, can be divided into mechanical and chemical methods, in which the former approach relies on horizontal and multi-lateral wells to increase contact reservoir zone, or liner and cement squeezes to block short-cut flow (Prada et al., 2000). Those mechanical techniques often failed, because water either leaks past the packing devices to outside of plugging zone (Hoefner, 1989). The latter approach, which is the scope of this study, uses a chemical solution to form gels in high permeability zones. Several methods have been investigated, with mitigated results, including phenol-formaldehyde resins, chemical precipitation, and inorganic gels (sodium silicate gels) and gelling polymer (Nasr-El-Din and Taylor, 2005). Stahl and Schulz, 1988 studied the cross-linked polymer for water diversion and presented two methods to evaluate gel characteristics including beaker tests and gel evaluation. They concluded that both the gelation time, therein defined as the time at which viscosity starts to increase and the viscosity of the polymer are the main influencing parameters (Chou and Bae, 1994). It was further shown that water shut-off treatment using polymer as starting material is severely challenged by the heterogeneity of the candidate formation. In this regard, alternative approaches consisting of blending polymer with silica gel has been proposed (Bryant et al., 1996; Hamouda and Amiri, 2014; Hoefner, 1989; Jousset et al., 1990; Skrettingland et al., 2014; Stahl and Schulz, 1988; Sydansk and Argabright, 1988; Taylor and Nasr-El-Din, 2003). However, the details mechanisms and chemical analyses of this silicate gel are poorly understood on previous studies. It appears from the literature that in order to form the gel, a foreign material (gelling activator) is required, none of which are carbon dioxide (CO_2).

1.2.2 Previous Gel Characterization

Stahl and Schulz (1988) conducted the laboratory evaluation of crosslinked polymer gel for water diversion and proposed two methods, beaker and core testing, for gel characterization and evaluation.

- **Beaker test:**

Gel time:

Gel time is arbitrarily defined as the time at which viscosity starts to increase or the time at which the apparent viscosity reach at a specific value (Green and Willhite, 1998). The time required for gelation to occur is an important design for gel placement. With gel system, chemicals are mixed at the surface and injected as a viscous solution to the underground formation. The solution is designed to react and gel at the designated time after being placed in the formation. Gel time is determined from the intercept of the extrapolations from the two straight line sections of a viscosity-versus-time curve as shown in **Figure 1.6** (Green and Willhite, 1998; Stahl and Schulz, 1988). This concept is similar to what McDonald (2015) did by taking the gel time at highest viscosity.

For short gelation time, a Brookfield Viscometer is used for viscosity monitoring. But for long gel times, a ball viscometer is recommended because it is not efficient to continuously monitor the solution viscosity with the viscometer (Bookfield DVI) (Stahl and Schulz, 1988).

This method has been found to give reproducible results for gel time up to 10 days or more (Green and Willhite, 1998).

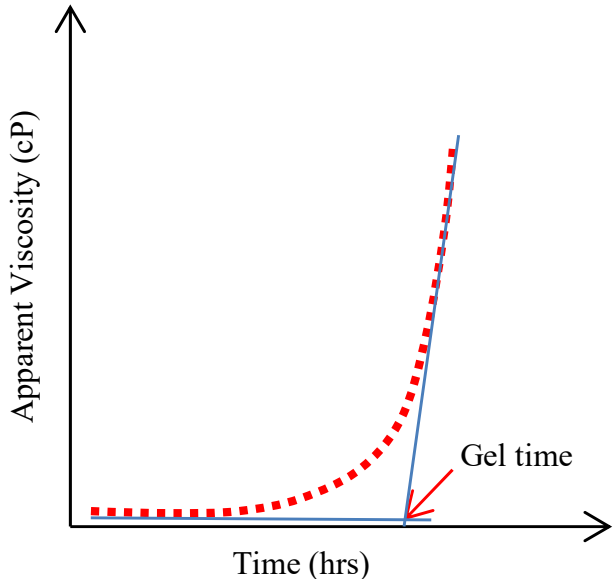

Figure 1.6 Gel time determination

Gel Strength:

Gel strength is a variable related to process performance, but it is not defined precisely. Methods of measurement based on the use of shear viscosity, dynamic viscosity, a penetrometer device, gel breakdown pressure, or visually observed flow characteristics have been proposed (Green and Willhite, 1998).

The term “gel strength” is being used as a general term to include both the gel’s yield pressure and its apparent viscosity as a function of pressure and its apparent viscosity as a function of shear rate (Meister, 1985).

Another approach is to monitor the value of storage modulus, G’. Lukach and Sun (1986) found that a strong gel has a storage modulus of approximately 100 dynes/cm^2 and a weak gel refers to a storage modulus of approximately 10 dynes/cm^2. A strong gel is a better candidate compared to weak gel for plugging a large fracture.

The simple bottle test can also be used in which the gel solution is observed when a bottle holding a gel is tilted in a specified way or inverted. The gel strength code of bottle test was provided by Sydansk & Argabright (1988) as illustrated in **Table 1.4** and **Figure 1.7**.

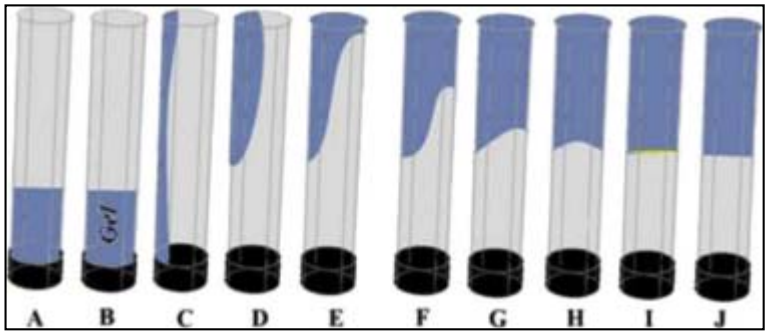

Figure 1.7 Gel strength determination (Sydansk and Argabright, 1988)

Table 1.4 Bottle test-gel strength code (Sydansk and Argabright, 1988)

Type	Definition
“A”	No detectable gel formed.
“B”	Highly flowing gel.
“C”	Flowing gel.
“D”	Moderate flowing gel.
“E”	Barely flowing gel.
“F”	Highly deformable non-flowing gel.
“G”	Moderately deformable non-flowing gel.
“H”	Slightly deformable non-flowing gel.
“I”	Rigid gel.
“J”	Ringing rigid gel.

Gel Stability:

A major cause of gel instability in polymer system is syneresis. Syneresis is defined as shrinkage of the gel by expelling out the liquid from a gel. It appears as a breaking up of the gel. The mechanism of syneresis is thought to be due to an over crosslinking of polymer (Bryant et al., 1996; Green and Willhite, 1998; Stahl and Schulz, 1988).

Syneresis is commonly believed to be incompatible with the application of polymer gels to reduce the permeability of porous media (Bryant et al., 1996).

A simple measurement of gel syneresis is by visual observation. The volume of remaining gel is estimated and divided by the initial volume to give a percent syneresis. By plotting of this percent syneresis versus aging time gives a visual stability curve (Stahl and Schulz, 1988).

Rheological Properties of Gel:

Gel generally exhibits viscous behaviour when it is placed in the porous media for plugging. Thus, the rheological properties of gel help to understand a lot about the gel characteristics and the effects of reservoir condition on it.

Rheological behaviours of fluids divided into Newtonian and non-Newtonian fluid. A Newtonian fluid has a linear relationship between shear stress and shear rate with the constant viscosity (**Eq. 1.6**), whereas non-Newtonian fluid has no linear relationship and viscosity depends on the shear rate. A non-Newtonian behaves as shear shinning (**Figure 1.8**). The viscosity of fluid decreases as the shear rate increases, and as shear thickening (**Eq. 1.7**). The polymer gel is typically non-Newtonian fluid in shear thinning (Green and Willhite, 1998; James Sheng, 2010; Stahl and Schulz, 1988).

$$\tau = \mu\dot{\gamma} \tag{1.6}$$

$$\mu = K\dot{\gamma}^{(n-1)} \tag{1.7}$$

where

τ : shear stress (Pa)

μ: solution viscosity (Pa·s) (1 mPa·s=1 cP or 1000cP=1Pa·s)

$\dot{\gamma}$: shear rate (s^{-1})

K: power law constant (Pa. s^n)

n: power law exponent

n<1 Pseudoplastic or shear-thinning fluid

n=1 Newtonian fluid

n>1: Dilatant or shear-thickening fluid

The data can be correlated as function of polymer concentration in Eq. 1.7, $n=1/(1+0.002C^{0.943})$, $K=5.435+2.362\times10^{-5}C^{2.286}$ (Green and Willhite, 1998).

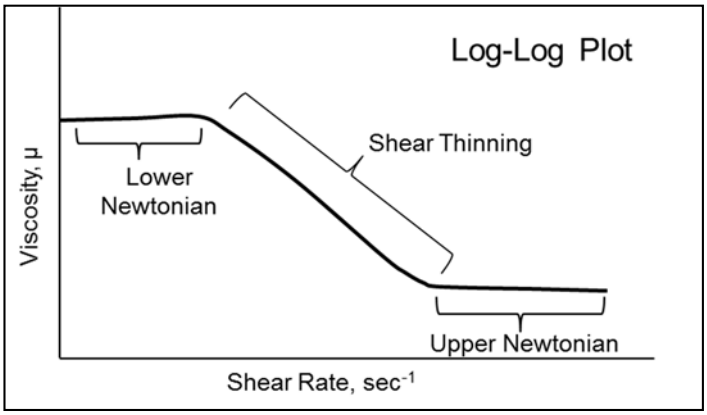

Figure 1.8 Rheology of a shear-thinning fluid (Green and Willhite, 1998)

The rheological behaviour of polymer gel is affected by shear rate, polymer concentration, temperature, salinity and divalent ion (Ca^{2+}, Ma^{2+}) (Green and Willhite, 1998; James Sheng, 2010).

Affecting Factors on Gel Properties:

There are many variables that can affect on the gelation time, gel strength and gel stability. Those major effects are chemical concentration/properties, temperature, salinity, divalent ion, pH and shear rate (Green and Willhite, 1998; James Sheng, 2010; Stahl and Schulz, 1988). Stahl & Schulz (1988) found that the high molecular weight polymers have faster gel times and higher gel strengths than low molecular weight polymer.

- ***Effects of chemical concentration*:** gel strength increases with an increase in the polymer concentration. However, syneresis is promoted as well at high concentration.
- ***Effects of salinity***: increasing the salinity of the solution reduces the gel time and decrease the gel strength in some cases. Sydansk & Argabright (1988) reported that the gel time of polyacrylamide is faster with increasing salinity at low salt concentration, but it is slower with increasing salinity at high salt concentration. Salinity also affects gel stability, and gels syneresis can occur at very low and very high salt concentration (Green and Willhite, 1998).
- ***Effects of shear rate***: normally the apparent viscosity decreases as the shear rate increases, hence the shear thinning of rheological characteristics is due to the reduction of internal friction of molecules (Green and Willhite, 1998).

- ***Effects of temperature*:** the redox-reaction process relies on the temperature. Normally gel time is shorter at high temperature. The increasing in temperature promoted the intensive syneresis (Green and Willhite, 1998).

- **Core Testing**

The second evaluation program tests the performance of gels under simulated flow conditions in reservoir core samples. In this section, the core sample must be an actual reservoir core sample or generic rock like Berea sandstone. There are two types of apparatus for the routine core testing (Stahl and Schulz, 1988).

- A core screening panel is designed for the rapid evaluation of gel system in the core. This step, only the total pressure drop across the core is measured.
- The second core test apparatus is designed for more detailed tests, such as injectivity/retention tests, gel placement evaluation, and gel stability tests under flowing condition.

1.2.3 Alkaline Flooding Using S-MS Solution

Sodium-metasilicate, hereinafter S-MS, is commonly used as powder detergents and industrial applications (PQ Corporation, 2015; SILMACO, 2016). They contain an optimum portion of alkali and soluble silica, which made S-MS a suitable gel precursor (Hamouda and Amiri, 2014; McDonald, 2012; Vinot et al., 1989). Injected in an oil-bearing matrix, S-MS solution, whose viscosity is similar to that of water; is suitable for formation areas located at long distance from the injector (Lakatos et al., 2009; Skrettingland et al., 2012). However, the solution should be thermally stable in high temperature reservoirs, and its gelation time also controllable at the same conditions (Amiri et al., 2014). Furthermore, S-MS is inorganic and do not present hazards such as low flash or flammability. Because of the alkali content that alter the interfacial tension of the trapped oil, S-MS solution has a long history as an alkaline flooding agent for light/medium/heavy oil formations (Chang and Wasan, 1980; James Sheng, 2010; Krumrine et al., 1985; Larrondo and Urness, 1985; Martin and Oxley, 1985).

Larrondo et al. (1985) conducted the experiment on the effect of salinity (0.075-8.075 wt% of NaCl) on the IFT of wellhead oil and sodium metasilicate solutions (0.1-2 wt%). They reported that at the alkali concentrations greater than 1 wt% of S-MS solutions showed the minimum IFT value in orthosillicate solution and sodium hydroxide solutions. As S-MS concentration increased, IFT value tended to decrease, but as the sodium

chloride concentration, the IFT value also decreased and slightly increased at the high salinity case (**Figure 1.9**).

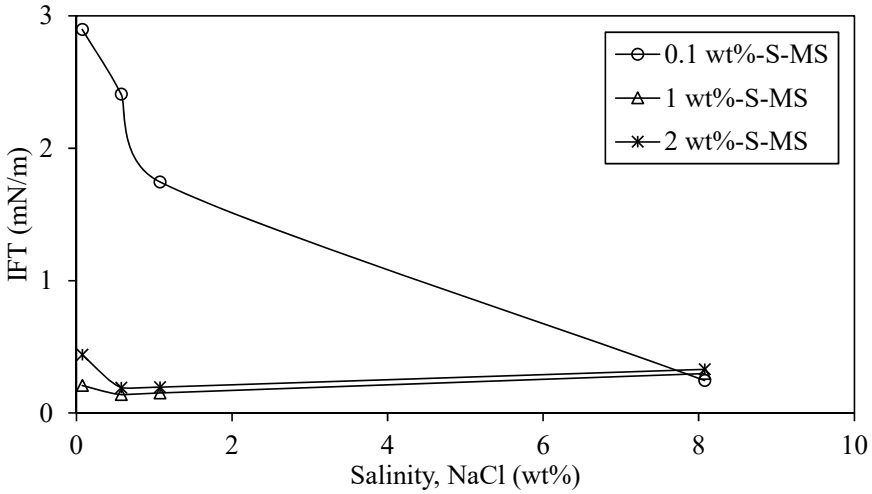

Figure 1.9 Effect of S-MS solution and salinity on the IFT (Larrondo and Urness, 1985)

The W/O emulsification was usually observed in the alkaline floodings. The role of forming W/O emulsification was discussed by Pei et al. (2013).

1.2.4 Effect of Salinity on Microemulsion Formed from Oil and S-MS Solution

The pipette test was undertaken to investigate phase behaviour. As shown in **Figure 1.10**, the microemulsion types were classified to Winsor I (Lower-phase microemulsion), Winsor II (Middle-phase microemulsion) and Winsor III (Upper-phase microemulsion). Sheng (2011) used the term O/W, bicontinous (O/W-W/O), and W/O microemulsions to describe water-external (Winter I), bicontinuous (Winter III), and oil-external (Winsor II). Generally, W/O emulsion is generated at low water/oil ratio (WOR), whereas O/W emulsion are formed at higher WOR.

The effect of salinity in the S-MS solution was also investigated by observing the phase behaviour of the microemulsion. In this study, it was focused to find the optimal salinity to form stable microemulsion which shows type Winsor III and low IFT ($<10^{-3}$ $mN.m^{-1}$) (James J. Sheng, 2011).

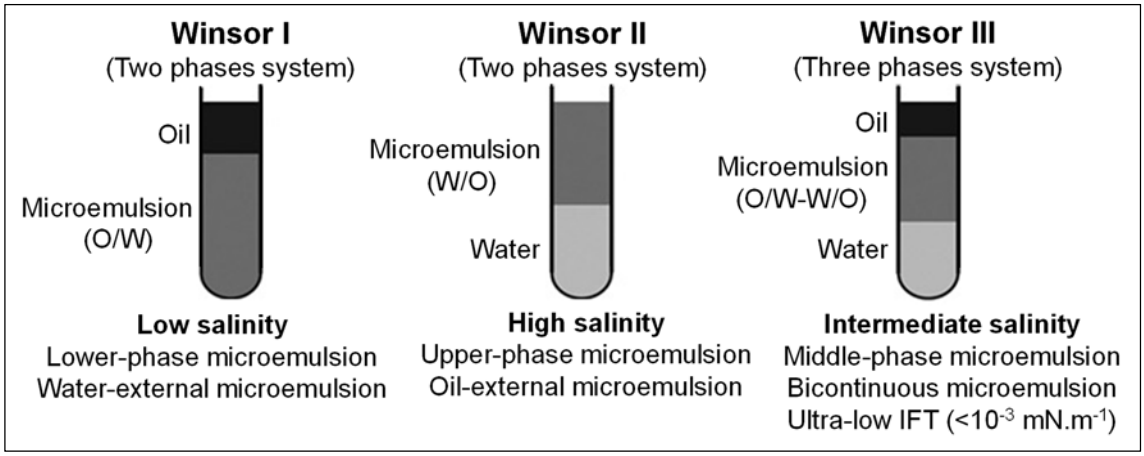

Figure 1.10 Three types of phase behavior system and the effect of salinity on phase behavior (Sheng, 2011)

By the reaction of alkaline solution with crude oil in a reservoir, the *in-situ* generated soaps (surfactants) facilitate the formation of both O/W and W/O emulsions with the help of low IFT, and the mobility ration improves displacing and displaced fluids. The flow of these two types of microemulsion induces the mechanism to enhance oil recovery by alkaline flooding (Ding et al., 2010; Green and Willhite, 1998; Sheng, 2011; Pei et al., 2013). In the low salinity solution, oil-in-water (O/W) emulsion was formed with the oil droplet particles smaller diameters than the pore throat size owing the low IFT by the alkaline flooding. Meanwhile in the high salinity, water-in-oil (W/O) emulsion was generated by *in-situ* formed soap in the reservoir. The water droplets in W/O emulsion break easily and coalesce to become larger particles during moving through the pores, so the oil mobility was improved by reducing apparent viscosity with decreasing water droplets (Green and Willhite, 1998; Sheng, 2011; Pei et al., 2013).

The effect of temperature on the stability of microemulsion was reported by Bera et al, (2012). They showed that the type of Winsor I of emulsion phase behaviour was observed at low salinity and low temperature, while the phase changes to the type of Winsor III as the temperature increases above 42ºC, and the type of Winsor II in the system at the high salinity and low temperature. As temperature increases, the type of Winsor II start to generate. At moderate salinity near the optimal salinity, the middle phase microemulsion is very stable compared to other salinities. However, the volume of middle phase microemulsion decreases with increasing of temperature. But the change is no so high due to the high stability of microemulsion around the optimal salinity (Bera et al., 2012).

Using S-MS for conformance has been extensively studied. Taylor and Nasr-El-Din (2003a) stated that the silica gel formed when the S-MS solution is acidified to a pH value lesser than 10, however the challenge therein reported was controlling the gelation time

(McDonald, 2012; Kevin C. Taylor and Nasr-El-Din, 2003). In the field treatment, S-MS can form silicate gels using precursors or activators such as organic acid, urea, multivalent cation (Krumrine and Boyce, 1985; Nasr-El-Din and Taylor, 2005). Aforementioned precursors intend to lower the acidity of the solution to promote the formation of gel. Young and Blankenhorn, 1972 reviewed potential gelling activators among CO_2, hydrogen chloride (HCl) and amides. CO_2 is easy to handle and to adjust, because it can be injected into a well and spread in a reservoir due to its higher relative permeability compared to that of liquid fluids. Moreover, using captured CO_2 as precursor is also an alternative approach for carbon sequestration.

On the basis of S-MS solution features discussed above, it is rational to think that it can be used for a dual purpose, including blocking channelling passes in the reservoir and chemical agent for alkaline flooding (**Figure 1.11**).

Both functions could subsequently enhance oil recovery given that S-MS solution remaining after alkaline flooding could become the starting material for the channel plugging. In theory, S-MS solution is injected as the alkaline flooding agent into the formation. The oil is produced from high permeable zones. At the water breakthrough, CO_2 is injected and the reservoir is shut-in. An *in-situ* gelation is then expected, which would plug short-cut passes, reducing thereby the permeability. As a result, the sweep efficiency, the oil recovery, is improved. It is worth pointing that this production scheme would be also altered the parameters, which influence the oil recovery by alkaline flooding (hard formation brine) or the gel formation (hard formation brine/high temperature) (Kristensen et al., 1995; Mayer et al., 1983; Skrettingland et al., 2014).

Therefore, the scope of this work, which is a preliminary study, aims to prepare, to characterize and to evaluate the potential of the *in-situ* gel as plugging/binding agent in heterogeneous reservoirs. An aqueous S-MS solution is used as starting material and CO_2 as precursor. To unveil the mechanisms of gel formation, both physical and chemical analyses were considered. The permeability tests were further performed to validate the *in-situ* gel formation in porous media. The effect of *in-situ* gel performance in the heterogeneous reservoir for enhanced oil recovery was investigated and evaluated through the heterogeneous Berea sandstone core flooding.

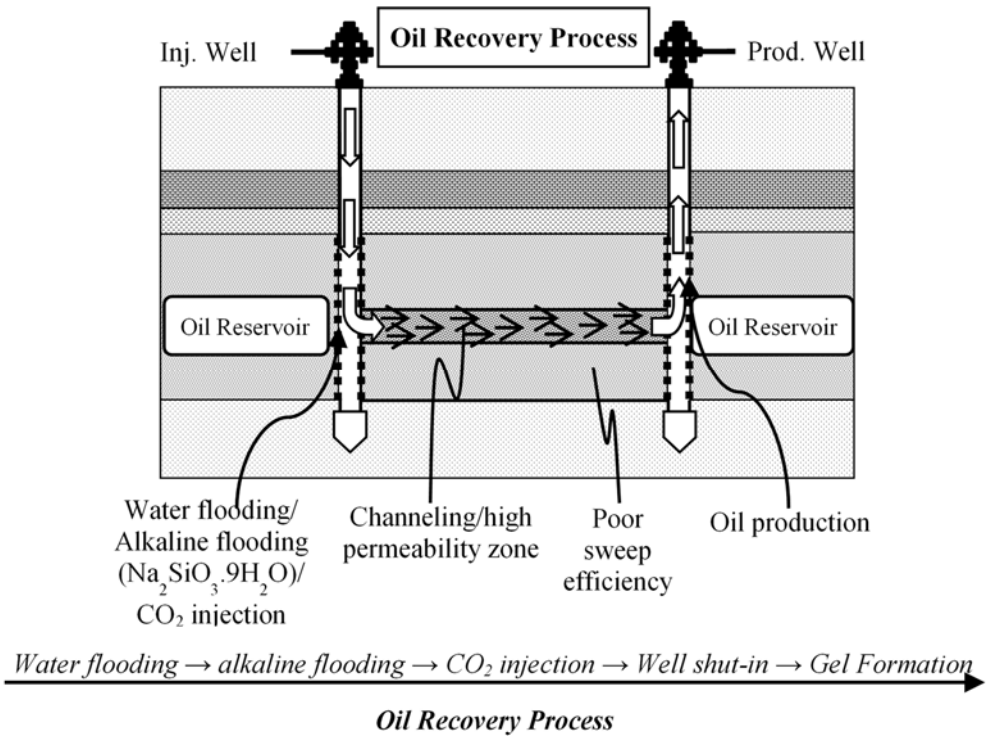

Figure 1.11 Conceptual oil recovery process in heterogeneous reservoir

1.3 Objectives

This research principally aims to characterize and evaluate the potential of the *in-situ* gel as blocking agent in heterogeneous reservoirs for enhanced oil recovery (EOR). The details of each objective are listed as follows:

- To screen, characterize and evaluate a potential of the *in-situ* gel as blocking agent in high permeability zones forming by the reaction between the sodium metasilicate solution as gelling solution, and dissolved CO_2 gas as precursor.
- To investigate the effect of sodium metasilicate solution on IFT reduction, wettability alteration, and emulsification as alkaline flooding agent for improving the oil recovery in the high permeability zones.
- To investigate the effects of *in-situ* gel as blocking agent in heterogeneous reservoir for enhanced oil recovery by using the heterogeneous Berea sandstone core.

1.4 Outline of Dissertation

The dissertation is compiled of six chapters according to the research objectives. The brief explanation of each chapter is in following:

Chapter 1 introduces about the oil recovery mechanism from primary to tertiary process, the approach of enhanced oil recovery method, its challenges in heterogeneous reservoir,

and the objectives of this present research. The approach of enhanced oil recovery method was highlighted comprehensively in this chapter for both megascopic and microscopic oil displacement efficiency.

Chapter 2 overviews the experimental research process with an overview of qualitative and quantitative methods, data collection, recording and analysis. It also presents the materials, such as crude oil and chemicals, used in gel formation coreflooding experiments and interfacial tension measurement (IFT) between oil and the water solutions including the experimental setups measurement instrument. Furthermore, Raman spectroscopy and scanning electron microscopy/energy dispersive x-ray (SEM-EDS) spectroscopy that were used to analyse molecular compounds and chemical characterization of the gel formed in the experiments is explained. The sandstone core was used to measure the threshold pressure gradient (TPG) after *in-situ* forming SC-gel in it. The cylindrical heterogeneous core (43.4 mm in diameter and 72.2 mm in length) was constructed by combining two semi-cylindrical Berea sandstone cores with different permeability (300 and 50 mD). It was used for coreflooding test after injecting saline water and the Japanese light crude oil (JLO-I) into the core to evaluate the blocking effect in the heterogeneous reservoir.

Chapter 3 explains about the *in-situ* gel screening, characterization and evaluation as blocking performance in high permeability zones by using the sodium metasilicate ($Na_2SiO_3 \cdot 9H_2O$; S-MS) as the gelling solution and dissolved CO_2 gas as a precursor. The experiments were carried out to characterize and evaluate the gel system based on the chemical and physical analysis by changing of sodium metasilicate solutions (1-10 wt%), CO_2 gas pressure (subcritical to supercritical condition), temperature (25-80ºC), salinities (NaCl, 0.1-10 wt%) and divalent ion (Ca^{2+}, 10-10000 ppm). Raman and scanning electron microscopy/energy dispersive x-ray (SEM-EDS) spectroscopy were used to determine the surface morphology, elemental composition, and structure of the gels. The physical characterization method was focused on the gel time, gel strength, and thermal stability of the gel. Firstly, the in-situ gel samples were prepared and formed in the high pressure cell by injecting the rang of CO_2 gas pressure (2-5.5 MPa) into 45 mL of different S-MS solution concentrations (1-10 wt%) at temperature of 25°C. Gel samples were taken in every shut-in time for the measurement of physical properties (pH, density), apparent viscosity (Brookfield DV-I Prime), flowing behaviour of gel (gel strength code), and the volume change of the gel under various temperature of 25°C, 55°C and 80°C (thermal stability of the gel). The baseline concentration of S-MS solution was selected for the

detailed investigation of the effect of supercritical CO_2 injection, salinity (NaCl), divalent ion (Ca^2+), and crude oil interaction with the gel property, as well as the gel behaviour in the porous media. The effect of *in-situ* gel as blocking performance was evaluated by the measurement of air flowing permeability and threshold pressure gradient (TPG) using Berea sandstone saturated with the *in-situ* gel.

Chapter 4 evaluates the effect of *in-situ* SC-gel as blocking performance in heterogeneous reservoir for enhanced oil recovery. The effect of on IFT reduction, wettability alteration and emulsification, as alkaline flooding agent for improving the residual oil recovery remaining in the high permeability zone was also investigated in this chapter. IFT and contact angle measurement were carried out by using a surface tension-meter (DropMaster DMS-401) for S-MS solution (0.01-0.2 wt%) and Japanese light/heavy crude oil. The phase behaviour test was conducted for emulsification investigation, including the phase system, emulsion type and stability of emulsion by using S-MS solutions (0.5-2 wt%), Japanese crude oil, and different salinities (0.1-10 wt% of NaCl), under the temperature of 55ºC. S-MS solution has two functions as an alkaline flooding agent and base fluid to form SC-gel with CO_2 gas as a blocking agent. Two half Berea sandstone cores fully saturated by Japanese light oil (JLO) was combined together to make a cylindrical heterogeneous sandstone core consisting of two different permeability zones and a thin fracture at the contacting interface of both half core. This cylindrical heterogeneous sandstone core was used for the coreflooding test that was carried out to evaluate the effect of *in-situ* formed SC-gel formation as blocking agent in the high permeability zones to recover oil from low permeability zone. After mounting the core into the core holder, the heterogeneous core was prepared by injecting 1PV oil (JLO) at 0.1 mL/min to be oil saturation is 1 including the fracture zone. The fluid injection scheme in the coreflooding test was designed as follows: (1) water flooding (2 wt% of NaCl concentration) at the same flow rate until produced oil became 0 (for around 6.5 PV), (2) alkaline flooding by injecting S-MS1wt%-solution at 0.1 mL/min for 0.5 PV, (3) injecting S-MS 5wt%-solution at the same flow rate for 0.3 PV as the base solution for in-situ formation of SC-gel, (4) CO_2 gas injection at 2 MPa during 10s from the cell (75 mL), (5) shut-in the core for *in-situ* gel formation during 2 days, (6) Second water flooding at 0.1 mL/min for 2 PV to produce extra oil from the core. Therefore, the effect of *in-situ* formed gel as blocking agent on the enhanced oil production process was investigated. During the coreflooding test, pH, pressure difference, oil and water production volume were monitored since from early stage of water flooding.

Chapter 2: Experimental Research Process

2.1 Introduction

Many researches have been conducted to study about the conformance the water-shut off by using the polymer and silica based gel in this decade. Those studies provided a lot of concepts for gelation characterization and evaluation.

Gelation time, gel strength, and long term gel stability are the gel properties that describe the gelation (Green and Willhite, 1998). Stahl and Schulz (1988) conducted the laboratory evaluation of crosslinked polymer gel for water diversion and gave two methods for gel characterization and evaluation. First, the beaker tests are conducted over a range of conditions to determine the gel time, gel strength, and gel stability, which are related to the placement, the magnitude of permeability reduction and the long life of gel treatment. At this point, the most favourable system is selected for the further testing. Second the gel evaluation is continued with more complex flow tests in reservoir core samples. The core tests are the best indicators available under the potential reservoir performance with the prior selected gel system and are used to make the final selection of gel system for field testing. Green and Willhite (1998) also agreed with this concept.

The beaker test is used to determine the gel time, gel strength and gel stability. Stahl & Schulz (1988) suggested to make a simple screening test and to consider about the time consuming due to the complex process of gelation affected by many variables.

2.2 Materials and Methods of Gel Characterization and Evaluation of Present Research

2.2.1 Materials

A various concentrations of S-MS solution (1-10 wt%) was used as the starting material reacting with the dissolved CO_2 (99.9 % of purity) as a precursor for the in-situ gel formation. A lyophilized powder of sodium metasillicate nonahydrate ($Na_2SiO_3.9H_2O$, S-MS), supplied by Junsei Chemicals (Japan), was diluted with the distilled water for the solution preparation. To investigate the effects of salinity and the water hardness on the gel formation, different solutions of sodium chloride (0.1-10 wt% of NaCl) and calcium chloride (10-10000 ppm of $CaCl_2$) were used. Both salts were purchased from Junsei Chemicals (Japan) and used as received.

Japanese light crude oil (JLO-I) was taken as a candidate oil for the investigation of the effect of crude oil interaction on the gel behavior. JLO-I has a density of 0.892 g/cm^3, 27 API gravity, and a viscosity of 15.45 mPa·s (or cP). All properties of JLO were measured at room temperature of 25ºC.

2.2.2 Gel Formation

Six solutions in S-MS concentration ranging from 1 to 10 wt% were prepared using distilled water. The physio-chemical properties of each solution including pH, density and viscosity were measured using pH meter (AS800), pycnometer and viscometer (Brookfield DV-I Prime) at room temperature (25 ºC). Gel formation was conducted at 25 ºC using 45 ml of S-MS solution (1-10 wt%) with various shut-in times (up to 6 h) and CO_2 pressures (2.0, 4.0 and 5.5 MPa) in a high pressure cell (**Figure 2.1)**.

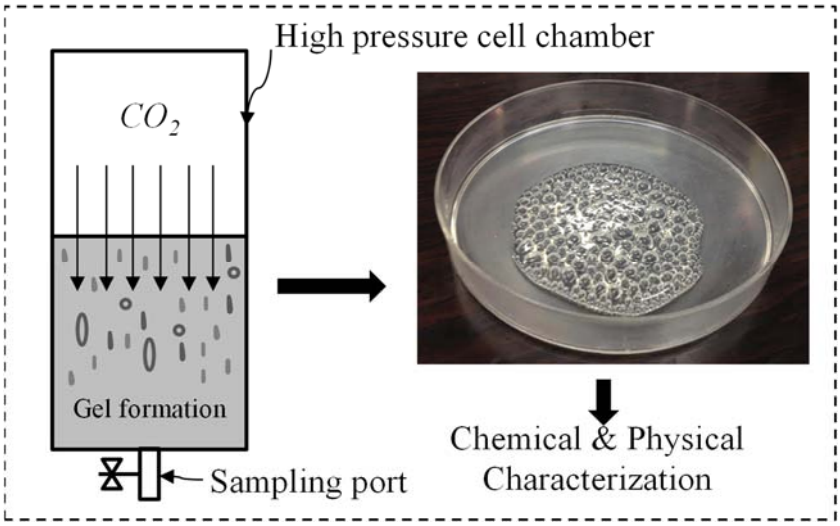

Figure 2.1 In-situ gel formation as per conducted in this study

The gel sample formed in the cell at each shut-in time, CO_2 pressure, and S-MS concentration were taken immediately after depressurization, and the gel properties such as pH, apparent viscosity, and gel strength were measured. Subsequently, beaker testing was carried out to screen and classify the gel samples based on its properties. After screening, the gel samples were also prepared at temperature and pressure conditions of supercritical CO_2.

2.2.3 Chemical Characterization

Scanning electron microscopy/energy dispersive x-ray spectroscopy (SEM-EDS) was used to investigate the surface morphology of the gels and determine the elemental composition of the gels. Raman spectroscopy was used to confirm the chemical structure of the gel formed.

Prior to analysis, the gel samples were dried at 110ºC for 24 h. SEM images were taken using a low vacuum high sensitive scanning electron microscope (Hitachi, SU 3500). Raman spectra were obtained by microscopic laser Raman spectroscopy (ARAMIS, Aramis Horiba, Japan) at 532 nm line of an Ar laser.

2.2.4 Physical Characterization

Gel characterization consisting of gel viscosity, gelation time, gel strength and gel stability was conducted by changing the S-MS solution concentration, CO_2 gas pressure, and temperature.

Gel viscosity: The rheological properties were measured using a viscometer (Brookfield Viscometer DV-I) with shear rate from 5 to 100 rpm. The apparent viscosity was then plotted against the elapsed time (viscosity-time curve) for gelation time determination.

Gelation Time: Gelation time, defined as the time at which the apparent viscosity deviated (Green and Willhite, 1998), was determined from the intercept of the extrapolations from the two straight line sections of the viscosity-time curve. Gelation time was determined from the six solutions at which the hardest gels were obtained and the thermal effects on the gel properties were investigated in 25, 40, and 55 ºC. The gelation time of the hardest gel was also evaluated in glass beads (average 1.5 mm in diameter) as porous-media in both subcritical and supercritical CO_2 conditions as shown in **Figure 2.2**.

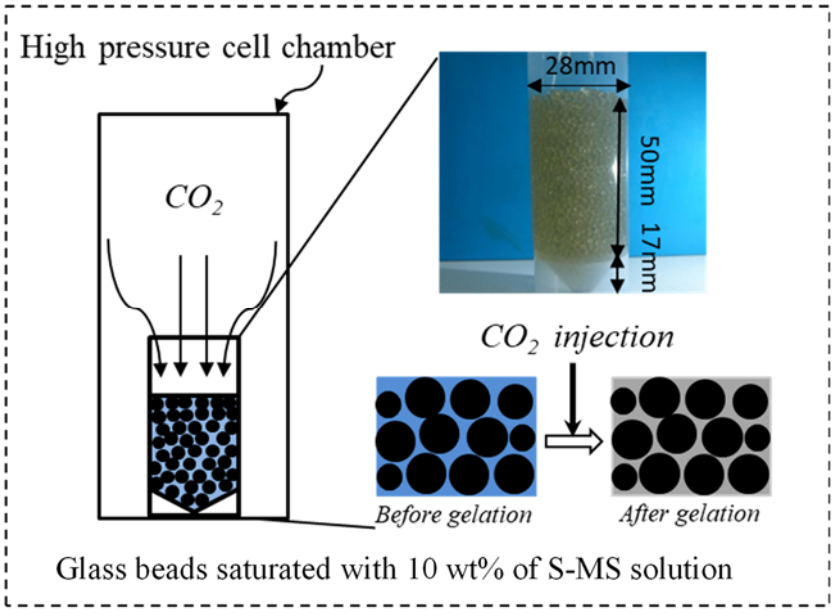

Figure 2.2 Gel formation test in porous media

Gel Strength: The gel strength was evaluated from the gel strength code previously proposed (Sydansk and Argabright, 1988) based on visual observation as shown in **Figure 1.7** and **Table 1.4**.

In the present study, flow behaviour of the gel was observed by flipping 3 mL-gel in a 10 mL-glass tube. To prevent the sampling effect on the gel strength observation and to confirm the preliminary screening result, 15 mL of glass bottle containing 10 mL of S-MS solutions (1-10 wt%) was put into the high pressure cell for forming the *in-situ* gel at designing temperature, CO_2 gas pressure and shut-in time. After gelation, the 15 mL of a glass bottle containing the gel sample was taken out from the high pressure cell and flipped immediately for gel strength observation without sampling. The gel strength was also investigated under the supercritical condition of CO_2 gas (at temperature range of 35-55 ºC under a constant 7.5 MPa of CO_2 gas pressure).

The CO_2 phase behaviour depends on the temperature and pressure. Therefore, gas easily dissolves into the aqueous solution after injection by controlling temperature and pressure in the cell. The gas dissolution can be recognized based on the pressure drop through time and it stops dissolving after reaching at the equilibrium condition. The equilibrium condition means the CO_2 gas saturation and pressure are constant through time (Or et al., 2016). Based on this mechanism, the CO_2 gas solubility and molar number of dissolved CO_2 gas can be measured from:

$$C_s = \frac{n_{dis}}{m_{solution}} \tag{2.1}$$

where

C_s : CO_2 gas solubility in the oil (mmol.g^{-1})

n_{dis}: molar number of dissolved CO_2 gas (mmol)

m_{oil}: mass of solution (g)

$$n_{dis} = \frac{10^3}{M}\left[\frac{V_i}{v(P_i, T_i)} - \frac{V_e}{v(P_e, T_e)}\right] \tag{2.2}$$

where

(P_i, V_i, T_i): initial condition after gas injection

(P_e, V_e, T_e): equilibrium condition after dissolution

n_{dis}: molar number of dissolved gas (mmol)

M: molecular mass of gas (g.mmol^{-1})

v: gas specific-volume ($m^3.kg^{-1}$) (calculated using PROPATH^{TM})

Gel Stability: This study mainly focused on the thermal stability of the gel based on visual observation and measurements of remained ratio of the gel sample under constant temperatures (25 to 80 ºC). The gel stability was then defined as the ratio (gel remaining ratio, %) of the remained gel volume after the elapsed time divided by the total initial volume. The tests were carried out by continuous monitoring of sampled gel (10 mL) in the glass pipette for one month at 25, 55 and 80 ºC.

2.2.5 Evaluation of *In-situ* Gel as a Blocking Agent

The blocking effect of the *in-situ* gel was evaluated by forming the in-situ gel in a Berea sandstone core fully saturated with water, then the measurements of gas permeability and threshold pressure gradient (TPG) were conducted (**Figure 2.3**).

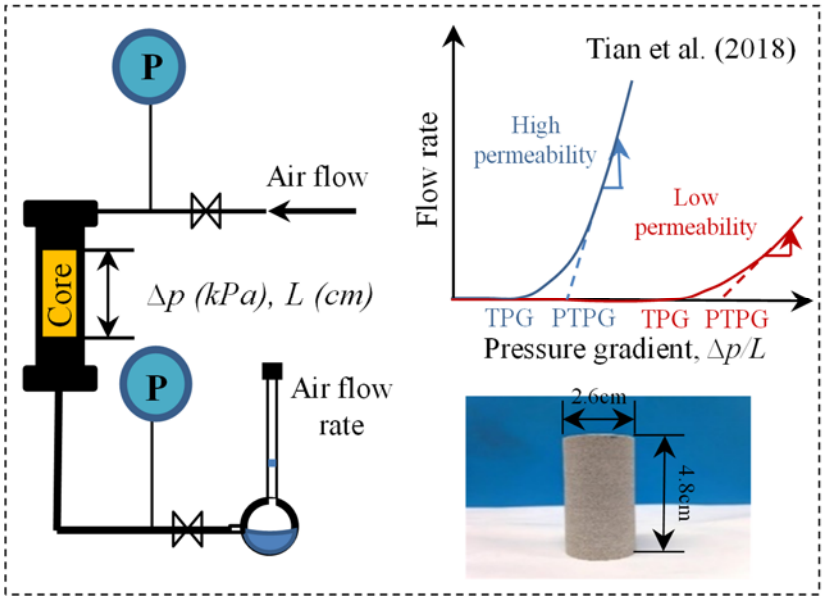

Figure 2.3 Schematic evaluation of gas permeability in Berea sandstone core

10 wt % of S-MS solution was injected into a dried Berea sandstone core sample (length = 4.8 cm, diameter = 2.6 cm, permeability = 0.12 μm^2), then in-situ gel was formed after CO_2 injection. The flow rate and pressure drop were measured to evaluate the permeability of CO_2 gas from the measurement results using air, because this measurement was performed at almost atmospheric pressure so the correction for gas compressibility was not required.

2.3 Materials and Methods of Evaluation of S-MS Solution as Alkaline Flooding Agent

2.3.1 Materials

Sodium metasilicate were used as alkaline agent diluted in the distilled water to form the alkaline solution with the range of concentration from 0.01 to 2 wt%. Sodium metasilicate was supplied from Junsei Chemical (Tokyo, Japan).

Fourteen brine solutions (0.1-10 wt% of NaCl) were prepared primarily from sodium chloride purchased by Junsei Chemical (Tokyo, Japan).

The light /heavy crude oil samples were applied in this experiment. Light crude oil (JLO-II) has 42.03°API and specific density of 0.8151 at 15°C. Heavy crude oil (JHO) sample has 16.6°API and specific density 0.955 at 15°C.

2.3.2 Measurement Methods

Interfacial Tension Measurement:

The interfacial tension measurement was performed based on the pendant drop method by using the tension-meter (DropMaster DMS-401) at the room condition (25°C, atmospheric pressure). IFT was measured at the interface of Japanese light/heavy crude oil and sodium metasiclicate solution (0.01-0.2 wt%). The pendant oil drop was formed at the tip of the stainless steel needle using a special design syringe delivery system. After the oil drop was formed in the cell holder of the sodium metasilicate solution, its digital images were well focused and captured using a CCD camera-based measurement system. IFT was automatically calculated by computer based system and all data was stored in the computer memory (**Figure 2.4**).

Basically, the IFT can be calculated by following equation:

$$\sigma = \frac{\Delta\rho g d_e^2}{H} \tag{2.3}$$

where

σ: interfacial tensing (mN/cm)

$\Delta\rho$: density difference between the two fluids (g/cm^3)

d_e: maximum diameter of the real drop (cm)

g: gravitational constant at the point of measurement (cm/s^2)

H: shape factor (estimated from based on d_s/d_e)

d_s: diameter of the tip of the actual needle in cm.

Finally, the measured IFT was correlated linearly with the varied concentrations of S-MS solution for the critical micelle concentration determination.

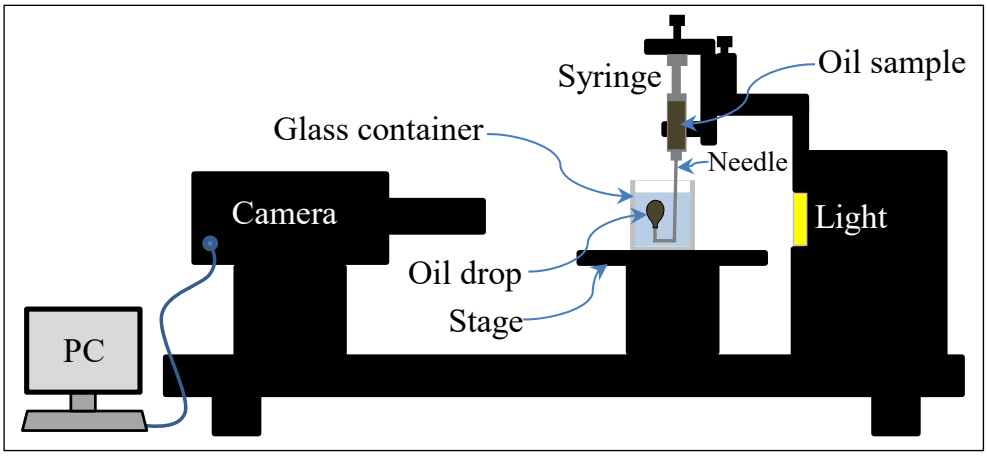

Figure 2.4 Surface tension meter (DropMaster DMS-401)

Contact Angle Measurement:

The contact angle measurement of Japanese crude oils (JLO-II and JHO), glass slide and S-MS solutions (0.01-0.07 wt%) was conducted using the surface tension-meter under the room condition (25°C, atmospheric pressure). The schematic diagram of contact angle measurement is shown in **Figure 2.5**.

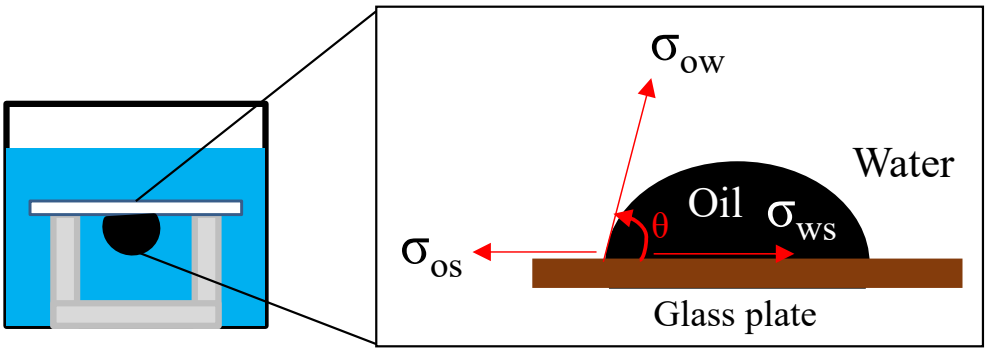

Figure 2.5 Schematic figure of wettability measurement

Emulsification Investigation:

As discussed in section 1.2.3, the phase behaviour of emulsification was classified into Winsor I, II and III based on three-phase fluids system. In this study, the oil particle size distribution of oil/water droplets in the microemulsion types and microemulsion stability versus elapsed time were investigated. The effect of salinity in the S-MS solution was also investigated by observing the phase behaviour of emulsification. In this study, it was focused to find the preferable salinity to form stable microemulsion which shows type Winsor III that is formed in low IFT ($<10^{-3}$ mN.m^{-1}) between S-MS solution and crude oils (James J. Sheng, 2011).

The phase behaviour tests were conducted using an array of 10 mL-glass tubes by mixing different combinations of solution concentrations of S-MS (0.5-1-2 wt%), brine water (0.1-10 wt% of NaCl) and Japanese light/heavy crude oil samples (JLO-II/JHO). For all test, a constant volume ratio of water salinity and oil was equal 1 (WOR=1). The details of experimental procedure were reported by Seng (2011). The glass tubes were thoroughly a mixer (Scientific Industries, Vortex Genie 2) for 2h. All fluids mixtures were then placed in an oven that temperature was kept at 55 ºC. The microemulsion phase behaviour was investigated up to 3 weeks. The microemulsion stability was studied from the time-curve of volumes of oil, solution and microemulsion in the glass tubes. The type and particle size distribution of microemulsion were analysed using the optical microscope.

2.4 Blocking Test of SC-Gel in Enhanced Oil Recovery

2.4.1 Porous Media

The heterogeneous Berea sandstone core was used in this study by combining two half Berea sandstone cores with different porosity and permeability properties (Cores I and II) as shown in **Figure 2.6**. The interface between two half core represents the fracture within the core. The core properties are given in **Table 2.1**.

a) Section view b) Side view c) Fracture view

Figure 2.6 Heterogeneous Berea sandstone core before oil saturation

Table 2.1 Properties of each half Berea sandstone core

Half Berea sandstone core	Length (cm)	Section area (cm^2)	Porosity (%)	K_{gabs} (mD)
Core-I	7.22	7.34	13.17	50
Core-II	7.19	7.61	15.33	500

2.4.2 Fluids and Chemicals

S-MS 1wt%-solution was prepared by diluting the lyophilized powder of sodium metasilicate nonahydrate ($Na_2SiO_3.9H_2O$, S-MS) into the distilled water. S-MS 5wt%-solution was used as the base fluid reacting with CO_2 gas of 99.9% purity to form *in-situ*

SC-gel in the high permeability zone. The formation brine in the core has a salinity of 2 wt% of NaCl concentration. S-MS and NaCl were purchased from Junsei Chemicals (Japan). **Table 2.2** shows the properties of all chemical solutions used in this study.

Table 2.2 Properties of chemical solutions

Chemical solutions	pH	Viscosity (mPa·s)	Density(g/cm^3)
S-MS-1 wt%	12.34	1.123	1.00
S-MS-5 wt%	12.92	1.165	1.01
NaCl-2 wt%	6.87	1.153	1.01

2.4.3 Crude Oil

Japanese light crude oil was (hereinafter coded as JLO-I) selected for oil saturation in the Berea sandstone core. JLO-I has a density of 0.892 g/cm^3, 27 API gravity, and a viscosity of 15.45 mPa·s (or cP). All properties of JLO-I were measured at room temperature (25ºC).

2.4.4 Core Flooding Test System

The evaluation of the potential of in-situ formed SC-gel as blocking performance in heterogeneous reservoir for enhanced oil recovery was conducted through the coreflooding test system using the heterogeneous sandstone core under the room temperature (25 ºC). **Figure 2.7** shows the illustration of the coreflooding system and apparatus using in this study.

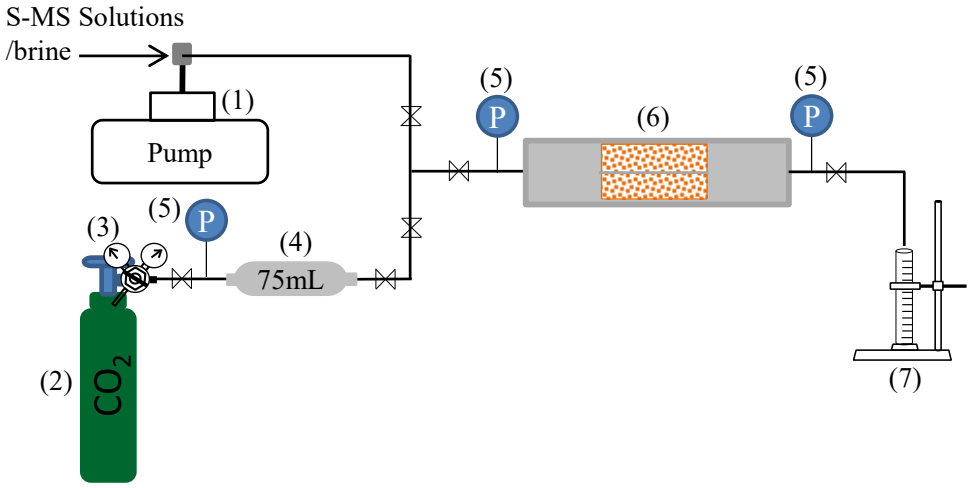

Figure 2.7 Schematic figure of coreflooding apparatus: (1) injection pump, (2) CO_2 gas cylinder, (3) gas regulator, (4) CO_2 storage high pressure cell, (5) pressure indicator, (6) mounted plug, (7) fractionator

2.4.5 Heterogeneous Berea Sandstone Core

After the measurement of porosity of each half Berea sandstone core by gravimetric method saturated by the distilled water, Both half-sandstone core were dried overnight at 105 °C to remove an interstitial water, then the mass of each core was recorded immediately after drying. The dried half cores were saturated with JLO for 48 hours using the air vacuums, then the mass of each half core was weighted again for the calculation of oil volume saturation. Two half-sandstone cores saturated by JLO was combined together to make a cylindrical heterogeneous sandstone core consisting of two different permeability zones and a fracture at the middle interface of both half core (**Figure 2.8**). The combination was well prepared using super sealing tape. Then, the heterogeneous sandstone core was mounted to a Hassler-type core holder, upon which 3 MPa of overburden pressure was applied. JLO was injected at 0.1 mL/min of injection rate for 1 PV to be oil saturation=1.0 including in the fracture zone. The total oil volume within the the cylindrical heterogeneous core was calculated by mass balance in and out, and determined as the initial oil in place (OOIP). The properties of heterogeneous core are shown in **Table 2. 3**.

a) Two half cores after oil saturation using the air vacuum

b) Combination of each half core after oil saturation

Figure 2.8 A Cylindrical heterogeneous Berea sandstone core formed by combining two half core with different permeability after oil saturation

Table 2.3 The properties of heterogeneous Berea sandstone core after combination

	Length (cm)	Section area (cm^2)	Average porosity (%)	Average gas permeability (mD)
Heterogeneous Berea sandstone core	7.19	7.61	15.33	500

2.4.6 Coreflooding Scheme

After the oil saturation, the water flooding (2 wt% of NaCl concentration) was conducted at the same flow rate until no more oil production. 1 wt% of S-M solution was then

injected as alkaline flooding at 0.1 mL/min for 0.5PV. Followed by 5 wt% of S-MS concentration at the same flow rate for 0.3PV for the *in-situ* gel formation. Then CO_2 gas was injected from 75 mL of a high pressure cell under 2 MPa of CO_2 gas pressure immediately (**Figure 2.10**), then the coreflooding system was shut-in for the *in-situ* gel formation up to 2 days at which the pressure drop was recorded. Meanwhile, the pH, pressure drop, oil and water/solution volumes in produced micro-emulsion were also monitored during the core flooding to investigate fluids properties in the core. After 2 days of shut-in time for gel generation, the water flooding was applied again at the same flow rate of 0.1mL/min for 2 PV to investigate the effect of *in-situ* gel as blocking agent in improving the performance of water flooding for enhanced oil recovery. The detailed injection scheme of the coreflooding test system was highlighted in **Table 2.4**.

Table 2.4 The details injection scheme in coreflooding test system

Injection scheme	Injection rate (mL/min)	Injection size (PV)
• Water flooding (Brine-2 wt%)	0.1	Until no more oil production
• Alkaline flooding (S-MS-1 wt%)	0.1	0.5
• Gelling solution injection (S-MS-5 wt%)	0.1	0.3
• CO_2 gas injection	Released from 75 mL of high pressure cell with 2 MPa of CO_2 gas pressure	
• Shut-in	Shut-in for 2 days	
• Water flooding	0.1	2

Chapter 3: *In-situ* Characterization and Evaluation as Blocking Agent

3.1 Introduction

Prevention of channelling flows during enhanced oil recovery targeting heterogeneous or fracture type reservoirs and leakage flows from saline aquifers containing CO_2 remains a challenge. The present study aims at preparing, characterizing and evaluating the potential of *in-situ* gel as plugging/binding agent in heterogeneous reservoirs using the reaction between water solution of sodium metasilicate ($Na_2SiO_3 \cdot 9H_2O$; S-MS) and dissolved carbon dioxide (CO_2). Both Raman and scanning electron microscopy/energy dispersive x-ray (SEM-EDS) spectroscopy have taken place for chemical characterization. Physical characterization of the *in-situ* gel including the gelation time, gel strength and stability, were investigated in respect of S-MS concentration, temperature, salinity (NaCl), divalent ion concentration (calcium, Ca^{2+}) as well as CO_2 injection pressure (subcritical CO_2 and supercritical CO_2 injection). The baseline concentration of S-MS solution will be selected for the next evaluation of blocking performance in the porous media, the glass beads and Berea sandstone core. The gas permeability and threshold pressure gradient were measured using the air flow through the sandstone core saturated with water to investigate the blocking effect of *in-situ* gel. The materials and method of characterization and evaluation of in-situ gel as blocking performance were explained in chapter 2.

3.2 Screening of Baseline Concentration

Monitoring on the increase in acidity in the cell found that the gels are formed subsequent to pH reduction as shown in **Figure 3.1**. This increase in acidity occurred in the primary solution and suggests the threshold concentration.

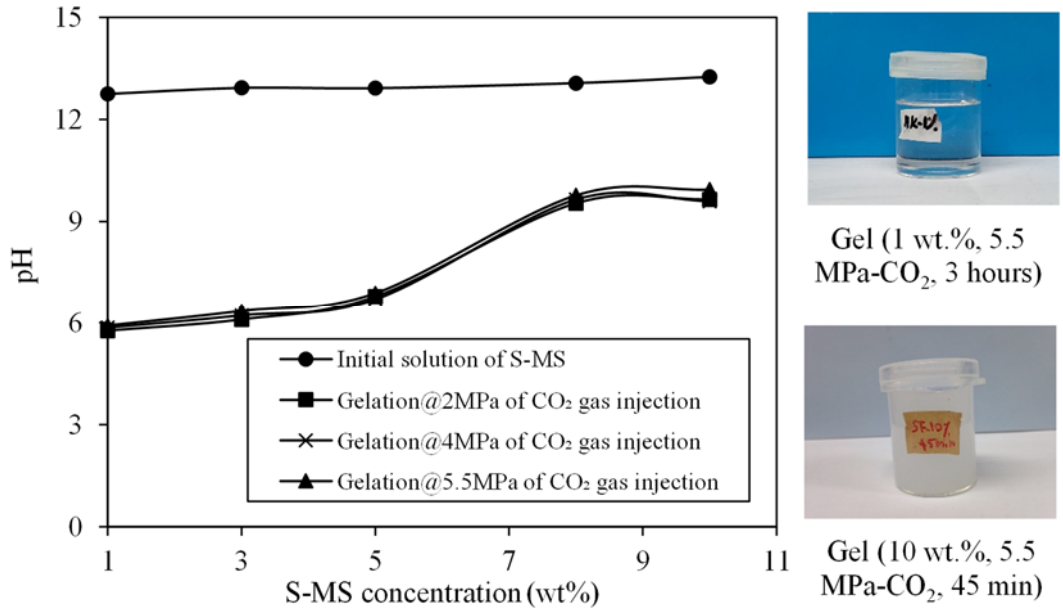

Figure 3.1 pH monitoring during the gel formation

Dissolution of CO_2 decreases the pH from the initial pH of 13 to less than 5.9 regardless of the injection pressure. The acidity within the solution decreased slightly with increasing of S-MS concentration to an order of CO_2 gas injection pressure. Furthermore, the formed gel was weak at a concentration of S-MS solution lower than 5 wt%, at which the pH was around 6, plausibly because of the low concentration of S-MS.

This observation contrasted with the above finding at higher concentration (above 5 wt%) at which the pH ranged from 7 to 9.5. A similar result has been reported by (McDonald, 2012). These results also show that the gel hardness, increased with higher CO_2 injection pressure and S-MS concentration. Therefore, the gels prepared from 5, 8, and 10 wt% of S-MS concentration were selected for further analyses.

3.3 Spectral Characterization of Gel

SEM analysis, which shows the surface morphology of the gel, revealed a soft texture at low S-MS concentration (**Figure. 3.2a**).

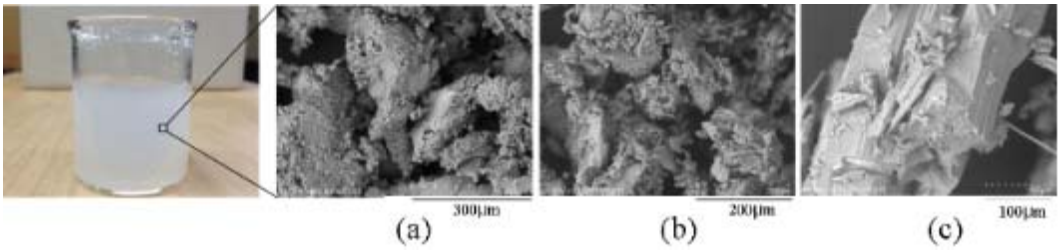

Figure 3.2 SEM images obtained from S-MS solutions and CO_2 at different concentrations; (a) 5 wt%, (b) 8 wt%, and (c) 10 wt%

In contrast, the gel structure appeared both less loose (**Figure 3.2b**) and coarser (**Figure 3.2c**) at higher concentrations, suggesting stronger molecular bonding. Further information was conveyed by the Raman spectra of the samples (**Figure 3.3**).

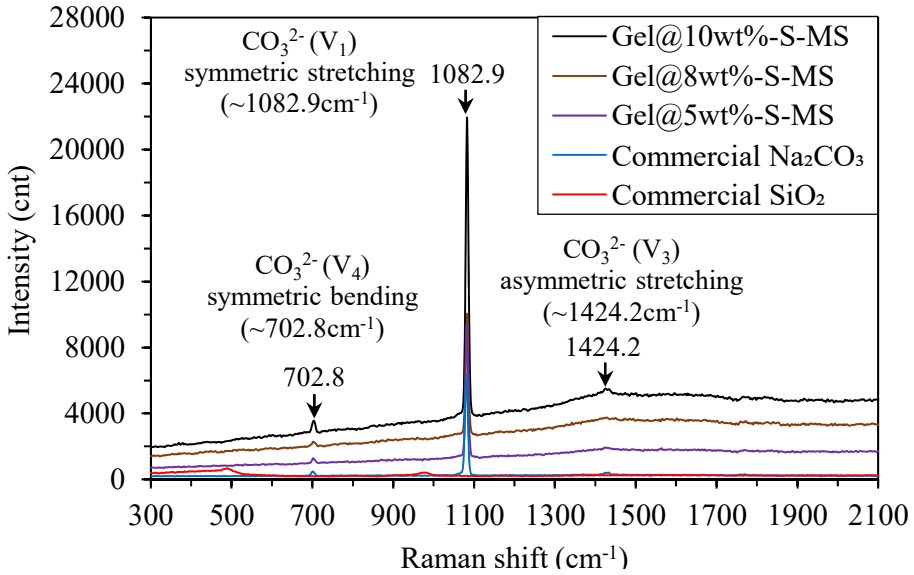

Figure 3.3 Raman spectra of gel samples

Characteristic bands (at 703, 1083 and 1424 cm^{-1}) were observed, all of which were more pronounced with higher concentration of S-MS. The peaks at 703 and 1082 cm^{-1} were associated with the symmetric stretching of carbonate ions (CO_3^{2-}), and the peak at 1424 cm^{-1} was associated with the asymmetric stretching of the carbonate ions (Brooker and Bates, 1971; Vargas Jentzsch et al., 2013). These results suggested that the formed gel was a carbonate rather than siliceous. By comparing the Raman spectra of the formed gels with those of commercial sodium carbonate (Na_2CO_3), it is found that their peaks appeared at the same wavelengths.

Therefore, gel formation was probably triggered by aqueous dissociation of S-MS and formation of silicates as shown in **Eqs. (3.1), (3.2) and (3.3)**,

$$Na_2SiO_3.9H_2O_{(s)} \rightarrow 2Na^+_{(aq)} + SiO^{2-}_{3\,(aq)} + 9H_2O \quad (3.1)$$

$$SiO_3{}^{2-} + H_2O \rightarrow SiO_4^{4-} + 2H^+ \quad (3.2)$$

$$Na_2SiO_3.9H_2O + H_2O \rightarrow (2Na^+ + SiO_4^{4-} + 2H^+ + 9H_2O) \quad (3.3)$$

Eq. (3.3) explains why crystalline silica (SiO_2) was not detected in the Raman spectra. Silica was converted to silicic acid. With the injection of CO_2, the gas dissolves in the aqueous solution to yield carbonates,

$$CO_{2\,(g)} \rightarrow CO_{2\,(aq)} \quad (3.4)$$

$$CO_{2\,(aq)} + H_2O \rightarrow CO_3^{2-} + 2H^+ \quad (3.5)$$

The carbonates are plausibly responsible for increasing of the acidity in the initial S-MS solution (**Figure 3.4**). As the concentration of CO_2 increases within the solution, with higher concentration of CO_3^{2-} ions, the carbonated gel (SC-gel) is formed by the following reaction,

$$(2Na^+ + SiO_4^{2-} + 2H^+ + 9H_2O) + CO_{2\,(aq)} + H_2O \rightarrow (2Na^+, CO_3^{2-}) + (4H^+, SiO_4^{4-}) + 9H_2O \quad (3.6)$$

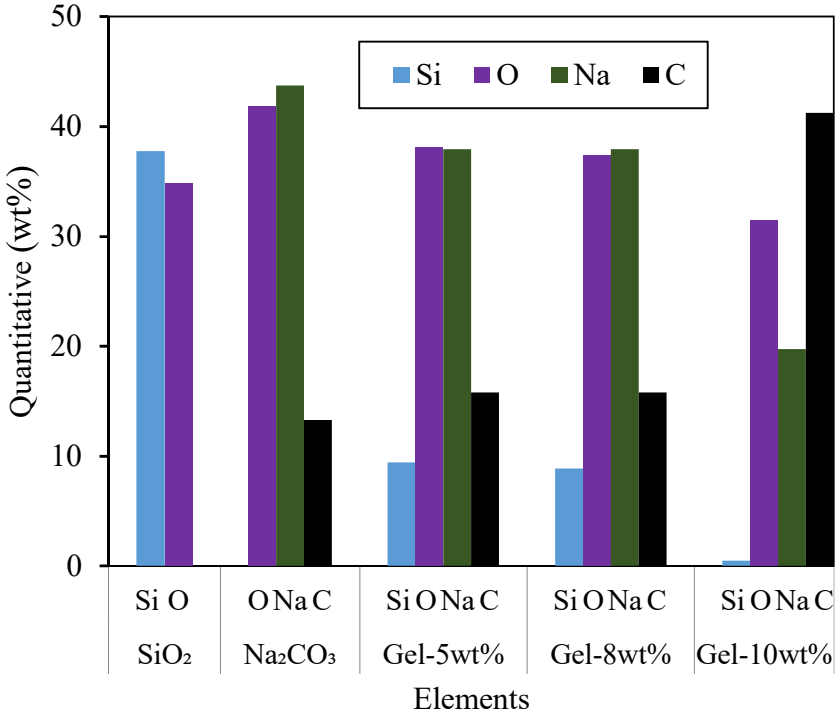

Figure 3.4 Elemental composition of samples prepared at different S-MS concentrations and dissolved CO_2 under pressure of 5.5 MPa

This reaction pathway was confirmed by EDS analysis (**Figure 3.4**) which revealed that SC-gel predominantly contained carbon (C, originating from CO_2), sodium (Na, from S-MS), and oxygen (O from both CO_2 and S-MS). The concentration of silicon (Si) was decreased based on the chemical leads to gel formation (**Eq. (3.3)**), so the decrease in Si is plausibly explained by **Eq. (3.2)**. In fact, it is believed that the formation of silicate (SiO_4^{4-}) is reversible and could be altered by the concentration within the mother liquor (S-MS).

3.4 Physical Properties of Gels

3.4.1 Gel Formation Time

Figure 3.5 shows the curve of viscosity versus time after CO_2 injection for three selected solutions of S-MS.

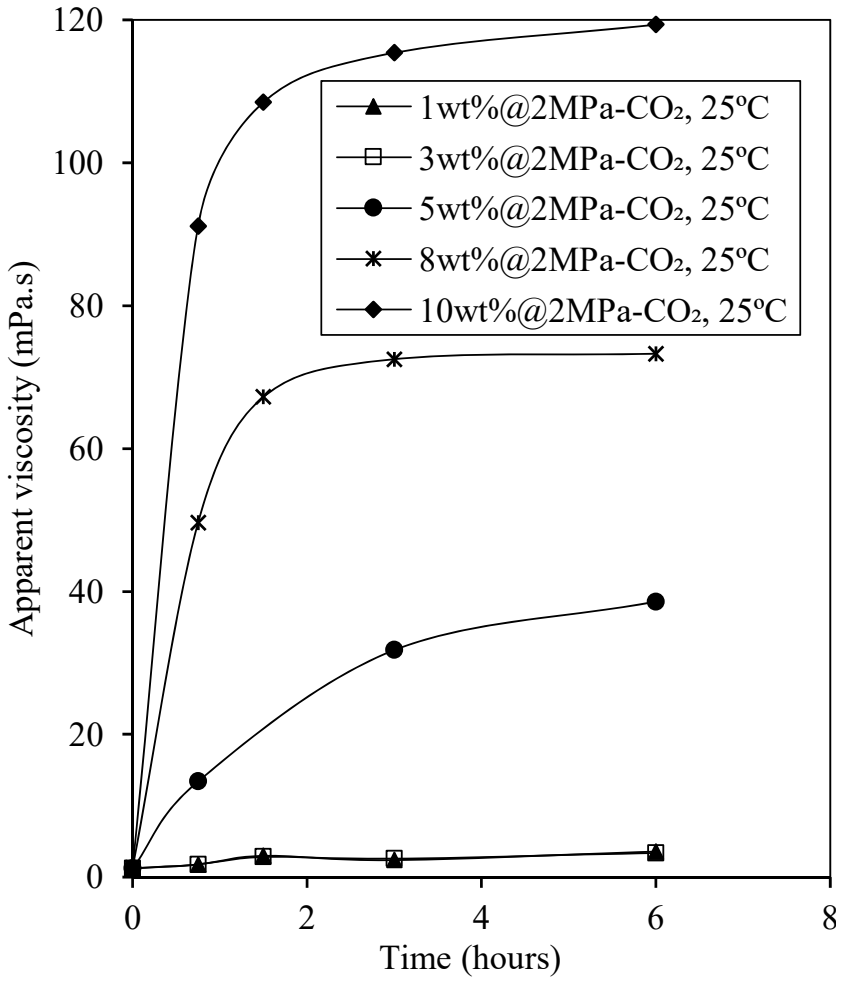

* Gel apparent viscosity measured at the shear rate, 132 s^{-1}

Figure 3.5 Gelation time as function of S-MS concentrations

Gelation time at constant CO_2 gas pressure of 2 MPa was 1 to 4 h depends on the initial concentration of S-MS. Longer gelation time was required for lower concentrations of S-MS (≤5 wt%) because of the lower reaction rate. Therefore, gelation time decreased at higher concentration. On the other hand, the SC-gel became more viscous at higher concentration of S-MS solution. For example, the gel viscosity formed by 5 and 10 wt% of S-MS solution was approximately 40 and 180 mPa·s (or cP), respectively (**Figure 3.5**).

Increasing the temperature from 25 to 55 ºC each, at 10 wt% of S-MS solution under 5.5 MPa of CO_2 injection pressure, revealed the delay in gelation time up to 1 day at 40 and 55 ºC whereas the gelation time at 25 ºC is around 1 h with an abrupt decrease of apparent viscosity (**Figure 3.6**).

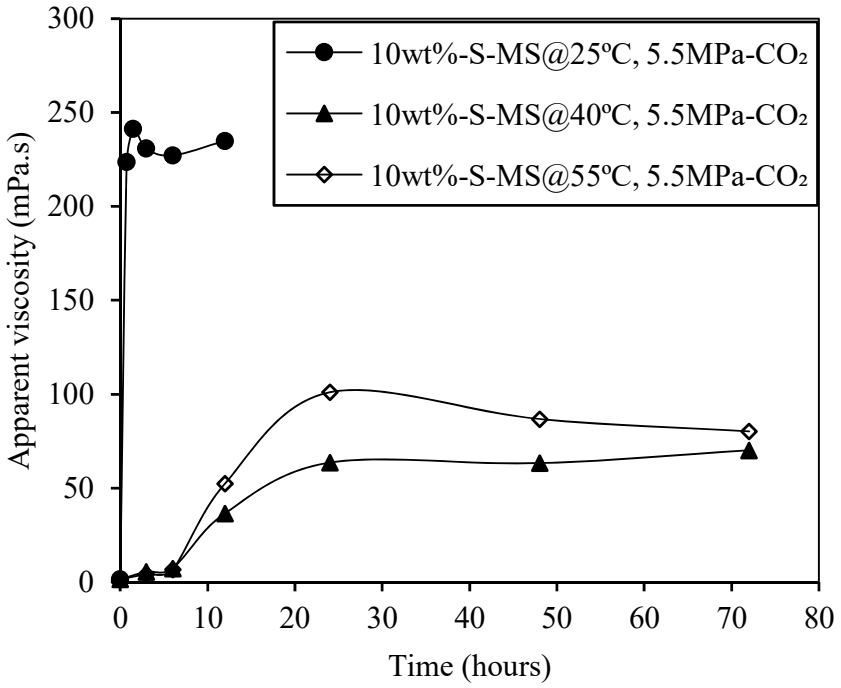

* Gel apparent viscosity measured at the shear rate, 132 s^{-1}

Figure 3.6 Effect of temperature on gelation time and gel strength

This result contrasted with previous findings that higher temperature resulted in a significant decrease in the gelation time (Green and Willhite, 1998; Nasr-El-Din and Taylor, 2005). These studies also found a different type of gel is formed. CO_2 solubility is normally decreases at higher temperature (Mosavat et al., 2014). The CO_2 solubility decreases with lower concentration of CO_3^{2-} ions, so the SC-gel formation time becomes longer (**Eqs. (4), (5), (6)**). The delay in gelation time will promote the gel formation and gel replacement with formation water at longer distances from the injector in a deeper zone with high permeability. Nevertheless, both gelation time and apparent viscosity are sensitive to temperature. Therefore, reservoir temperature will be an important operation parameter for the application of *in-situ* gel formation.

Gelation time was also measured in the porous media consisting of glass beads 1-2 mm (average 1.5 mm) in diameter and saturated with 5 and 10 wt% of S-MS solution at room temperature of 25 ºC. CO_2 gas was injected and the pressure within the cell was maintained at 5.5 MPa and under the supercritical CO_2 condition at 35 ºC, 7.5 MPa of CO_2 gas pressure (**Figure 3.7**).

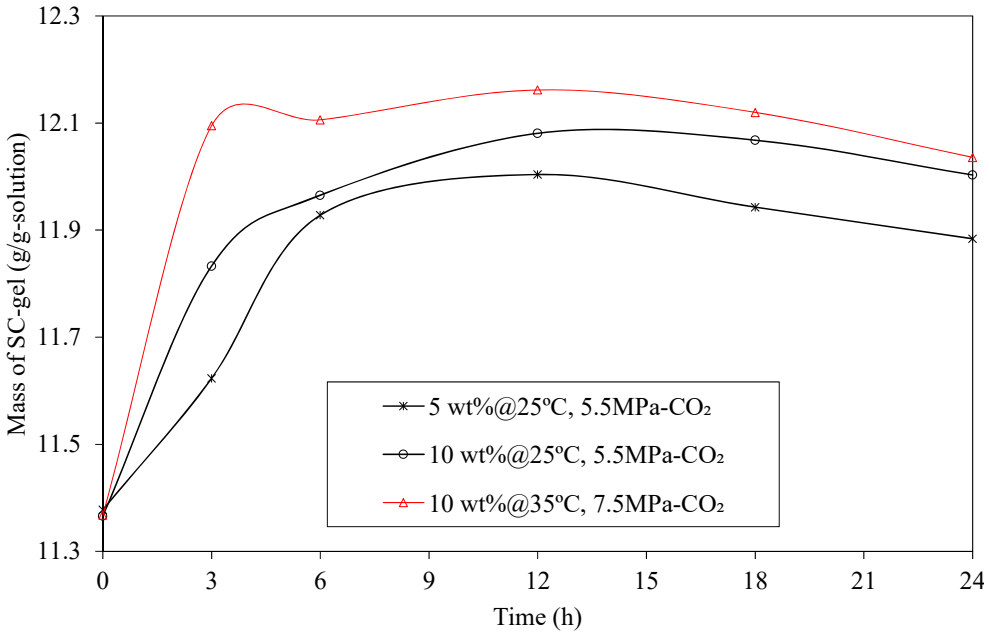

Figure 3.7 Mass of in-situ gel (g/g-solution) formed in porous media consisting of glass-beads

The SC-gel was generated in the pore spaces between grains and bonded the glass beads together using both concentrations (5 and 10 wt%) of S-MS (**Figure 3.8**). As the SC-gel was formed, the color of solution became milky. The gelation time was 12 h, much longer than that of the solution only, because of the limited CO_2 diffusion rate in the porous media.

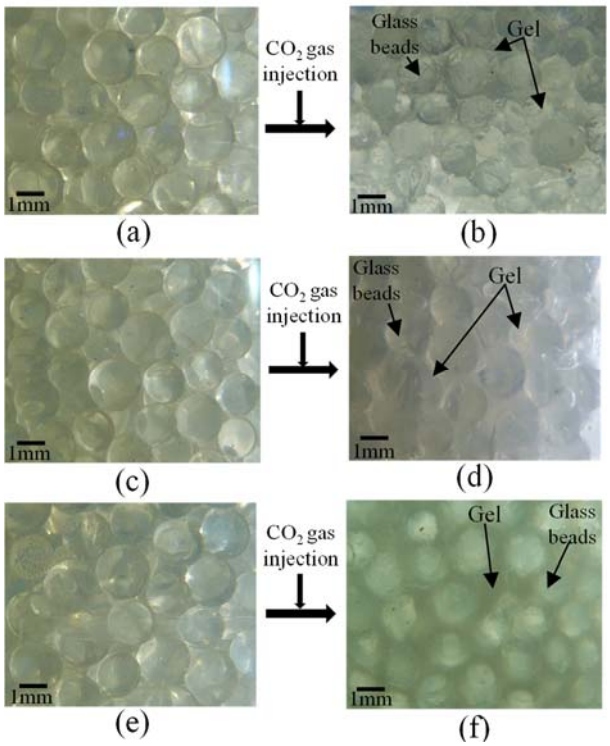

Figure 3.8 In-situ gel formation in porous media, (a) glass beads saturated by 5 wt% of S-MS before gelation; (b) glass beads bonded by gel after gelation by 5 wt% of S-MS, under 5.5 MPa of CO_2 pressure, 25℃, 24 h; (c), (e) glass beads saturated by 10 wt% of S-MS before gelation; (d) glass beads bonded by gel after gelation in supercritical CO_2 injection, 7.5 MPa, 35℃, 24 h

The mass of the gel formed by 5 wt% of S-MS solution was lighter than 10 wt% with the same gelation time due to higher concentration of S-MS generated denser SC-gel (**Figure 3.7**). The mass of gel was increased under the supercritical CO_2 injection and well bounded the glass beads (**Figure 3.8f**). This result shows that the gel formed under supercritical CO_2 condition was performed better than the subcritical CO_2 condition.

3.4.2 Rheological Properties of *In-Situ* Gel

Figure 3. 9 shows the relationship between the apparent viscosity and shear rate of the SC-gel samples generated from three concentrations of S-MS solutions (5, 8 and 10 wt%) under the subcritical CO_2 injection (25ºC, 5.5MPa of CO_2 gas pressure).

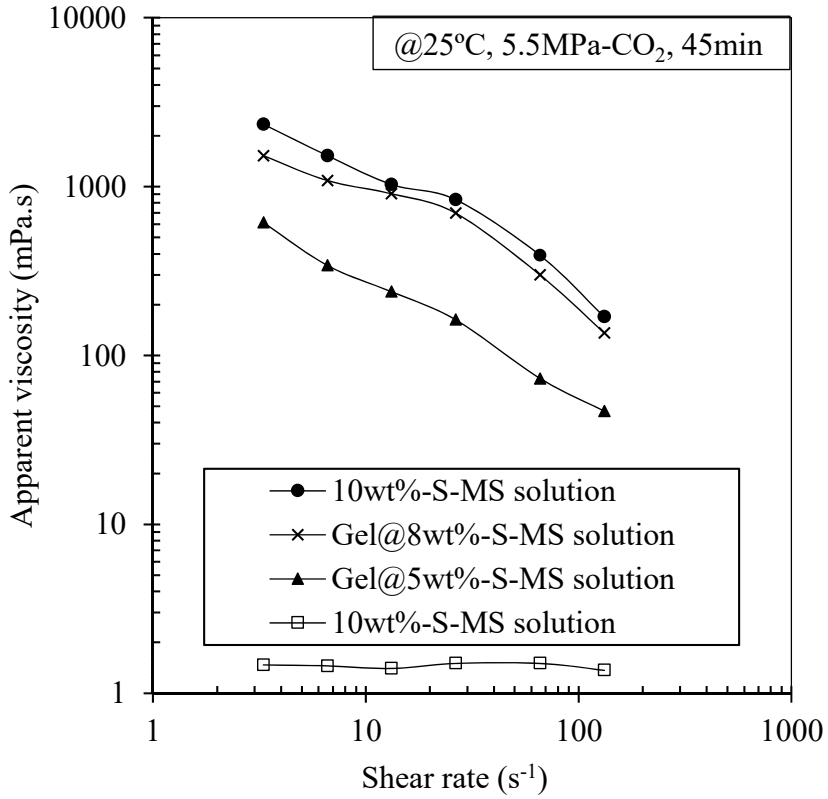

* Gel apparent viscosity measured at the shear rate, 132 s^{-1}

Figure 3.9 Rheological properties of SC-gel

SC-gel appeared more viscous, with the rheological properties of non-Newtonian fluid. Three formed gels exhibited shear thinning behaviour of a pseudo plastic fluid similar to that of polymer solutions. The yield stress was evaluated to be 0.5 to 1.0 Pa. The apparent viscosity of the polymer solution decreases as the shear rate increases because the polymer molecules can align with the shear field to reduce the internal friction (Green and Willhite, 1998).

3.4.3 Gel Strength

Gel Formation in Subcritical CO_2 Condition:

Figure 3.10 shows the effects of S-MS concentration and CO_2 gas pressure on the SC-gel strength measured based on the gel strength code (**Table 2.1**).

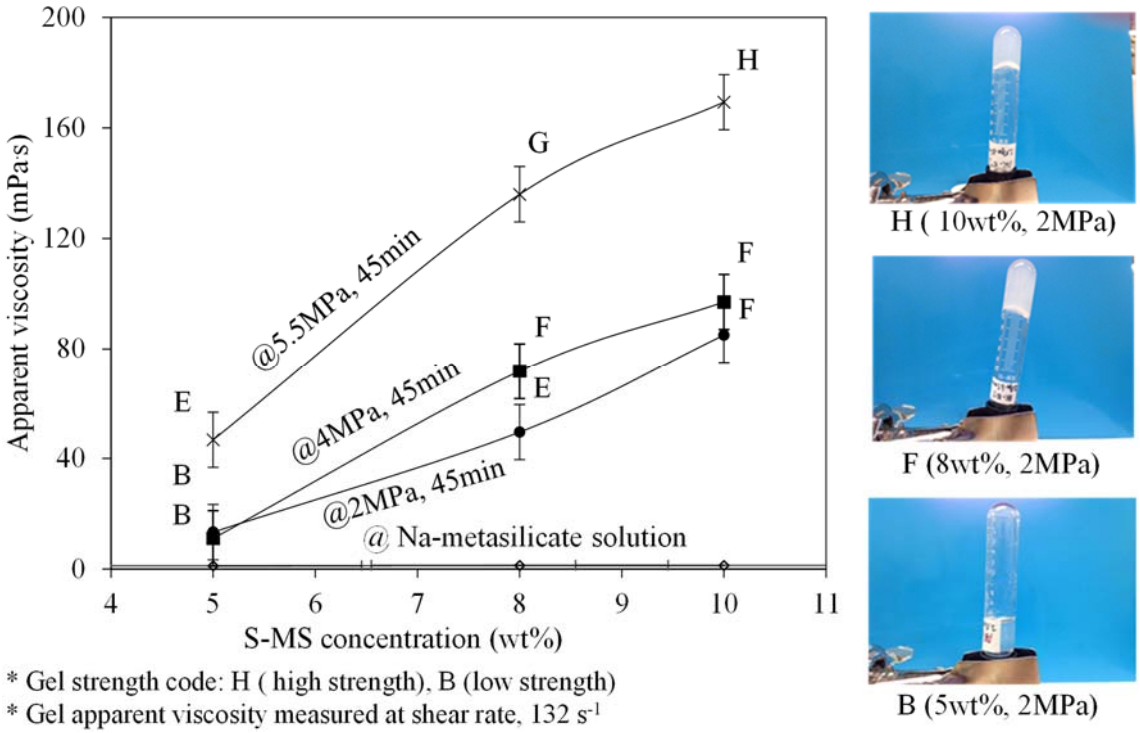

Figure 3.10 Effects of S-MS concentration, and CO_2 gas pressure on SC-gel strength

The gel samples formed using 5, 8 and 10 wt% of S-MS solution at 25 ºC could be classified from (B) to (H) based on the ease of flow. Highly flowing gel (B) and non-flowing gel or strong gel (H) were formed from 5 and 10 wt% solutions, respectively. The gel strength increased with S-MS concentration and CO_2 gas injection pressure. The gel was formed by chemical reactions that do not cause large changes in gel properties by depressurization. The viscosity of the gel is also not so sensitive to the pressure (less than 5.5 MPa in this study), as the drilling fluid viscosity is not sensitive to pressure. Even if depressurization does affect the gel property, our measurements show that the properties of the irreversible gel are formed chemically and remain stable against pressure change. However, to prevent the sampling effects, the gel strength was reconfirmed by direct observation without sampling on the gel sample containing in 15 mL glass bottle which was formed at different S-MS solutions (0.1-10 wt%), room temperature, and 5.5 MPa of CO_2 gas pressure for 45 min in the high pressure cell.

Figure 3.11 indicated that the very weak gels (code-A) were formed at low concentration of S-MS solution, below 5 wt% under the condition mentioned above. The strong gels,

(code F, I and J), were also observed at different order concentrations of S-MS solution from 5 to10 wt%. This similar results were found in **Figure 3.11**.

All SC-gel samples formed from 10 wt% concentration were coded as "J" (high strength), whereas the SC-gels formed from 5 wt% of S-MS solution were coded as "F" after the gel strength conformation without sampling. Therefore, 10 wt% of S-MS solution were selected for in-situ gel formation at 40 and 55 ºC with CO_2 gas injection pressure of 5.5 MPa to characterize the effects of temperature on the gel properties. The gel strength was reduced from high strength "J" at 25 ºC to low strength "D" at 40 and 50 ºC with decrease in apparent viscosity from 50 to 80 mPa·s.

Gel Formation in Supercritical CO_2 Condition:

Figure 3.12 shows the results of gel strength generated from the different concentrations of S-MS solution (1-10 wt%) under the supercritical CO_2 condition (35 ºC, 7.5 MPa-CO_2 pressure, 24 h-shut-in time).

The gel strength was improved by forming the *in-situ* gel under the supercritical CO_2 condition. However, the very weak gel was observed at the low concentration of S-MS below 5 wt%. Code-B gel was formed with the code-B (can be seen by the naked eyes) at S-MS concentrations of 2 to 3 wt%, and code-A gel was formed at S-MS concentration of 1 wt% (cannot be seen by the naked eyes). The high concentration of S-MS, 5-10 wt% generated all stronger code H, I, and J. It can be proved through the flow behaviour, gel surface and colour.

Based on this result, SC-gel strength can become stronger and more irreversible under the supercritical CO_2 gas injection, because the higher CO_2 solubility enhances the gel formation in the solution.

The effect of temperature on the gel strength was also performed using 5 and 10 wt% of S-MS solution under the supercritical CO_2 gas injection with the constant 7.5 MPa of CO_2 pressure at varied temperature up to 55 ºC.

The results show that all SC-gels formed from S-MS 5 wt%-solution were strong due to higher gel strength (Code-H). Furthermore, the strongest Code-J was formed at S-MS 10 wt%-solution and 7.5 MPa CO_2 gas (**Figure 3.13**). The appearance of gel formed from S-MS 10 wt%- solution is stronger than that formed from 5 wt% (**Figure 3.13**). Based on the gel strength code observation, the strength of the gel formed under supercritical CO_2 injection are all most stable at increasing the temperature. It means that the SC-gel formed

from subcritical condition of CO_2 gas was stronger than that formed from subcritical CO_2 gas.

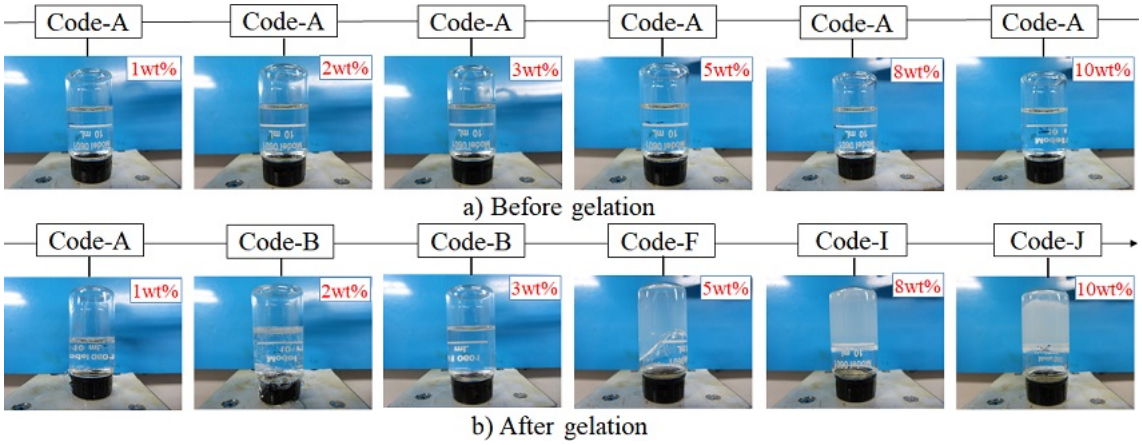

Figure 3.11 Effects of S-MS concentrations (1-10 wt%) on the gel strength in subcritical CO_2 condition (25℃, 5.5 MPa of CO_2 pressure, and 45 min of shut-in time

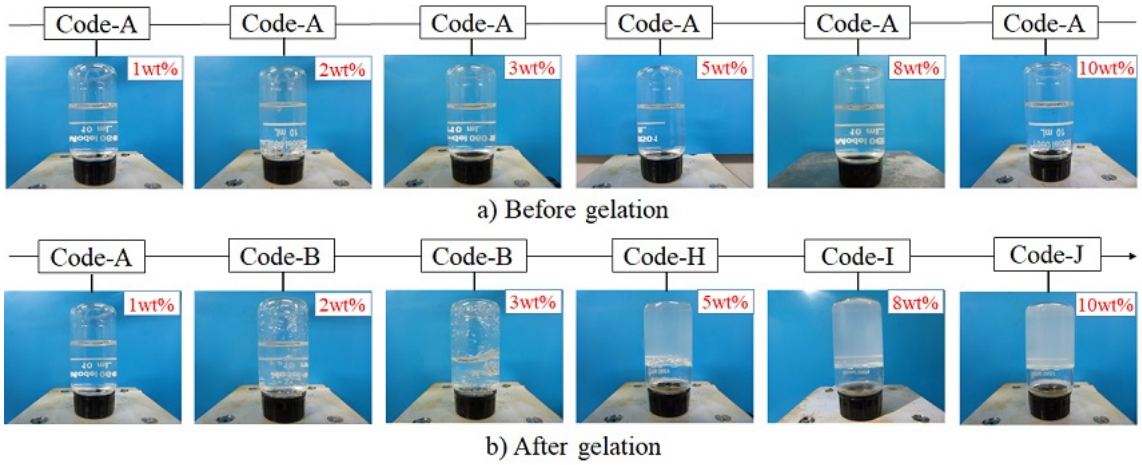

Figure 3.12 Gel strength investigation in supercritical CO_2 condition (35℃, 7.5MPa of CO_2 pressure, and 24 h of shut-in time)

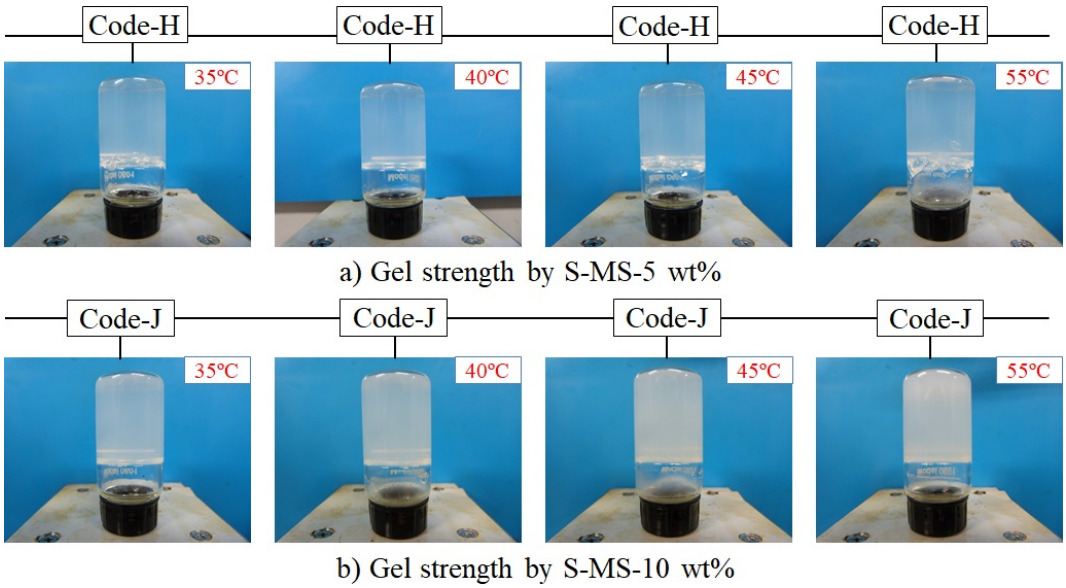

Figure 3.13 Effect of temperature on the gel strength in supercritical CO_2 condition (35-55 ℃, 7.5 MPa-CO_2 pressure, and 24 h of shut-in time)

Figure 3.14 shows the effect of temperature on the apparent viscosity of gel forming by 5 and 10 % of S-MS solution under the supercritical CO_2 injection with a constant pressure of 7.5 MPa. The apparent viscosity of gel was decreased with increase of temperature.

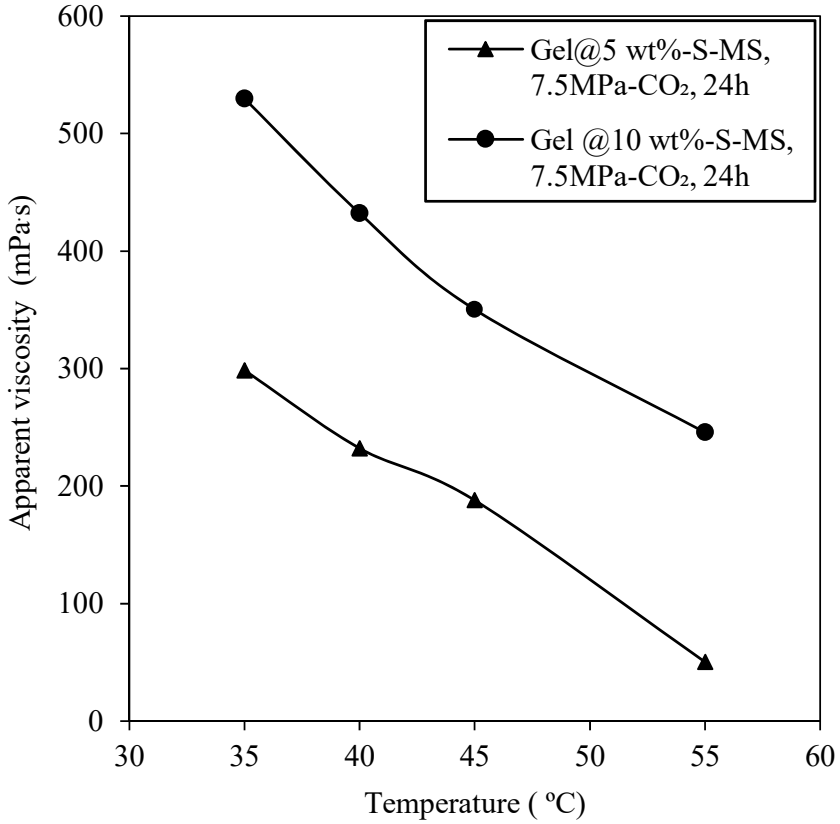

* Gel apparent viscosity measured at the shear rate, 132 s^{-1}

Figure 3.14 Effect of temperature on gel apparent viscosity in supercritical CO_2 injection

In the case of S-MS 5wt%-solution concentration, gel viscosity was decreased from 300 to 60 mPa·s in the temperature range from 35 to 55ºC, whereas the gel viscosity formed at S-MS 10wt%-solution was reduced from 530 to 250 mPa·s at the same range of temperature. Based on these results, the gels generated by both concentrations of S-MS solution with supercritical CO_2 gas injected had the apparent viscosity higher than the gel forming with subcritical CO_2 gas. So it can be concluded that SC-gel formed from supercritical CO_2 has better properties in the gel strength and gel stability.

3.4.4 Gel Stability

Figure 3.15 shows the results of remaining ratio (remaining gel volume %) vs. time up to 35 days.

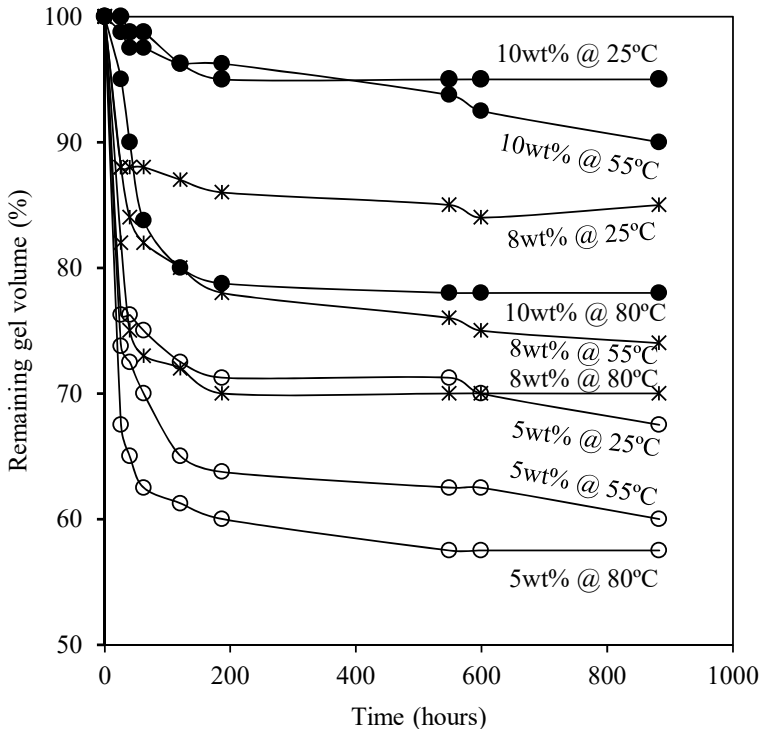

Figure 3.15 Gel stability as function of different S-MS concentrations and temperatures

The remaining ratio-time curves decreased sharply before 200 h, especially in the cases of low S-MS concentration and high temperature. However, the stability was improved with a remaining ratio over 55 % after 200 h, even at higher temperature (80 ºC). The remaining ratio of SC-gel decreased with lower solution concentration and increased with lower temperature (**Figure 3.16**).

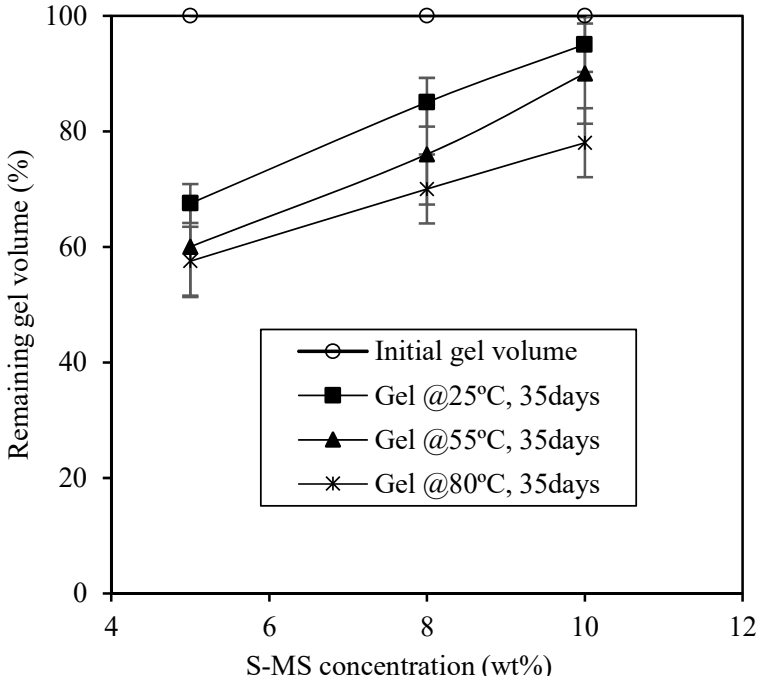

Figure 3.16 Effect of temperature on the gel stability

3.5 Parameters Influencing Gel Formation

Effect of Salinity:

Different concentrations of sodium chloride (0.5-10 wt%) were added into S-MS solution to evaluate the effect on the gel strength (**Figure 3. 17**).

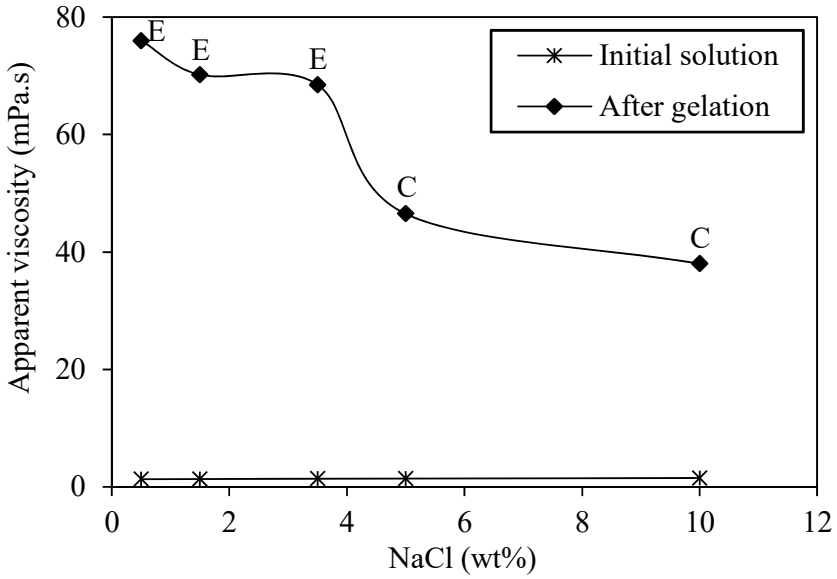

* Moderate gel strength: E. Low gel strength: C
* Gel apparent viscosity measured at shear rate, 132 s^{-1}

Figure 3.17 Effects of salinity (NaCl) on the gel strength (10 wt% of S-MS, 0.1-10 wt% of NaCl@25 ºC, 5.5 MPa-CO_2 gas pressure)

The pH of S-MS solution with 0.5 wt% concentration of NaCl was around 13 and slightly decreased with higher salinity. No precipitation was observed after adding the salt (0.5 to 10 wt%) to the S-MS solution. However, both gel strength and viscosity were decreased presumably due to the common ion effect or salting out effect (Iler, 1979). Gel viscosity decreased with salinity higher than 3.5 wt% as shown in **Figure 3.17**.

Effect of Divalent Ions:

Different concentrations of calcium divalent ion, Ca^{2+} (10 to 10000 ppm), were added to the S-MS solution. Precipitation was clearly observed by adding the calcium divalent ion as shown in **Figure 3.18**. This precipitation was probably caused by the formation of calcium silicates,

$$CaCl_{2\,(s)} \rightarrow Ca^{2+} + 2Cl^{-} \quad (3.7)$$

$$Ca^{2+} + SiO_3^{2-} + SiO_4^{4-} \rightarrow CaSiO_3 + Ca_4(SiO_3)_2 \quad (3.8)$$

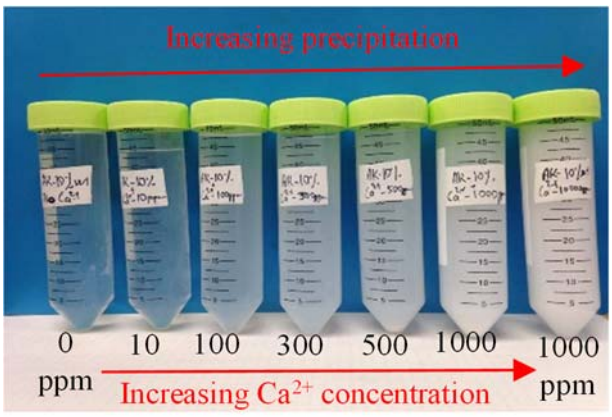

Figure 3.18 Precipitation with different Ca^{2+} concentrations (10 wt% of S-MS @25 ℃)

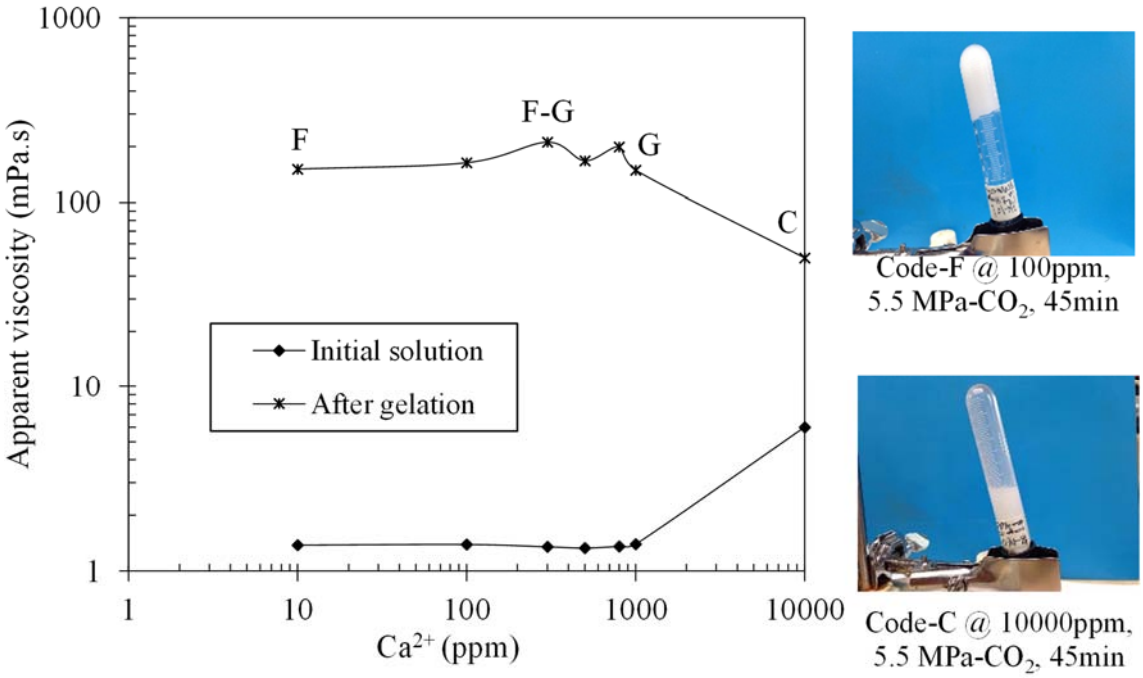

Figure 3.19 Effect of Ca^{2+} concentration on SC-gel strength

S-MS solutions including Ca^{2+} at concentrations of 10 to 10000 ppm were used for gel property measurements. **Figure 3.19** shows the effect of Ca^{2+} concentration on gel viscosity and gel strength. Precipitation was increased with higher Ca^{2+} concentration, and intensively from 1000 to 10000 ppm with viscosity of 6 mPa·s.

Based on these results, the S-SM solution is sensitive to hard brine containing divalent ions (Ca^{2+}, Mg^{2+}), so large preflush volume of soft water needs to be injected.

Interaction with Crude Oil:

Some amount of residual oil still remains in the high permeability layer where is the target of blocking zone by *in-situ* SC-gel. The effect of crude oil interaction must be considered

not only on the gel formation, but also on the possibility of removing oil from the high permeability zone.

S-MS 5 and 10 wt%-solutions were selected for studying the effect of crude oil interaction on the gel formation. 10 mL of each concentration of S-MS solution with the Japanese light crude oil was prepared in the ratio of 2mL up and down (1:9, 3:7, 5:, 7:3, 9:1) and was added into 15mL of glass bottle without any mechanical mixture, then put into a high pressure cell for the gel formation under subcritical CO_2 condition (temperature of 25ºC, 5.5MPa of CO_2 gas pressure, 45min of gelation time) (**Figure 3.20**). The observation was taken place from before, during and after gel formation. As shown in **Figure 3.20 and Figure 3.21,** the emulsion was occurred by adding the light crude oil into to each concentration of S-MS solution. This finding shows both concentrations of S-MS solution can form the emulsification by the interaction with the light crude oil. These S-MS solutions can improve the mobile of residual oil by IFT reduction results in forming emulsifications. The lower the IFT, the easier the emulsification occurs (James J. Sheng, 2011).

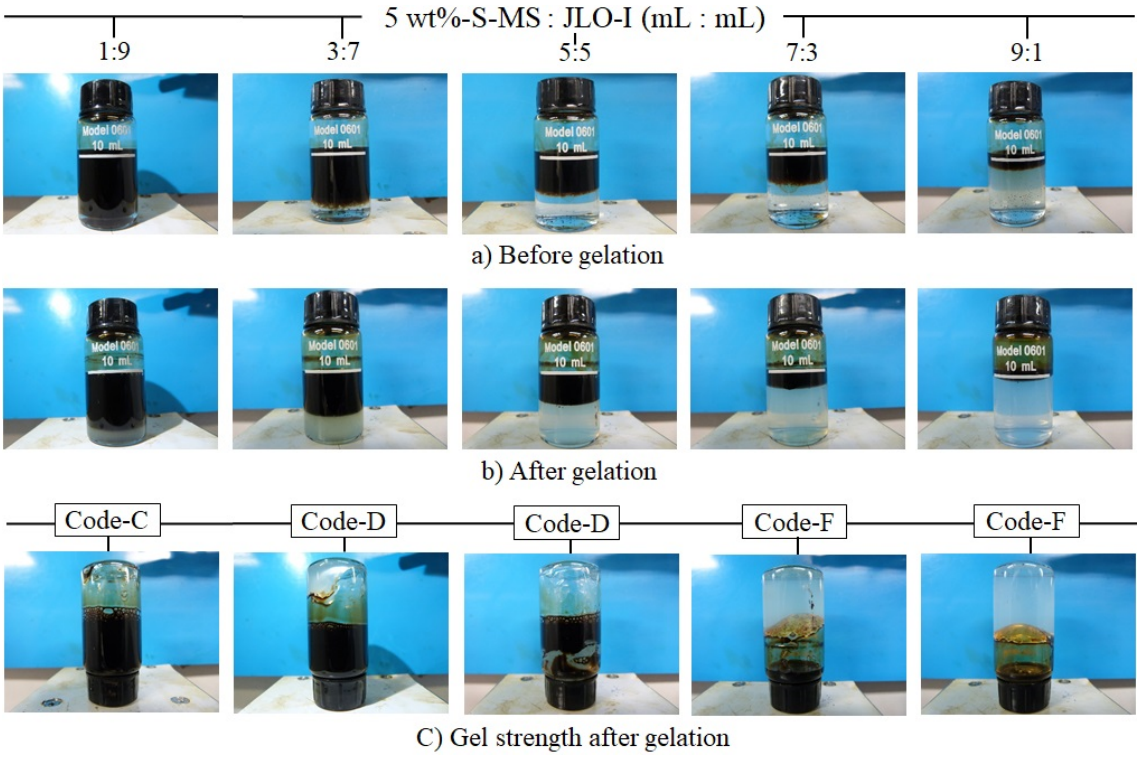

Figure 3.20 Effect of crude oil interaction on the gel behavior and gel formation in subcritical CO_2 condition (S-MS 5wt%-solution /JLO-I, 25ºC, 5.5 MPa-CO_2, 45min-shut-in time)

The effect of mixing JLO-I in the system forming the SC-gel from S-SM solutions and injected CO_2 was investigated. Based on the comparison between the cases with and without the JLO as shown in **Figures 3.20** and **3.21**, almost same performance of gel

formation was confirmed by both concentrations of S-MS 5 and 10 wt%-solutions with mostly same gel strength (code-F for 5 wt% and code-I for 10 wt% of S-MS solutions). There is not serious effect of JLO-I on gel strength and appearance of the gel when the oil volume ratio is over than 90 % of total volume in the case of 10 wt% of S-MS solution (**Figure 3.21**).

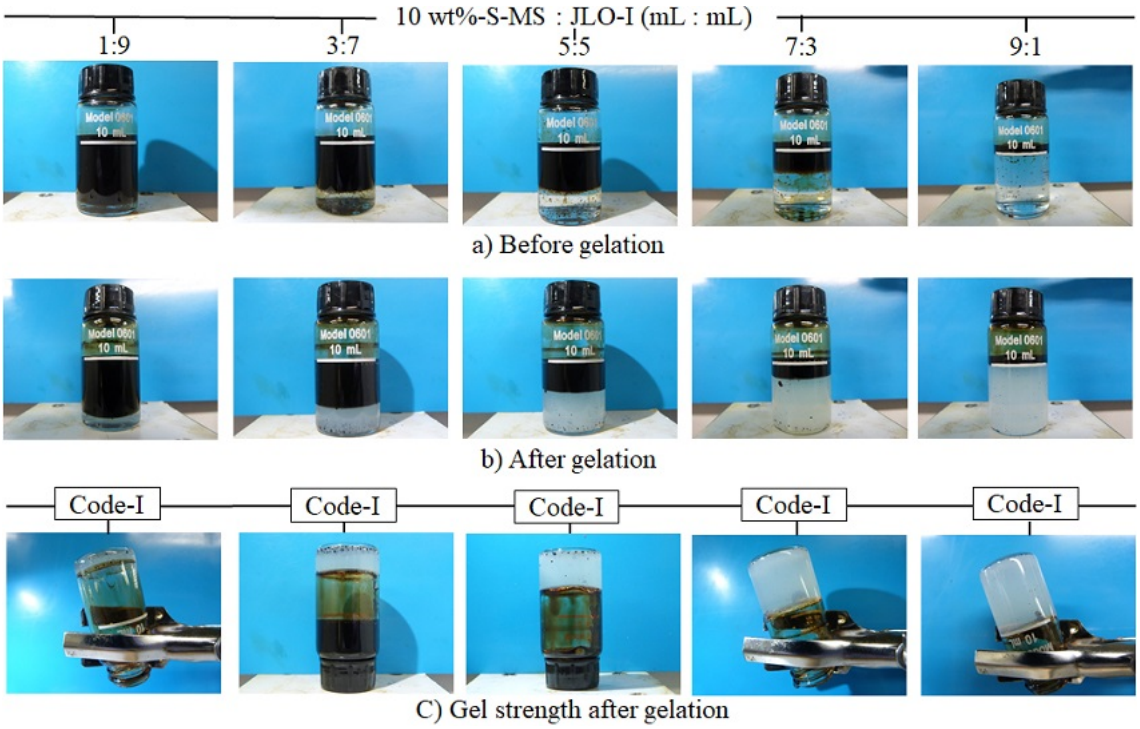

Figure 3.21 Effect of crude oil interaction on the gel behavior and gel formation in subcritical CO_2 injection (S-MS-10 wt%/JLO-I@25℃, 5.5 MPa-CO_2, 45 min-shut-in time)

However, the gel strength was decreased from high strength (code-F) to lower strength (code C and code-D) by increasing the volume ratio of Japanese light crude oil above the 5mL for the case of 5 wt% of S-MS solution, and the gel strength became the same high strength as the case of gel formation without adding the light crude oil after decreasing of volume ratio of light crude oil below 5mL (**Figure 3.20**).

The effect of crude oil interaction on the gelation time and gel formation was also monitored by using the volume ratio of 5:5 of 10 wt%-solution and JLO-I for a gel generation under the same condition above. The result shows that the emulsification was occurred intensively after adding the same volume of JLO-I into the 10 wt%-solution (**Figure 3.22**). The SC-gel was started forming in 15 min after CO_2 gas injection and continually up to complete gel formation in 45 min as shown in **Figure 3.22**. This gelation time is almost the same as gel formation using the S-MS solution alone without adding the JLO. When the SC-gel was started forming the emulsion was moved upward to the

initial interface between light crude oil and aqueous S-MS solution. This phenomenon could be explained that the phase change and density difference from aqueous S-MS solution to the plastic viscous SC-gel could force the emulsion interface move upward, improving the oil mobile.

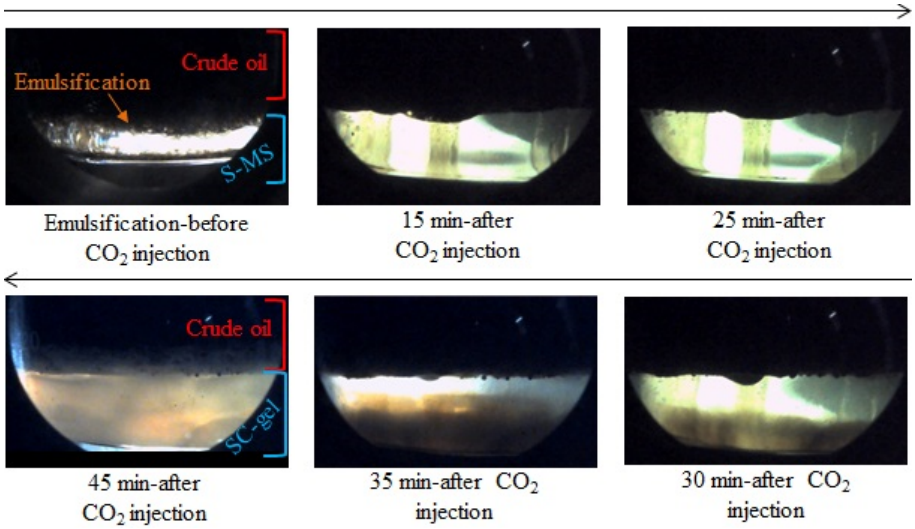

Figure 3.22 Effect of crude oil interaction with 10 wt% of S-MS solution on the gel formation (Volume ratio of S-MS/JLO-I=1@25℃, 5.5 MPa-CO_2, 45 min of gelation time)

3.6 Blocking Performance of *In-Situ* SC-Gel

The blocking performance of the *in-situ* gel, formed from 10 wt% of S-MS solution under CO_2 gas injection, was measured by the core permeable gas flow test. **Figure 3.23** shows the measurements of air flow rate vs. pressure drop, Δp for dry core, core saturated with water and core including the *in-situ* formed SC-gel.

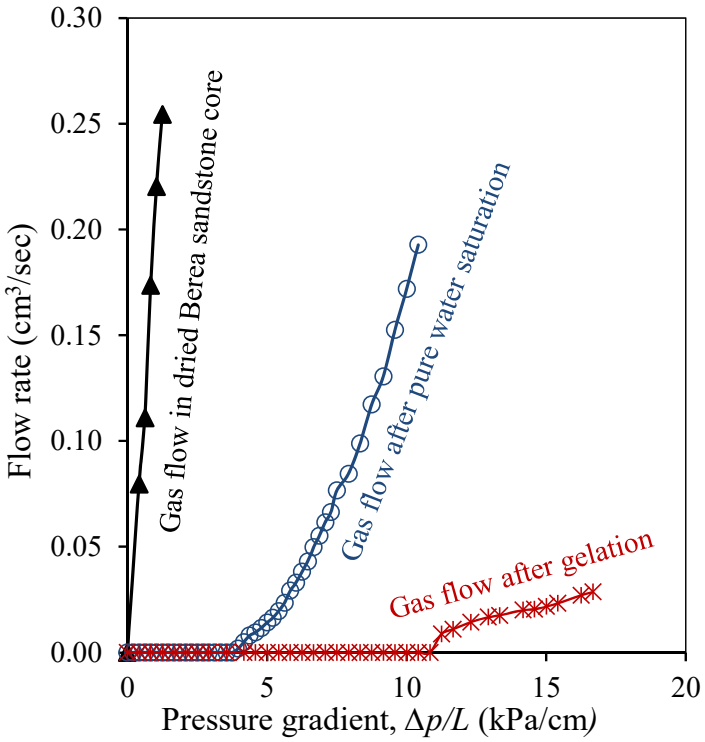

Figure 3.23 Blocking performance for gas permeable flow by the in-situ formed SC-gel in core samples

The air flow rate increased linearly with the pressure gradient in dried core, whereas air flow started at the pressure gradient of 4 kPa/cm in water saturated core, which is called the threshold pressure gradient (TPG) as defined in **Figure 2.6**. The TPG increases with lower permeability and smaller pores and throats (Tian et al., 2018; Zhu et al., 2011). Investigation of the effect of TPG on gas flow in the tight sandstone gas reservoir found that the biggest pores and throats of cores start to contribute to gas flow at TPG, similar to the physical phenomenon of entry pressure, and more pores and throats contribute to the flow forming a concave curve by increasing the pressure gradient (Tian et al., 2018). After the concave curve, the increasing ratio of airflow rate against the pressure gradient became constant, and the extrapolation line intersects the horizontal axis (flow rate=0) at a pressure gradient of 5.8 kPa/cm, which is called as the pseudo threshold pressure gradient (PTPG) as shown in **Figure 3.23** (Lu, 2012). After the pressure gradient exceeds the PTPG, the number of the pores and throats become stable in the core, so the curve becomes a straight line. In the case of the core including formed *in-situ* gel, air flow starts approximately from 11 kPa/cm of TPG that is almost 2.6 times of that of the solution. These results show that in-situ gel formed in sandstone pores has effective blocking performance compared with water.

Figure 3.23 also shows the effect of *in-situ* SC-gel on permeability change in the Berea sandstone core. The pressure gradient is proportional to the gas permeability after

breaking air flow. Therefore, the gas permeability of the core filled with *in-situ* SC-gel is almost 1/80 and 1/10 those of dry and water-filled cores, respectively, as shown in **Table 3.1**.

These findings of the threshold pressure gradient and permeability show that *in-situ* SC-gel can reduce reservoir permeability by the blocking performance.

Table 3.1 Gas permeability reduction by in-situ SC-gel

Berea sandstone core	Gas permeability (mD)
Dried core	77
Water saturated core	13
Gel formed core	1.1

3.7 Conclusions

The properties of *in-situ gel*, expected to be a cost-effective and environmentally safe blocking material, such as gelation time, gel strength and gel stability, were characterized and evaluated using various sodium metasilicate ($Na_2SiO_3 \cdot 9H_2O$, S-MS) concentrations, CO_2 gas pressures, temperatures, salinity or NaCl wt%, and divalent ion (Ca^{2+}) concentrations. Results can be summarized as follows:

- Gel formed from S-MS and CO_2 gas is a sodium carbonate gel (SC-gel) based on Raman spectroscopy and SEM-EDS results.
- Gelation time was decreased with higher S-MS concentration and CO_2 gas pressure, and by higher temperature. Gel strength and stability were also increased with higher S-MS concentration and CO_2 gas pressure, and especially under the supercritical CO_2 condition.
- Gel strength and stability were affected by temperature, salinity (NaCl, wt%) and divalent ion (Ca^{2+}) concentration. The high concentration of S-MS solution from 5-10 wt% generated the stable gel with high gel strength (> Code-E) in the subcritical CO_2 injection (CO_2 gas pressure >4 MPa) and (> code-F) under the supercritical CO_2 condition (35-55 ºC, 7.5 MPa-CO_2 pressure). The highest strength and most stable gel was formed by 10 wt.% of S-MS concentration in the subcritical CO_2 condition (gas pressure > 4 MPa) for temperature (< 55 ºC) and the presence of salt/divalent ion (< 500 ppm). The gel strength and stability were much improved after forming by 5-10 wt% of S-MS solution in the supercritical CO_2 condition with a constant gas pressure of 7.5 MPa, at varied temperature from 35 to 55 ºC.

- Presence of high salt/divalent ion concentration, reduced gel strength and gel stability, so preflushing of reservoir water is required to apply this method.

- The SC-gel formation was confirmed by adding all volume ratio of JLO-I into high concentrations of S-SM solution (5-10 wt%). This interaction has no serious impact on the SC-gel strength. The emulsification and the phase change during the gelation could improve the residual oil mobile in the high permeability zone expectedly.

- Threshold pressure gradient and permeability of the core saturated by the SC-gel was 2.6 times higher and about 1/10 lower, respectively, compared with the core saturated with water. These core testing results indicated that *in-situ* SC-gel formation showed good performance as a blocking agent.

- *In-situ* formed SC-gel formation can be a potential blocking agent to stop short-cut paths to improve oil recovery and also CO_2 sequestration.

Chapter 4: The Effect of *In-situ* Sodium Carbonate Gel as Blocking Agent in Heterogeneous Reservoir for Enhanced Oil Recovery

4.1 Introduction

The amount of oil that is recoverable from a reservoir by two mechanisms. The first mechanism is displacement oil trapped in microscopic pores of the rock reservoir by injected fluid. It is called as microscopic displacement efficiency. The second mechanism is displacement of volumetric fraction of oil by injected fluid. It is called as macroscopic sweep efficiency.

When a displacement process has taken place in a heterogeneous reservoir with large variations in vertical permeability, injected fluids tend to flow through the higher permeability zones leaving only a small fractional volume of injected fluids come across the low permeability zones (**Figure 4.1**). This bypassing part of the reservoir by injecting fluids leads the excess water production to recover oil that results in exceeding economic limits.

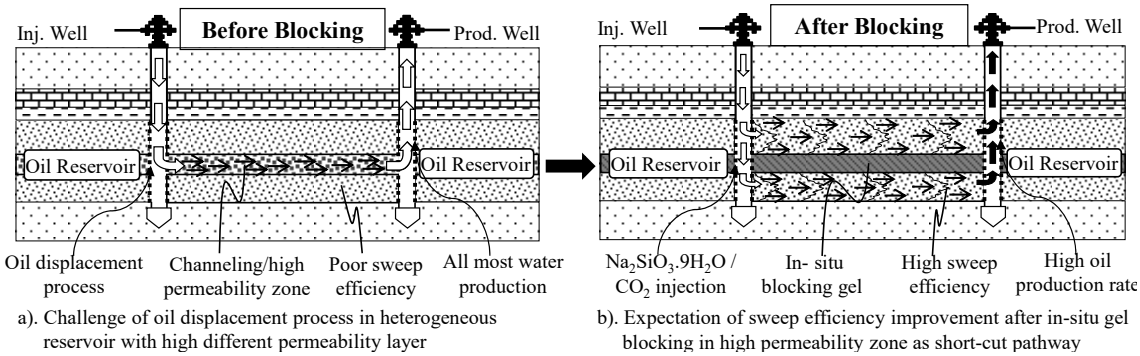

Figure 4.1 Schematic figure of challenge of oil displacement process in heterogeneous reservoir and the effectiveness of in-situ blocking SC-gel in high permeability zone

Sodium metasilicate (S-MS) has been commonly used as a powder detergents and industrial applications (SILMACO, 2016). By containing an optimum portion of alkali and soluble silica, S-MS is a suitable gel precursor which already explained in the previous chapter. Because the alkali content alters the interfacial tension of the trapped oil, S-MS solution has a long history as an alkaline flooding agent for light/medium/heavy reservoirs (James Sheng, 2010; Krumrine and Boyce, 1985; Larrondo and Urness, 1985; Mayer et al., 1983). James Sheng (2010) reviewed that the mechanisms of alkaline flooding responsible for improving oil recovery are (1) emulsification and entrainment of

oil, and (2) wettability reversal from oil-wet to water-wet. Based on previous researches, it is clear that S-MS solution can be used for the alkaline flooding.

In this research, the SC- gel formed from S-MS solution and CO_2 gas as the blocking agent has been also investigated to apply to oil recovery from heterogeneous reservoirs. On the basis of S-MS solution features discussed in previous chapters, S-MS solution can be used for a dual purpose that are chemical agent of alkaline flooding and blocking agent to control excess water flow. Both functions could subsequently enhance oil recovery from that S-MS solution remaining after alkaline flooding could become the base solution for forming SC-gel with CO_2 gas injected after. The oil can be recovered from high permeability zones by usual waterflooding and alkaline flooding. After the flooding, CO_2 is injected then shut-in to form the SC-gel in the reservoir. This *in-situ* gelation is expected to be a plugging agent to decrease short-cut passes due to reducing permeability of high permeability zones or layers. As a result, oil recovery is expected to be improved due to increasing sweep fluids flow in low permeability zones.

In this chapter, firstly the performances of S-MS solution as alkaline flooding agent are discussed based on interfacial tension (IFT) reduction, wettability alteration, and emulsification of the crude oil. Secondary, the results of the coreflooding test to investigate the *in-situ* formed SC-gel as blocking agent in the high permeability zones are presented in order to confirm increasing oil recovery by macroscopic displacements (sweep efficiency) in the low permeability zone where residual oil is not fully swept compared with high permeability zone.

4.2 Static Interfacial Tension of Oil (IFT) between Oil and S-MS Solution

The effect of the sodium metasilicate on IFT reduction is illustrated in **Figure 4.2**. The IFT was measured by using the pendant drop technique at the room condition. The results shown in the figure shows that the IFT at the interface between JLO-II and S-MS solution was decreased gradually with the increase of S-MS concentration, while IFT could not be determined in 0.2 wt% of S-MS concentration because the turbidity in aqueous phase made it impossible to form a stable oil droplet at this concentration (**Figure 4.2**).

The critical micelle concentration (CMC) of S-MS concentration was determined as 0.07 wt% at IFT =1mN/m. These results indicated that S-MS has a high potential as alkaline flooding agent for EOR.

On the other hand, IFT at the interface between JHO and S-MS solution was extremely decreased at lower S-MS concentrations. The IFT at the interface between light crude

oil/S-MS solution could not be measured at 0.05 wt% of surfactant concentration (**Figure 4.3**).

The minimum IFT value was lower than 0.1mN/m in S-MS concentration range of 0.18 to 0.2 wt% with light crude oil and 0.03 to 0.05 wt% with heavy crude oil.

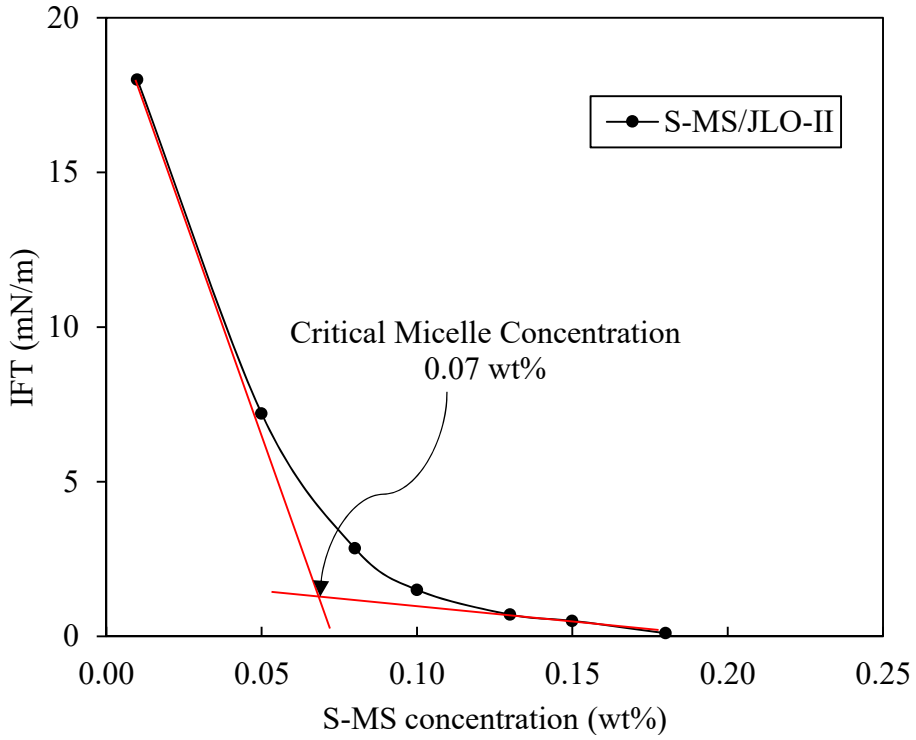

Figure 4.2 Effect of S-MS solution on IFT reduction (JLO-II)

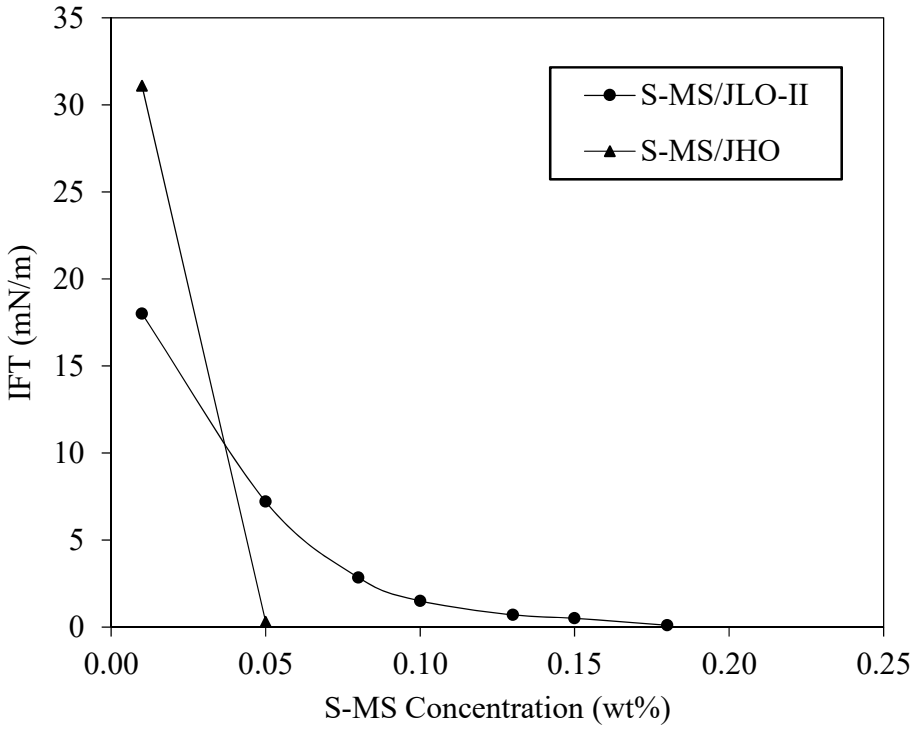

Figure 4.3 Comparisons of JLO-II and JHO on IFT vs. S-MS solution concentration

4.3 Wettability Alteration of Oil in S-MS Solution

Figure 4.5 shows the effect of S-MS concentrations on the wettability alteration of JLO-II/JHO on the glass surface that is assumed to be almost similar property of silica grains in the sandstone core. The contact angle of the oil droplet on the glass plate surface was increased gradually from 118 º to 160º for Japanese light oil (JLO-II) and from 128 º to 174 º for the Japanese heavy oil (JHO) with increasing of S-MS concentration from 0 to 0.05wt%. These results show that the S-MS solution has the ability to alter the wettability of both crude oils from oil-wet to water-wet on the glass surface.

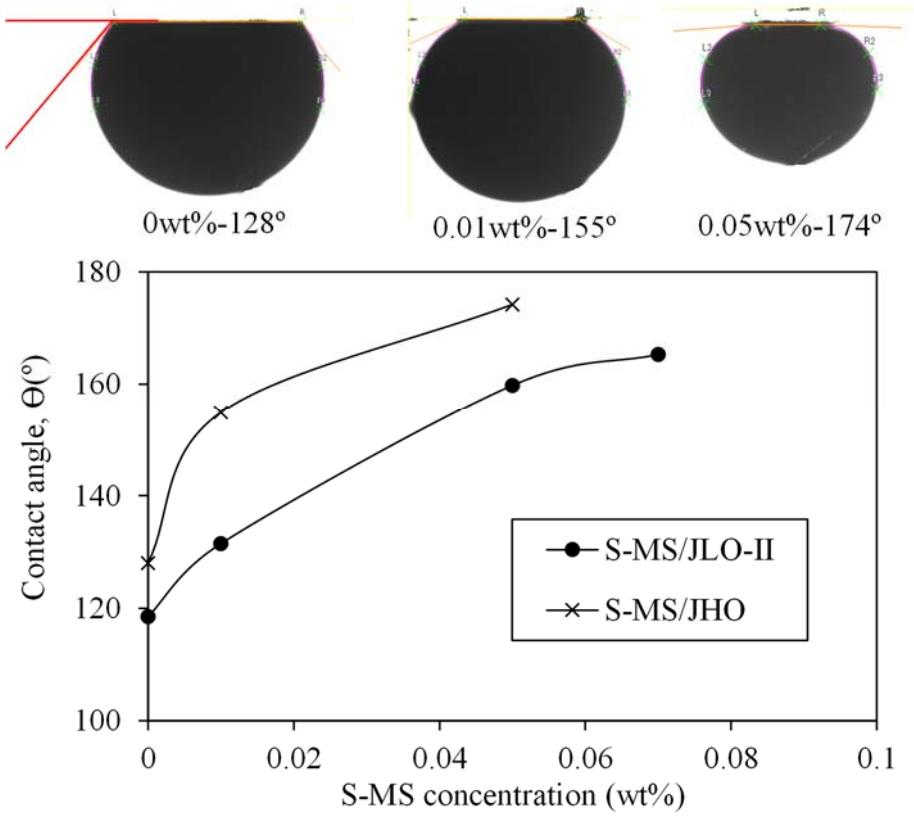

Figure 4.4 Contact angle of oil droplet vs. S-MS solutions (0.01-0.07 wt%) to evaluate wettability alteration of JLO-II/JHO

4.4 Analysis of O/W Emulsion formed with S-MS Solution

4.4.1 Phase Behaviour of Microemulsion formed with S-MS Solution

As shown in **Figure 4.5** and **Figure 4.6, t**he change of microemulsion phase behaviours (Winsor type I and III) was observed by the phase behaviour test using the S-MS solutions (0.5-1-2 wt%) with crude oil type (Japanese light and heavy crude oils) and brine water with range of salinity (0.1-10 wt% of NaCl). With increasing of salinity, the microemulsion was formed easily in short time. The Winsor type I was observed clearly at a lower salinity region (0.1-1.5 NaCl wt%) where there were two phases (water-microemulsion at the bottom and excess oil phase at the top) (**Figure 4.5**). The third phase

of Winsor type III was observed simultaneously in moderate to high salinity, 2-10 wt% NaCl. When the optimal salinity is considered, Winsor type III is the most suitable microemulsion for achieving the ultra-low IFT. Those properties of microemulsion were related to salinity as introduced in the section 1.2.3 (Bera et al., 2012; Green and Willhite, 1998; Sheng, 2011). The micromulsion behaviour showed darker and thicker structure at the high salinity above 5.5 wt% NaCl. It probably caused by high salt concentration effect, and found in both JLO-II and JHO (**Figure 4.5, Figure 4.6**).

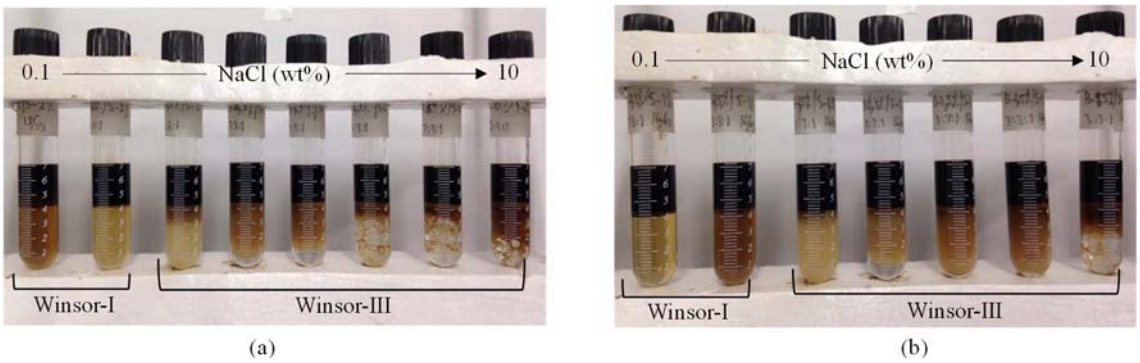

Figure 4.5 Effect of S-MS solution on emulsification of Japanese light crude oil and various salinities: (a) 2 wt%-S-MS/JLO-II/salinity (0.1-10 NaCl wt%)@ 55 ºC, and (b) 1 wt%-S-MS/JLO-II/salinity (0.1-10 NaCl wt%)

4.4.2 Microemulsion Stability

The microemulsion stability was monitored after mixing of three concentrations of S-MS solution (0.5-1-2 wt%) with Japanese heavy crude oil in different salinities (0.1-10 wt% of NaCl) by keeping in an oven controlled temperature of 55ºC. The phase behaviour of microemulsion was recoded up to 3 weeks. The results showed that the volume of microemulsion was decreased versus the elapsed time and extensively in the case of low S-MS concentration (**Figure 4.6**).

The microemulsion of Winsor-III was broken within an hour in 55ºC after forming by mixing with 0.5 wt% of S-MS solution. However, the microemulsion with 1 and 2 wt% of S-MS concentration were relatively stable during 3 weeks. The microemulsion formed using M-SM 2 wt%-solution was generated with largest volume ratio and most stable compared with other concentrations (**Figure 4.7, Figure 4.8**). The 60 % volume of the generated microemulsion was remained after 21 days at temperature of 55 ºC.

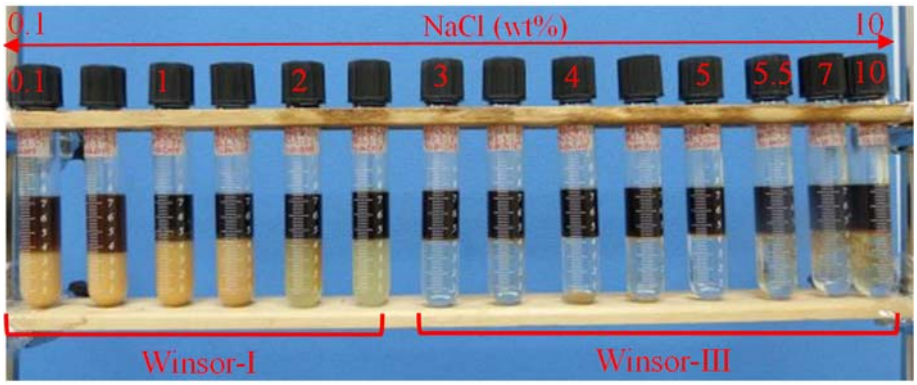

a) 0.5wt%-S-MS/JHO@55°C, 24h

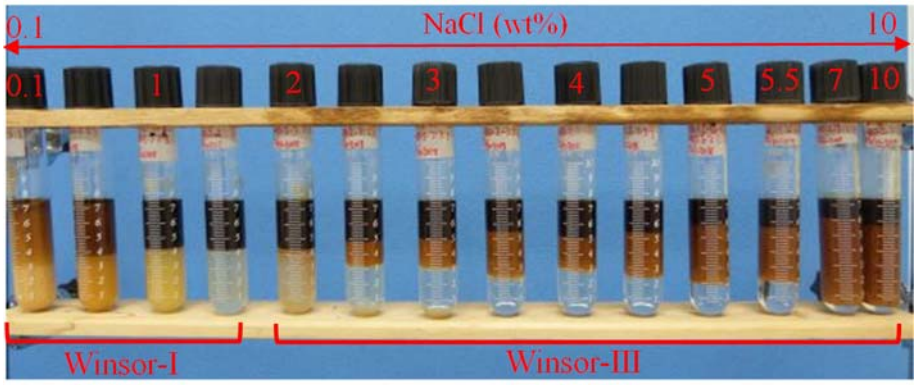

b) 1wt%-S-MS/JHO@55°C, 24h

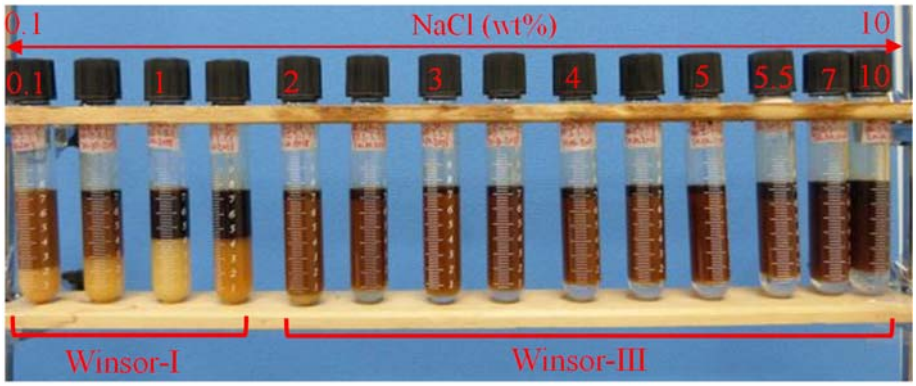

c) 2wt%-S-MS/JHO@55°C, 24 h

Figure 4.6 Effect of S-MS concentration on microemulsion stability of Japanese heavy oil (JHO) with range of salinity

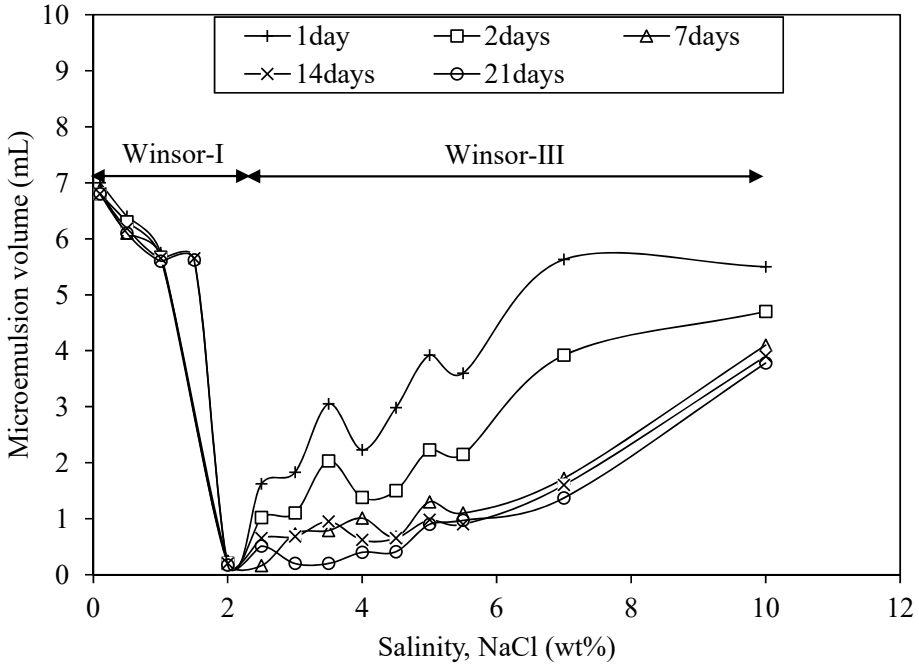

Figure 4.7 Microemulsion stability forming by mixing of 1 wt% of S-MS concentration/JHO/different salinities (0.1-10 wt% of NaCl)

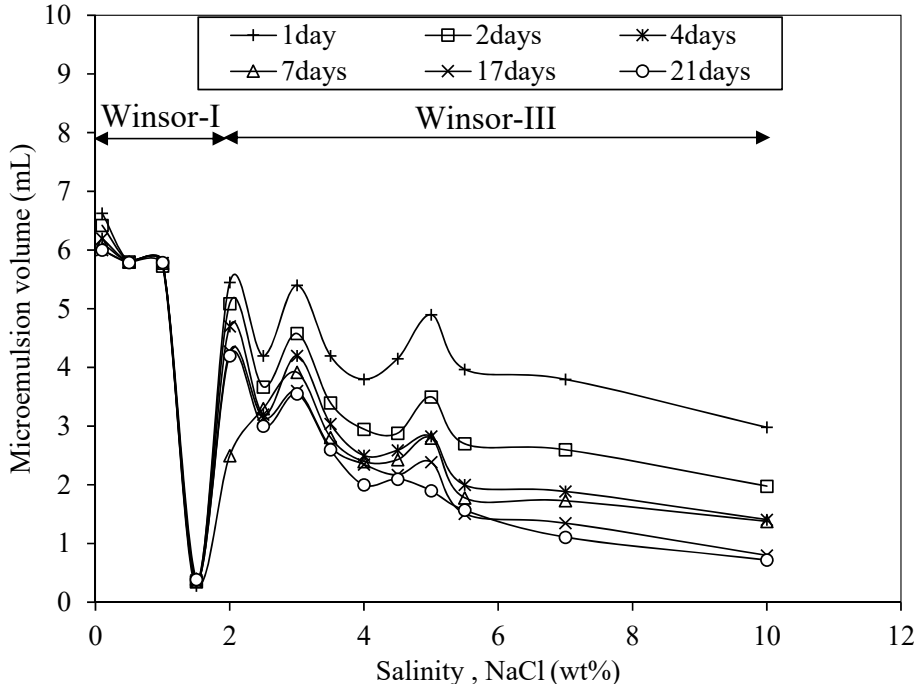

Figure 4.8 Microemulsion stability forming by mixing of 2 wt% of S-MS concentration/JHO/different salinities

4.4.3 Type of Microemulsion and Particle Size Distribution

The microemulsion type and particle size distribution were identified by optical microscope during the phase behaviour tests. **Figure 4.9** shows the microphotograph of microemulsion for Japanese heavy crude oil at 1 wt% of S-MS solution and different salinities after keeping 1 week at temperature of 55ºC.

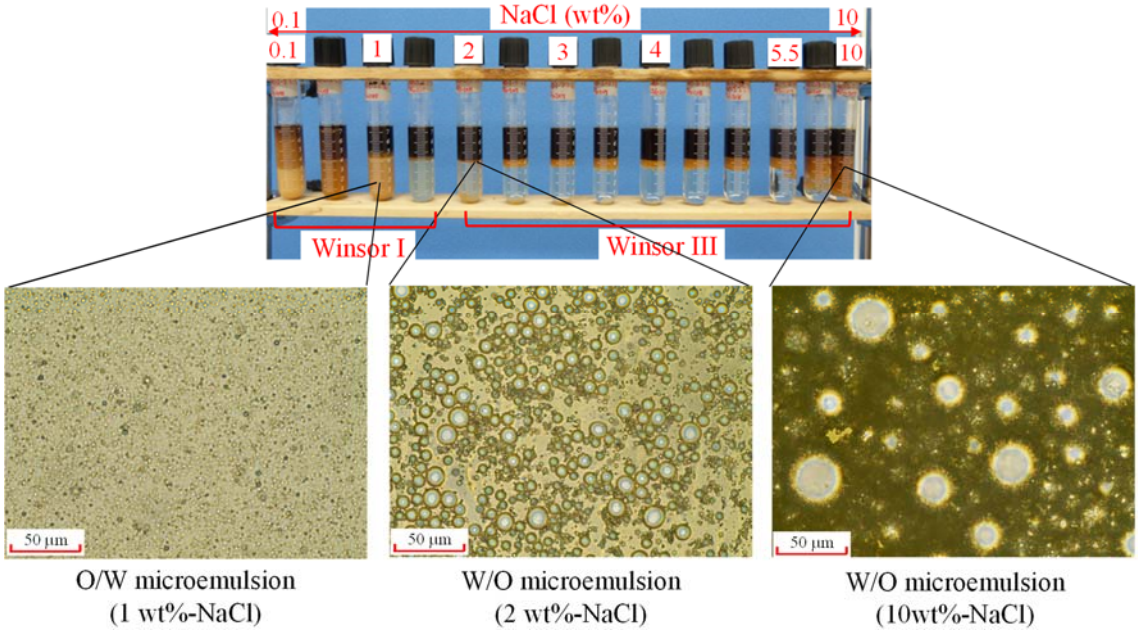

Figure 4.9 Microphotography of microemulsion of Japanese heavy oil (JHO) at 1 wt% of S-MS concentration and ranging salinities in 1 week

The results indicate that the salinity has a significant effect not only on the phase behaviour of microemulsion but also on the properties of microemulsion itself. The oil-in-water (O/W) microemulsion (yellow-brown color) was formed at low concentration of salinity less than 2 wt% of NaCl, while water-in-oil (W/O) micromemulsion was identified at higher salinity in the range 2 to 10 wt% of NaCl after mixing S-MS 1wt%-solution and JHO. The similar results was founded by previous reports (Akhlaghi Amiri et al., 2014; Ge et al., 2012; James J. Sheng, 2011; Pei et al., 2013, 2012). Seng (2011) highlighted that the W/O emulsion is not rigid and easily broken and coalesce to become larger water droplets that increase oil mobility through pore throats in a reservoir. This mechanism helps increasing oil recovery. These emulsions have higher viscosity than oil leading the mobility improvement as well (Ding et al., 2010).

The salinity also affects on the particle size of microemulsion. The particle size of microemulsion increased with increasing of the salinity concentration. At low salinity (<2 wt% of NaCl), the particles size of microemulsion was mostly less than 2 µm and the Winsor type I of the microemulsion phase was observed. The particles size of microemulsion was mostly ranged from 2-10µm at higher salinity from 2 to 5.5 wt% of NaCl at which the Winsor type III was indicated. The large water particles (10 to 50 µm) were observed in the microemulsion generated at the too high concentration of salinity larger than 5.5 NaCl-wt% (**Figure 4.10**). At too high salinity (> 5.5 wt% NaCl), the ratio of larger size of water droplets increased compared with the lower one due to increasing stability of water particles in the solution. This typical micromemulsion property is not

favourable for the improvement in oil recovery (Ge et al., 2012). Therefore, the salinity range from 2 to 5.5 NaCl-wt% was considered preferable salinity in which the Winsor type III microemulsion is produced.

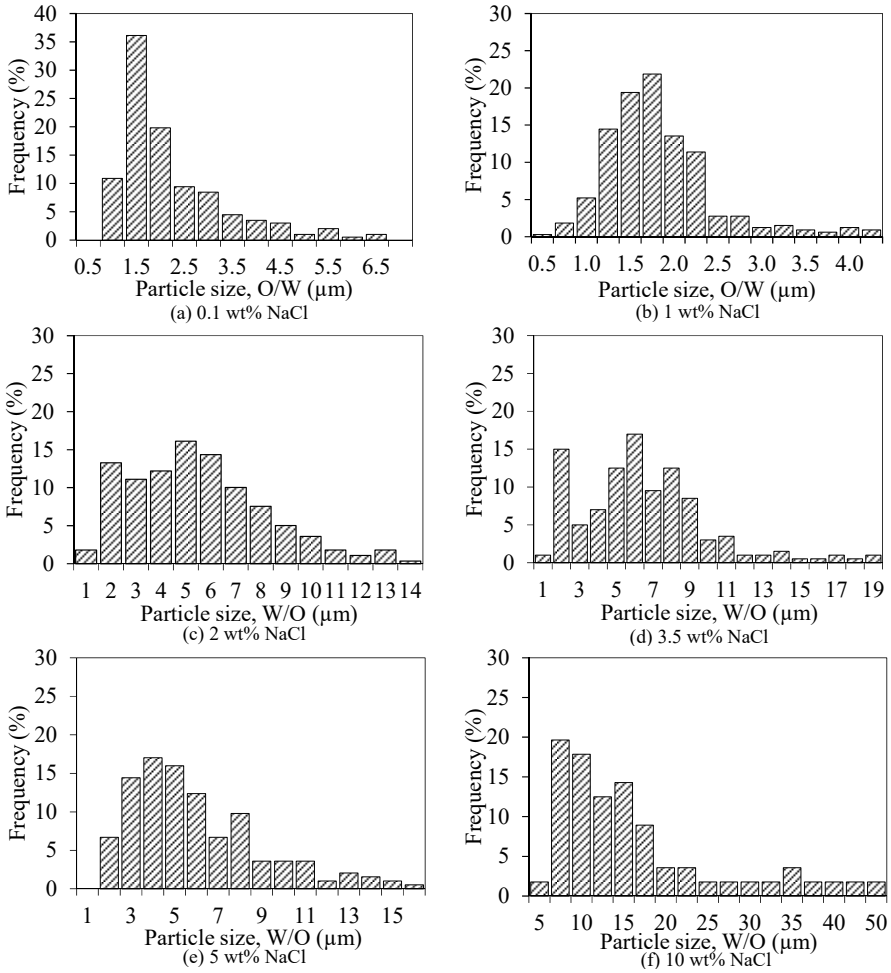

Figure 4.10 Droplet size distribution of formed O/W and W/O microemulsion in various salinities, 0.1-10 wt% NaCl

4.5 Core Flooding Results on the Effects of S-MS as Blocking Performance for Enhanced Oil Recovery (EOR)

After JLO-I saturation by the air vacuum and drainage in the heterogeneous Berea sandstone core used for the coreflooding system, 19.98 mL of total volume of JLO-I was stored as the original oil in place (OOIP) within the core. By following the first stage of water flooding (brine with the salinity of 2 wt% of NaCl concentration) at the flow rate of 0.1 mL/min until no more oil production equivalent to 6.5 PV, 56.7% of oil recovery factor was yielded on average. At the same, the pressure drop was weak and slightly increased from ranging 0.05-0.08MPa during the water flooding stage, suggesting a good interaction with the residual oil (**Figure 4.11**). The pH value was on average around 8.35 during the water flooding stage (**Figure 4.12**).

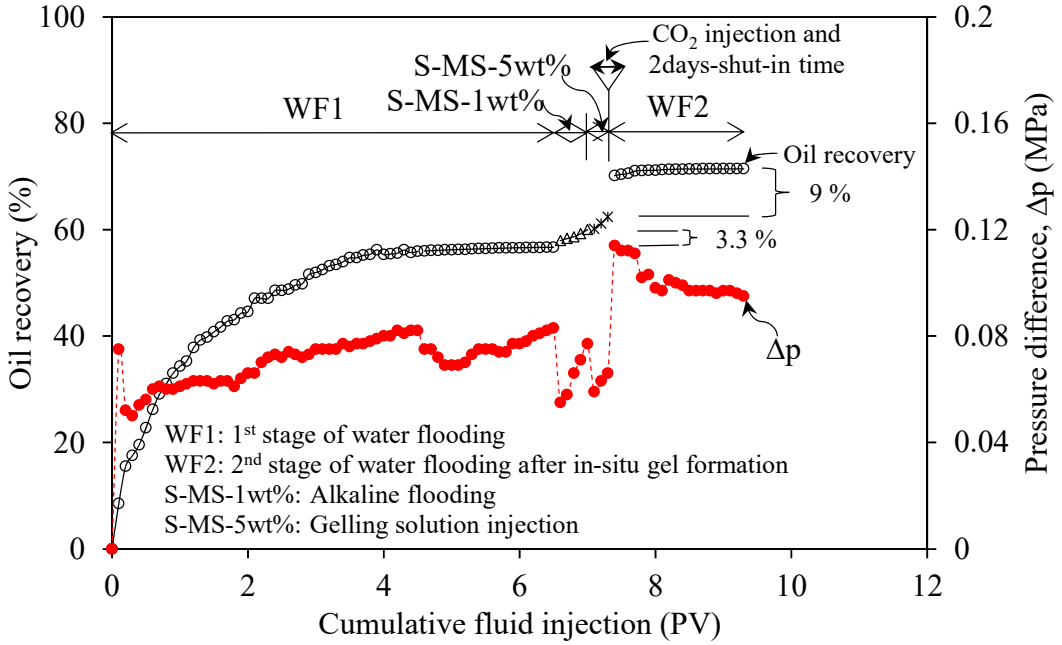

Figure 4.11 Oil recovery by applying the two functions of S-MS as alkaline flooding and in-situ SC-gel formation in the heterogeneous Berea sandstone core

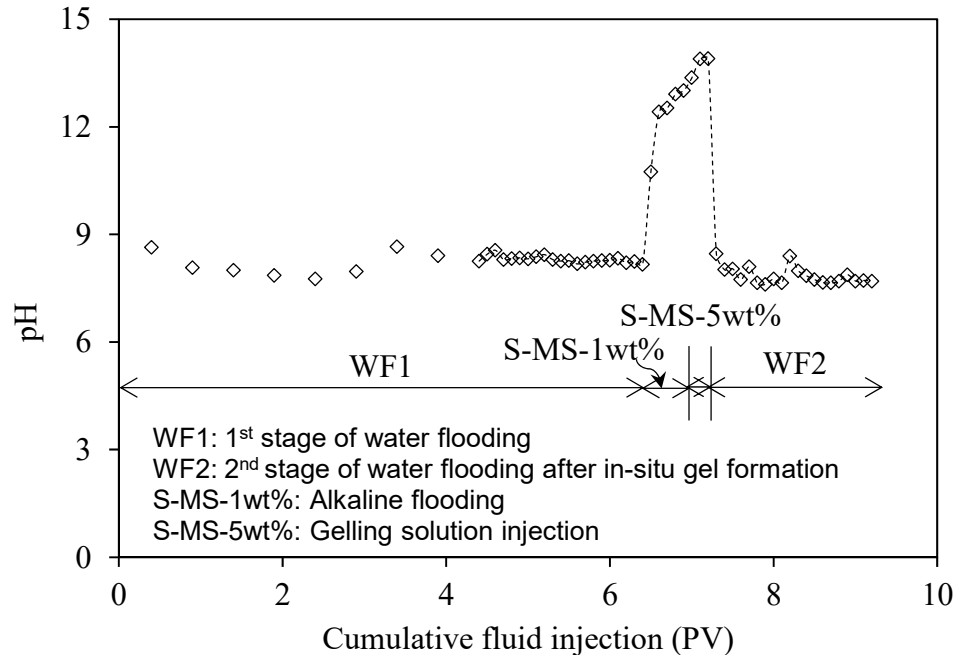

Figure 4.12 Monitoring results of pH of fluid in heterogeneous sandstone core

As the alkaline flooding, S-MS 1wt%-solution was injected at the flow rate of 0.1 mL/min due to 0.5 PV, 3.3 % of oil recovery factor was achieved during the flooding. The pressure difference during this alkaline flooding was slightly increased from 0.055-0.077 MPa which was less than that at the water flooding stage. The pH was increased from 8.4 at the water flooding stage to 13.0 due to the influencing of S-MS 1wt%-solution flooding. The emulsion phase behaviour of Winsor III was produced at this stage by observing the produced fluids (**Figure 4.13**) and the optical microscope. As shown in **Figure 4.13,** the black phase observed at the top in the produced fluids is W/O microemulsion that include

almost oil produced from the core. The presence of W/O microemulsion in the oil phase is probably due to the diffusion of *in-situ* soaps into the aqueous phase declines and more soap remained at the interface between oil and solution/water which is favourable to form water droplets in the oil phase. The second phase in yellow-brown colour observed at below the top one is the aqueous phase including minor O/W microemulsion. The second phase is almost aqueous phase including small amount of oil droplets. This aqueous phase is almost the S-MS solution injected as alkaline flooding agent. The increasing pressure drop during this stage due to forming the W/O and O/W microemulsions in the core. But, the oil recovery factor of this stage is not too high, because the residual oil volume in the high permeability zones was expected small.

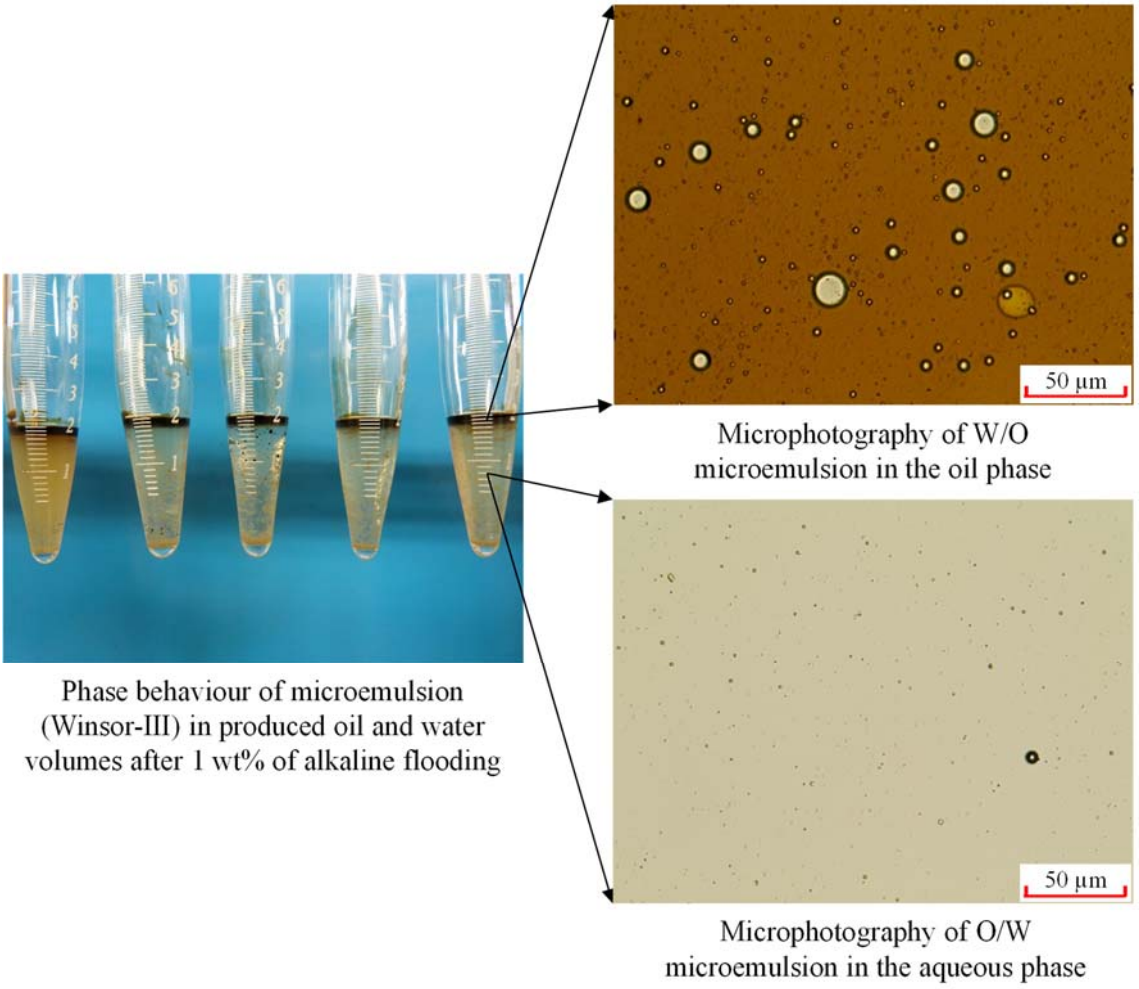

Figure 4.13 Photographs of produced fluids showing O/W and W/O microemulsion during 1 S-MS wt% alkaline flooding

The S-MS 5 wt%-solution was then injected for the *in-situ* gel formation at the same flow rate for 0.3 PV, 2.4 % of oil recovery factor was improved. The solution was also had a function as the alkaline flooding agent as well, so getting the oil improvement at this stage can be reasonable. The pH was abruptly increased up to 13. 9 which is higher than that in

1wt%-solution injection. At the same time, the pressure drop continued increasing with the elapsed time during this stage.

Figure 4.14 indicates the photographs of emulsion phase behaviour of Winsor III consisting mostly of W/O in the oil phase and minor O/W microemulsion in the aqueous phase produced by S-MS 5wt%-solution. The particles size of microemulsion forming by S-MS 5wt%-solution is much smaller than the one producing by S-MS 1 wt%-solution. The smaller particles of micromulsion is the most stable comparing the larger size.

CO_2 gas was injected into the core flooding system after S-MS 5wt%-solution by releasing from 75 mL of a high pressure cell of 2 MPa of CO_2 gas pressure (**Figure 5.4**). Then the coreflooding system was shut-in for two days to allow the CO_2 gas propagating through the heterogeneous core. The pressure drop was recorded through the shut-in time period. 2.0 MPa CO_2 gas pressure was stored in the high pressure cell of 75 mL.

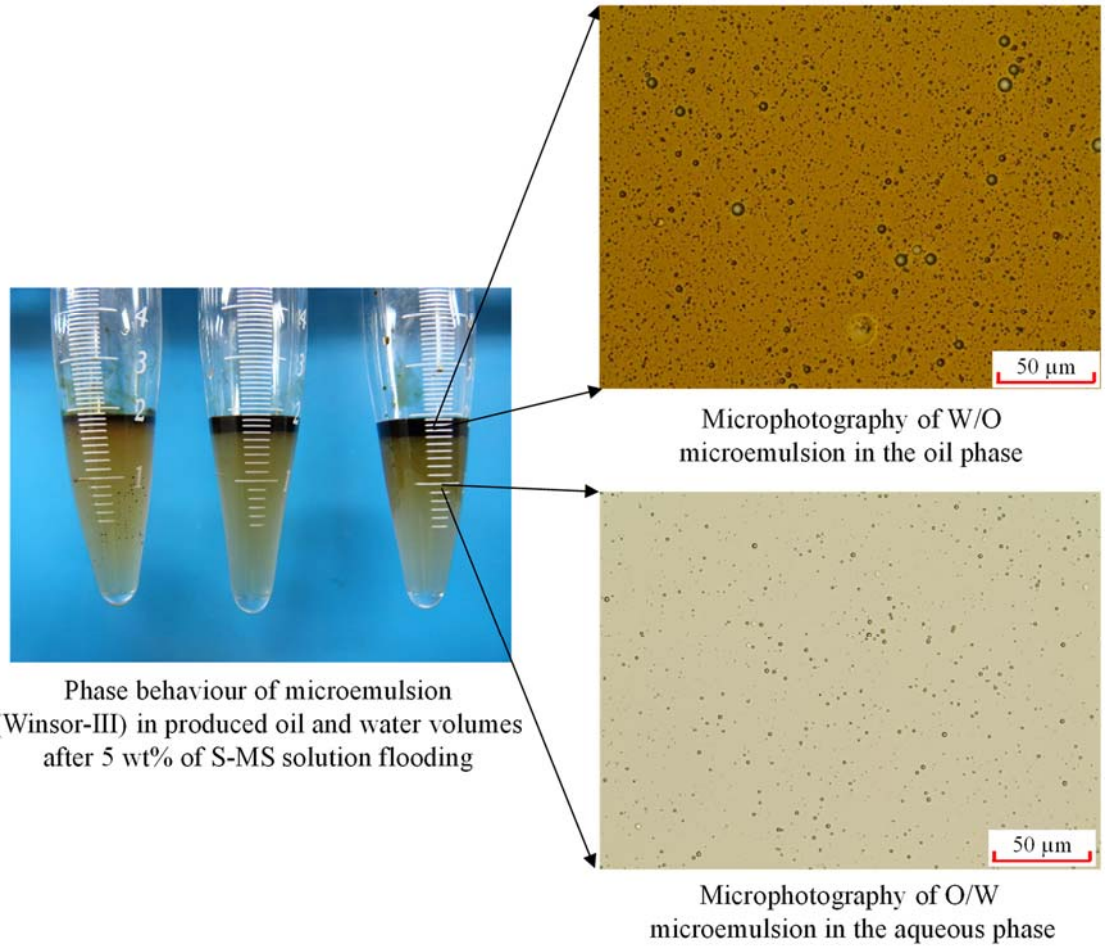

Figure 4.14 Photographs of produced fluids showing O/W and W/O microemulsion during 5 S-MS wt% solution flooding

The pressure in the core was almost equal to CO_2 gas pressure during CO_2 injection and shut-in stage. This suggests the stable CO_2 gas propagation within the coreflooding

system during the *in-situ* gel generation. The pressure was monitored from start of CO_2 injection (2.0MPa) to end of shut-in period as shown in **Figure 4.15**. The decreasing of CO_2 gas pressure of 0.38 MPa (=2.0 - 1.62 MPa) showed the quantity of CO_2 gas used to form the *in-situ* formed SC-gel within the core. When the CO_2 gas saturation is assumed 0.1, it can be calculated 0.28 mmol of CO_2 gas in the core.

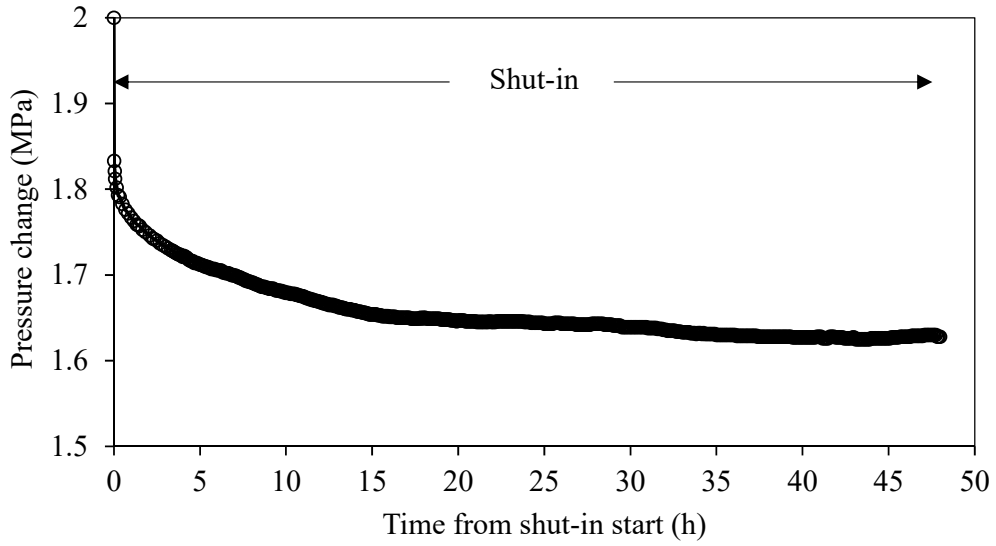

Figure 4.15 Monitoring of pressure decreasing during shut-in (2 days) for SC-gel formation

The pressure difference is all most 0.007 MPa and stable from starting CO_2 injection through the end of shut-in time period (**Figure 4.16**). This result suggested the stable CO_2 gas propagation within the coreflooding system for in-situ gel generation.

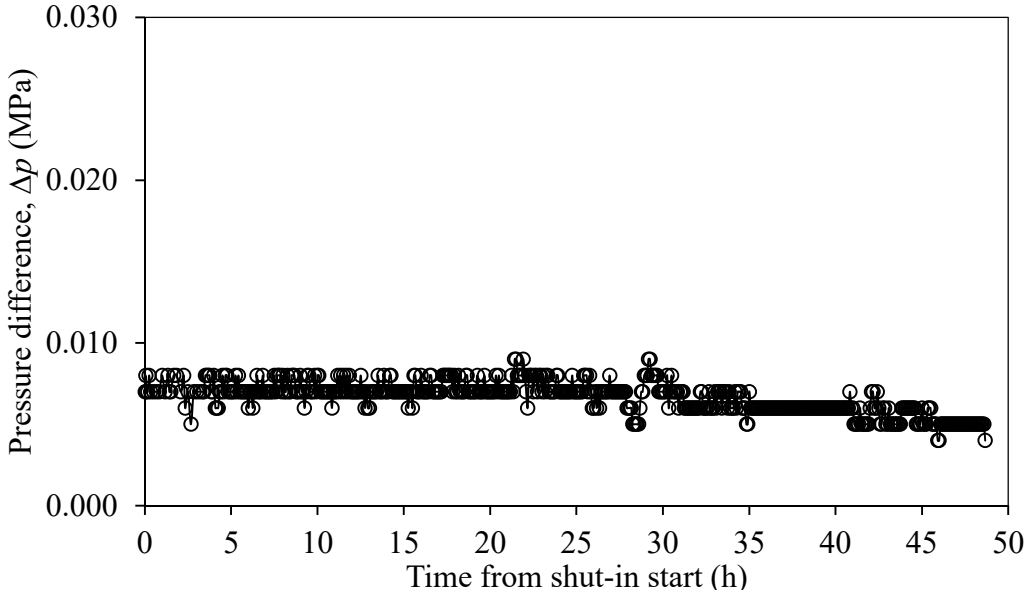

Figure 4.16 Pressure difference monitoring during the shut-in time period

After the shut-in for 2 days for *in-situ* SC-gel formation, the water flooding was conducted again at the same flow rate for 2 PV to evaluate the effects of *in-situ* SC-gel blocking on

increasing oil recovery. The result shows that the oil recovery factor of 9 % was achieved while the pressure drop was increased 1.5 time comparing the stage of water flooding by the SC-gel blocking. This finding shows the effectiveness of *in-situ* SC-gel as blocking agent in the high permeability half-zone in the core and improvement oil recovery from low permeability half-zone. However, the different pressure was started decreasing by increasing of injection size. There are two reasons causing the decrease of pressure drop. First one is probably the high oil recovery from the core system and second one is breaking the gel formed in the high permeability zones during the second water flooding stage. Only 0.3 PV of S-MS 5 wt%-solution as the slug size for in-situ gel formation was injected for gel formation, so the *in-situ* gel was not fully formed in the fracture zones and the high permeability half-zone. It made the *in-situ* gel not strong enough to resistance the water injection pressure. But, the pressure difference was gradually decrease at the end of the second water flooding.

To increase slug size of S-MS solution for *in-situ* gel formation up to 0.5 PV and alternated injected with CO_2 gas may be recommended to improve the gel formation as well as to strength the gel as blocking performance.

4.6 Conclusions

In this chapter, the effect of S-MS solution on the IFT reduction, wettability alteration, and emulsification as alkaline flooding agent were focussed, and the coreflooding test on enhanced oil recovery was carried out to confirm the performance of *in-situ* SC-gel formation as blocking agent using the heterogeneous Berea core sandstone. The results are summarized as following:

- The lower IFT were determined at low concentration of sodium metasilicate. At 0.07 wt% of the critical micelle concentration of sodium metasilicate, the IFT reached at 0.1 mN/m.

- The wettability can be altered by low concentration of sodium metasilicate solution from oil-wet to water-wet.

- The emulsification study showed that, the stable O/W and W/O microemulsion formed with JLO-II/JHO, different salinities and sodium metasilicate solutions at concentration from 1-2 wt%. As salinity changes from low to high, a phase behaviour take place the emulsion type from Winsor I to III. By mixing the S-

MS solution including salinity range from 2-5.5 NaCl-wt% and oil, the stable microemulsion phase of Winsor-III type with W/O microemulsion was produced.

- Injection of S-MS 1wt%-solution for 0.5 PV indicated the effectiveness as alkaline flooding.

- The high concentrations of S-MS solution of 5-10 wt%-solution were eligible used as gelling solution with CO_2 gas as precursor to form the *in-situ* SC-gel as blocking agent in high permeability zones.

- 2.4 % of oil recovery factor produced by S-MS 5 wt%-solution injection for 0.3 PV.

- The abrupt increase of pressure drop through the heterogeneous core by flooding before and after *in-situ* gel formation up to 1.5 time was observed during the water flooding after *in-situ* SC-gel formation. It shows the effectiveness of *in-situ* gel as blocking performance in high permeability zones. Before and during the *in-situ* gel formation process.

- 9 % of oil recovery factor by second water flooding after *in-situ* SC-gel formation were achieved.

- The *in-situ* SC-gel formation has a potential as a blocking agent in heterogeneous reservoir consisting of high different permeability zone by removing the residual oil trapped in low permeability half-zone.

Chapter 5 : Conclusions

The experimental studies of the effect of in-situ sodium carbonate gel forming from aqueous solution of sodium metasilicate reacts with dissolved CO_2 gas as blocking performance in heterogeneous reservoir consisting of high different permeability zones for enhanced oil recovery were successfully studied. The properties of *in-situ* SC-gel, expected to be a cost-effective and environmentally safe blocking material, such as gelation time, gel strength, gel stability, and the effect on enhanced oil recovery in the heterogeneous reservoir, were characterized and evaluated through laboratory experiments using various S-MS solution of concentrations range 1-10 wt%, CO_2 gas pressures (subcritical and supercritical CO_2 condition), different salinities (0.1-10 wt%), divalent ion (Ca^{2+}, 10-10000 ppm), and Japanese light/heavy crude oil.

5.1 Summaries of Present Research

5.1.1 *In-situ* SC-gel Characterization and Evaluation as Blocking Agent

The screening, characterization and evaluation of *in-situ* SC-gel as blocking agent were based on both chemical and physical method by using various sodium metasilicate ($Na_2SiO_3 \cdot 9H_2O$, S-MS) concentrations as the primary material and CO_2 gas (subcritical and supercritical condition) as precursor for *in-situ* gel formation in the high pressure cell apparatus. Influence parameters such as temperatures, salinity (NaCl, wt%), divalent ion (Ca^{2+}, ppm) concentrations and presence of crude oil were also taken into account in this study. SEM-EDS was applied for surface morphology and chemical element composition analysis through the gel samples. Physical characterization is focused on the gelation time, gel strength and gel stability.

The gelation time was decreased with higher S-MS concentration and CO_2 gas pressure, and by higher temperature. Gel strength and stability were also increased with higher S-MS concentration and CO_2 gas pressure, and especially in the supercritical CO_2 condition.

Gel strength and stability were affected by temperature, salinity (NaCl wt%) and divalent ion (Ca^{2+}) concentration. The high concentration of S-MS from 5-10 wt% generated the stable gel with high gel strength (> Code-E) in the subcritical CO_2 injection (CO_2 gas pressure >4 MPa). The highest gel strength and most stable SC-gel was formed by the S-MS 10 wt%-solution in the subcritical CO_2 condition (gas pressure > 4 MPa) at temperature (< 55 ºC) and the presence of salt/divalent ion (< 500 ppm). The gel strength

and gel stability formed from S-MS solution with concentration range of 5-10 wt% were much improved by forming in supercritical CO_2 condition (7.5 MPa at 35-55 ºC). However, these two properties can be reduced in the high salinity condition, and divalent ion concentration, therefore preflushing reservoir water is required to apply this method. The SC-gel was formed with high gel strength after contacting with crude oil. The emulsification during the gelation process could contribute to gel formation in the high permeability zone expectedly.

The core testing results show that the *in-situ* formed SC-gel had a good performance as a blocking agent. Threshold pressure gradient (TPG) and permeability of the core saturated by the SC-gel was 2.6 times higher and 10 time lower, respectively, compared with the core saturated with water.

This finding result of *in-situ* SC-gel herein was a new approach and can be a potential blocking agent to stop short-cut paths for oil recovery improvement and also CO_2 sequestration.

5.1.2 Effect of S-MS solution on IFT Reduction, Wettability Alteration, and Emulsification as Alkaline Flooding Agent

The various low concentrations of S-MS solution (0.1-2 wt%), Japanese light/heavy crude oil, and different salinities (NaCl, 0.1-10 wt%) were used for the effect of S-MS solution as alkaline flooding agent. The interfacial tension and contact angle were measured by using the surface-tension meter (DropMaster DMS-401).

By measuring the IFT versus the S-MS solution concentration, the critical micelle concentration of S-MS solution was determined at 0.07 wt%, where the IFT was 0.1 mN/m.

The contact angle of Japanese crude oil and glass slide was increased gradually from 118 º to 160º for the Japanese light oil and from 128 º to 174 º for Japanese heavy oil with increasing of S-MS concentration from 0-0.05 wt%. So the S-MS solutions can be used to alter the wettability from oil-wet with water-wet.

The emulsification was investigated by the phase behaviour test. The phase behaviour testing results showed that, the stable O/W and W/O microemulsion were formed by mixing JLO-II/JHO, different salinities and sodium metasilicate solutions at concentration from 1-2 wt%. The microemulsion was unstable and broken faster in the case of low concentration of S-MS below 1 wt%. As salinity changes from low to high, a

phase behaviour was taken place the type Winsor I to Winsor III. The salinity range from 2 to 5.5 wt% of NaCl concentration generated the phase behaviour Winsor III with relatively stable W/O microemulsion to achieve ultra-lowering the IFT as reported by the previous research.

5.1.3 Effect of *In-situ* SC-gel as Blocking Agent in Heterogeneous Reservoir for Enhanced Oil Recovery

The coreflooding test was carried out by using the heterogeneous Berea sandstone core consists from two different permeability half sandstone-cores and a fracture at the mid of the interface. Herein was proposed a new approach for the oil displacement process within the heterogeneous reservoir by applying the *in-situ* SC-gel as blocking agent in the higher permeability zones.

3.3 % of oil recovery was produced by 1 wt% of S-MS solution injection for 0.5 PV indicated that the low concentration of S-MS solution can be performed as alkaline flooding agent and injected prior before 5 wt% to remove the remaining oil in high permeability zones and also to prevent the chemical consumption from the reservoir rock on 5 wt% of S-MS as a buffer solution for *in-situ* gel formation.

The 5-10 wt% of S-MS solution can be used as gelling solution with CO_2 gas pressure as precursor to generate the *in-situ* SC-gel as blocking agent in high permeability zones. The pressure difference was abruptly increased up to 1.5 time of the core during the water flooding before and after *in-situ* gel formation. It shows the effectiveness of *in-situ* gel as blocking agent in high permeability zones with improving the oil displacement process of water flooding in the heterogeneous reservoir. The 9 % in oil recovery factor was increased by the second water flooding after *in-situ* SC-gel formation.

These results related to the *in-situ* SC-gel can be used as a blocking agent using in heterogeneous reservoir consisting of high different permeability zones. Furthermore, the S-MS solution can be used for alkaline flooding agent. The system using the S-MS solution and CO_2 injection to form *in-situ* gel formation has the potential to produce the residual oil trapped between pore grains of rock in both high and low permeability zones in the heterogeneous oil reservoirs.

5.2 Future Possibility and Recommendation

Based on the results of characterization and evaluation, the in-situ sodium carbonate gel has a high potential using as blocking agent to stop the channeling flow in the high permeability zones for enhanced oil recovery as well as CO_2 sequestration and leakage prevention. To make this finding more precise and eligible for implementation in the actual reservoir condition, some criteria should be discussed as follows:

- The effects of reservoir properties (reservoir rock, formation water, temperature) on the gelling solution and gel behavior need to be investigated in more details and comprehensively.

- The coreflooding test in supercritical CO_2 condition

- The kinetic properties on the gel formation are very important in term of gelation mechanism and also for simulation work, but they are not discussed in this study yet.

- To control the gel saturation in the whole high permeability zones is still challenging because when the gelling solution was injected and followed by CO_2 gas, the CO_2 gas tends to move upward due to density difference and break thought the production well. At the time the gelling solution was also swept out during the CO_2 gas injection. Therefore the injection scheme must consider and design carefully and precisely in order to allow the *in-situ gel* forming and saturating completely in the target high permeability zones within the reservoir.

References

Abdallah, W., Buckley, J.S., Carnegie, A., Edwards, J., Herold, B., Fordham, E., Graue, A., Habashy, T., Seleznev, N., Signer, C., Hussain, H., Montaron, B., Ziauddin, M., 2007. Fundamentals of wettability. Oilfield Rev. 19, 44–61.

Akhlaghi Amiri, H.A., Hamouda, A.A., Roostaei, A., 2014. Sodium Silicate Behavior in Porous Media Applied for In-Depth Profile Modifications. Energies 7, 2004–2026. ht tp s://doi.org/10.3390/en7042004

Bera, A., Ojha, K., Kumar, T., Mandal, A., 2012. Phase Behavior and Physicochemical Properties of (Sodium Dodecyl Sulfate + Brine + Propan-1-ol + Heptane) Mic roe mu lsio ns. J. Chem. Eng. Data 57, 1000–1006. https://doi.org/10.1021/je2013796

Blackford, J., Hattam, C., Widdicombe, S., Burnside, N., Naylor, M., Kirk, K., Maul, P., Wright, I., 2013. CO_2 Leakage from Geological Storage Facilities: environmental, societal and economic impacts, monitoring and research strategies, in: Gluyas, J., Mathias, S. (Eds.), Geological Storage of Carbon Dioxide (CO_2). Woodhead Publishing, pp. 149–178. https://doi.org/10.1533/9780857097279.2.149

Brooker, M.H., Bates, J.B., 1971. Raman and Infrared Spectral Studies of Anhydrous Li_2CO_3 and Na_2CO_3. J. Chem. Phys. 54, 4788–4796. https://doi.org/10.1063/1.1674754

Bryant, S.L., Rabaioli, M.R., Lockhart, T.P., 1996. Influence of Syneresis on Permeability Reduction by Polymer Gels. SPE Prod. Facil. 11, 209–215. https: //doi .org /10.2118/35446-PA

Carman, P.C., 1956. Flow of Gases Through a Porous Media. Academic Press.

Chang, M.-S.M., Wasan, D.T., 1980. Emulsion Characteristics Associated With An Alkaline Water Flooding Process. Presented at the SPE Oilfield and Geothermal Chemistry Symposium, Society of Petroleum Engineers. https:// doi.o rg/10.2118 / 9001-MS

Chou, S., Bae, J., 1994. Method for silica gel emplacement for enhanced oil recovery. US5351757A.

Ding, B., Zhang, G., Ge, J., Liu, X., 2010. Research on Mechanisms of Alkaline Flooding for Heavy Oil. Energy Fuels 24, 6346–6352. https://doi.org/10.1021/ef100849u

Ge, J., Feng, A., Zhang, G., Jiang, P., Pei, H., Li, R., Fu, X., 2012. Study of the Factors Influencing Alkaline Flooding in Heavy-Oil Reservoirs. Energy Fuels 26, 2875–2882. ht tps://doi.org/10.1021/ef3000906

Green, D.W., Willhite, G.P., 1998. in: Enhanced Oil Recovery, SPE Textbook. Henry L. Doherty Memorial Fund of AIME, Society of Petroleum Engineers, Richardson, TX, p. 545.

Hamouda, A.A., Amiri, H.A.A., 2014. Factors Affecting Alkaline Sodium Silicate Gelation for In-Depth Reservoir Profile Modification. Energies 7, 568–590. https ://d oi . org/10.3390/en7020568

Hoefner, M.L., 1989. Method for selectively plugging highly permeable zones in a subterranean formation. US4809781A.

Iler, R.K., 1979. The Chemistry of Silica: Solubility, Polymerization, Colloid and Surface Properties and Biochemistry of Silica, 1 edition. ed. Wiley-Interscience, New York.

IPCC, 2005. Carbon Dioxide Capture and Storage. UK.

Jousset, F., Green, D.W., Willhite, G.P., McCool, C.S., 1990. Effect of High Shear Rate on In-Situ Gelation of a Xanthan/Cr(III) System. Presented at the SPE/DOE Enhanced Oil Recovery Symposium, Society of Petroleum Engineers. https://doi.org /10.21 18/ 20 213-MS

Kristensen, R., Lund, T., Titov, V.I., Akimov, N.I., 1995. Laboratory evaluation and field tests of a silicate gel system intended for use under North Sea conditions. Geol. Soc. Lond. Spec. Publ. 84, 251–259. https://doi.org/10.1144/GSL.SP.1995.084.01.25

Krumrine, P.H., Boyce, S.D., 1985. Profile Modification and Water Control With Silica Gel-Based Systems. Presented at the SPE Oilfield and Geothermal Chemistry Symposium, Society of Petroleum Engineers. https://doi.org/10.2118/13578-MS

Krumrine, P.H., Mayer, E.H., Brock, G.F., 1985. Scale Formation During Alkaline Floo ding. J. Pet. Technol. 37, 1,466-1,474. https://doi.org/10.2118/12671-PA

Lakatos, I.J., Medic, B., Jovicic, D.V., Basic, I., Lakatos-Szabo, J., 2009. Prevention of Vertical Gas Flow in a Collapsed Well Using Silicate/Polymer/Urea Method. Presented at the SPE International Symposium on Oilfield Chemistry, Society of Petroleum Engineers. https://doi.org/10.2118/121045-MS

Lake, L.W., 1996. Enhanced Oil Recovery, 1st edition. ed. Prentice Hall, Englewood Cliffs, N.J.

Larrondo, L.E., Urness, C.M., 1985. Laboratory Evaluation of Sodium Hydroxide, Sodium Orthosilicate, and Sodium Metasilicate as Alkaline Flooding Agents for a Western Canada Reservoir. Presented at the SPE Oilfield and Geothermal Chemistry Symposium, Society of Petroleum Engineers. https://doi.org/10.2118/13577-MS

Lu, J., 2012. Pressure Behavior of a Hydraulic Fractured Well in Tight Gas Formation with Threshold Pressure Gradient. https://doi.org/10.2118/152158-MS

Martin, F.D., Oxley, J.C., 1985. Effect of Various Alkaline Chemicals on Phase Behavior of Surfactant/Brine/Oil Mixtures. Presented at the SPE Oilfield and Geothermal Chemistry Symposium, Society of Petroleum Engineers. https :// doi .or g/ 10 .21 18 /13575-MS

Mayer, E.H., Berg, R.L., Carmichael, J.D., Weinbrandt, R.M., 1983. Alkaline Injection for Enhanced Oil Recovery - A Status Report. J. Pet. Technol. 35, 209–221. https: //doi .org/10.2118/8848-PA

McDonald, M.J., 2012. Use of high ratio aqueous alkali silicates in drilling fluids. US20120245059A1.

Meister, J., 1985. Bulk Gel Strength Tester. Presented at the SPE Oilfield and Geothermal Chemistry Symposium, Society of Petroleum Engineers. https://doi .org/10 .2118/ 1 3567-MS

Mosavat, N., Abedini, A., Torabi, F., 2014. Phase Behaviour of CO_2–Brine and CO_2–Oil Systems for CO_2 Storage and Enhanced Oil Recovery: Experimental Studies. Energy Procedia, 12th International Conference on Greenhouse Gas Control Technologies, GHGT-12 63, 5631–5645. https://doi. org/10.101 6/j.egypro .2014 .1 1.596

Nasr-El-Din, H.A., Taylor, K.C., 2005. Evaluation of sodium silicate/urea gels used for water shut-off treatments. J. Pet. Sci. Eng. 48, 141–160. https://doi.org /10.1016/ j.petrol .2005.06.010

Or, C., Sasaki, K., Sugai, Y., Nakano, M., Imai, M., 2016. Swelling and Viscosity Reduction of Heavy Oil by CO_2-Gas Foaming in Immiscible Condition. SPE Reserv. Eval. Eng. 19, 294–304. https://doi.org/10.2118/179738-PA

Pei, H., Zhang, G., Ge, J., Jin, L., Ma, C., 2013. Potential of alkaline flooding to enhance heavy oil recovery through water-in-oil emulsification. Fuel 104, 284–293. https://doi. or g/10.1016/j.fuel.2012.08.024

Pei, H., Zhang, G., Ge, J., Tang, M., Zheng, Y., 2012. Comparative Effectiveness of Alkaline Flooding and Alkaline–Surfactant Flooding for Improved Heavy-Oil Recovery. Energy Fuels 26, 2911–2919. https://doi.org/10.1021/ef300206u

PQ Corporation, 2015. Typical Property Data forPQ®Sodium Metasilicates [WWW Document]. URL https://www.pqcorp.com/docs/default-source/typical-pro pe r t ie s/pq-corporation/sodium-metasilicates/17-2c-metasilicate---4-2015.pd f?sfv rs n =5 cc0c73d_8 (accessed 1.10.19).

Prada, A., Civan, F., Dalrymple, E.D., 2000. Evaluation of Gelation Systems for Conformance Control. Presented at the SPE/DOE Improved Oil Recovery Symposium, Society of Petroleum Engineers. https://doi.org/10.2118/59322-MS

SILMACO, 2016. Sodium Metasilicate: Green and Efficiënt [WWW Document]. URL http://www.silmaco.com/documents/10180/29033/Sodium+Metasilicate+-+Green+and+effici%C3%ABnt.pdf/57179204-a3a6-4f5c-8043-41701a67c843 (accessed 11.15.18).

Sheng, J. J., 2011, in: Modern Chemical Enhanced Oil Recovery. Elsevier, p. 391. https://doi.org/10.1016/C2009-0-20241-8

Sheng, J. J, 2010. Modern Chemical Enhanced Oil Recovery: Theory and Practice. Hardcover.

Skrettingland, K., Dale, E.I., Stenerud, V.R., Lambertsen, A.M., Nordaas Kulkarni, K., Fevang, O., Stavland, A., 2014. Snorre In-depth Water Diversion Using Sodium Silicate - Large Scale Interwell Field Pilot. Presented at the SPE EOR Conference at Oil and Gas West Asia, Society of Petroleum Engineers. https://doi.o rg/10.2 118/1 69727-MS

Skrettingland, K., Giske, N.H., Johnsen, J.-H., Stavland, A., 2012. Snorre In-depth Water Diversion Using Sodium Silicate - Single Well Injection Pilot. Presented at the SPE Improved Oil Recovery Symposium, Society of Petroleum Engineers. https://doi. org/10 .2118/154004-MS

Stahl, G.A., Schulz, D.N., 1988. , in: Water-Soluble Polymers for Petroleum Recovery. Plenum Press, New York, pp. 313–325.

Sydansk, R. D., Argabright, P.A., 1988. Conformance Improvement in a Subterranean Hydrocarbon-Bearing Formation Using a Crosslinked Polymer.

Sydansk, Robert D., Argabright, P.A., 1988. Conformance improvement in a subterranean hydrocarbon-bearing formation using a crosslinked polymer. US4744419A.

Taber, J.J., Martin, F.D., Seright, R.S., 1997. EOR Screening Criteria Revisited - Part 1: Introduction to Screening Criteria and Enhanced Recovery Field Projects. SPE Reserv. Eng. 12, 189–198. https://doi.org/10.2118/35385-PA

Taylor, K. C., Nasr-El-Din, H.A., 2003. Laboratory Evaluation of In-Situ Gelled Acids for Carbonate Reservoirs. SPE J. 8, 426–434. https://doi.org/10.2118/87331-PA

Taylor, K. C., Nasr-El-Din, H.A., 2003. Thermally responsive aqueous silicate mixture. US6660694B1.

Tian, W., Li, A., Ren, X., Josephine, Y., 2018. The threshold pressure gradient effect in the tight sandstone gas reservoirs with high water saturation. Fuel 226, 221–229. https://doi.org/10.1016/j.fuel.2018.03.192

Vargas, J. P., Ciobotă, V., Rösch, P., Popp, J., 2013. Reactions of alkaline minerals in the atmosphere. Angew. Chem. Int. Ed Engl. 52, 1410–1413. https://doi.org/10. 1002/ anie.201208319

Vinot, B., Schechter, R.S., Lake, L.W., 1989. Formation of Water-Soluble Silicate Gels by the Hydrolysis of a Diester of Dicarboxylic Acid Solublized as Microemulsions. SPE Reserv. Eng. 4, 391–397. https://doi.org/10.2118/14236-PA

Young, C.W., Blankenhorn, C.F., 1972. Method for plugging highly permeable zones. US3645336A.

Zhu, W., Song, H., Huang, X., Liu, X., He, D., Ran, Q., 2011. Pressure Characteristics and Effective Deployment in a Water-Bearing Tight Gas Reservoir with Low-Velocity Non-Darcy Flow. Energy Fuels 25, 1111–1117. https://doi.org/10 .1021/ ef 1014633

Zolotukhin, A.B., Ursin, J.-R., 2000. Fundamentals of petroleum reservoir engineering. Høyskoleforlaget AS–Norwegian Acad. Press Stavanger Nor.